Mechanisms of Immune Control in HIV-1 Virus Controllers

by

Tinashe Edward Nyanhete

Department of Immunology
Duke University

Date:_____
Approved:

_____
Georgia Tomaras, Supervisor

_____
Qi-Jing Li

_____
Mari Shinohara

_____
Guido Ferrari

_____
Thomas Tedder

Dissertation submitted in partial fulfillment of
the requirements for the degree of Doctor
of Philosophy in the Department of
Immunology in the Graduate School
of Duke University

2020

ABSTRACT

Mechanisms of Immune Control in HIV-1 Virus Controllers

by

Tinashe Edward Nyanhete

Department of Immunology
Duke University

Date:_____
Approved:

Georgia Tomaras, Supervisor

_____
Qi-Jing Li

_____
Mari Shinohara

_____
Guido Ferrari

_____
Thomas Tedder

An abstract of a dissertation submitted in partial fulfillment of the requirements for the degree of Doctor of Philosophy in the Department of Immunology in the Graduate School of Duke University

2020

Copyright by
Tinashe Edward Nyanhete
2020

Abstract

There is a lack of a clear understanding of what constitutes a potent natural immune response capable of mediating post-infection protection in an HIV-1 infection setting. Thus, the goal of my dissertation was to dissect the immune responses to HIV-1 infection associated with protection using a model for natural control from HIV-1 infection. The first objective was to expand our understanding of what constitutes an effective CD8+ T cell response, while the second objective was to bridge Fab and Fc-mediated antibody effector functions associated with natural control of HIV-1 infection.

The conventional T cell paradigm dictates CD8+ T cell recognition of peptides in the context of MHC class I. Remarkably, a paradigm shifting study demonstrated that induction of MHC class E and II-restricted CD8+ T cells was associated with the clearance of SIV infection in rhesus macaques. However, the induction of the unconventional class II-restricted CD8+ T cells in a natural HIV-1 infection setting, their ontogeny, distribution across different HIV-1 disease states and their role in viral control remain unclear.

In the first part of my dissertation research, I hypothesized that HIV-1 specific class II-restricted CD8+ T cells are present in patients naturally controlling HIV-1 infection (Virus Controllers). I also hypothesized that HLA class II-restricted CD8+ T cells capable of suppressing viral replication in autologous CD4+ T cells are ‘ex-CD4+ T cells’ with CD8-like anti-viral effector functions.

I not only showed that HIV-1 specific HLA class II-restricted CD8+ T cells are present in HIV-1 VCs, but that memory class II-restricted CD8+ T cell responses were more often detectable in VCs than in chronic viremics, and absent in healthy donors. I also demonstrated that VC CD8+ T cells inhibit virus replication in both a class I- and II-dependent manner and that in two VC patients the class II-restricted CD8+ T cells with an anti-viral gene signature expressed both CD4+ and CD8+ T cell lineage-specific genes. These data demonstrated that anti-viral memory class II-restricted CD8+ T cells with hybrid CD4+ and CD8+ features are present during natural HIV-1 infection. The presence of these atypical CD8+ T cells during HIV-1 infection redefines what may constitute an effective CD8+ T cell response. Moreover, my findings provide a potentially effective target for CD8+ T cell vaccine strategies given that these cells are readily detectable at a higher frequency in HIV+ patients spontaneously controlling virus replication compared to chronic patients.

The second objective of my dissertation was to bridge the Fab-mediated neutralization and Fc-mediated humoral effector functions associated with natural control of HIV-1 infection by determining whether neutralization breadth was coordinated with the Fc effector function, antibody-dependent cellular phagocytosis (ADCP), in HIV-1 VCs. The Fc domain of antibodies enhances the in vivo neutralization potencies of broadly neutralization antibodies while the Fc effector functions antibody-dependent complement deposition (ADCD) and

antibody-dependent cellular trogocytosis (ADCT) have been associated with the development of neutralization breadth. However, the potential coordination of ADCP, an Fc effector function associated with decreased infection risk and also enriched in HIV-1 VCs, with neutralization breadth and how such a relationship might mediate enhanced virus control remain unclear.

In the second part of my dissertation research, I hypothesized that the development of nAb breadth was coordinated with ADCP breadth in HIV-1 VCs. I also hypothesized that the HIV-1 VC broadly neutralizing antibody (bNAb) polyclonal response targeted both known bNAb epitopes and previously unidentified vulnerable epitopes on the HIV-1 Envelope. By utilizing a novel polyclonal epitope mapping approach, I also hypothesized that the polyclonal antibody responses (neutralizing and non-neutralizing) to natural HIV-1 infection can be mapped by electron microscopy.

I discovered a coordination between the nAb breadth and virion ADCP breadth in a subset of HIV-1 VCs characterized by the targeting of the CD4bs, V3 glycan and MPER known bNAb epitopes on the HIV-1 envelope that potentially act in synergy to mediate the broad nAb and ADCP responses observed in this patient cohort. The HIV-1 VCs with bNAb activity contain a potent class of CD4bs bNAbs that has never been reported in HIV-1 VCs without autoimmunity before, together with a novel gp120-gp41 interface binding antibody class. Thus, these findings not only suggest the presence of potent humoral responses in HIV-1 VCs,

but also suggest a possible role of ADCP in modulating the bNAb response in a low viremia setting.

Taken together, these findings highlight the presence of novel immune responses and multi-compartment associations in a subset of patients mediating natural control of viral infection and hence indicating the need to further investigate and elucidate the mechanistic processes behind these immune responses and relationships. This body of work sheds light on the complex anti-viral immune response in HIV-1 VCs and provides potential novel targets for future HIV vaccine design.

Dedication

To my parents, siblings, mentors, everyone affected by the HIV/AIDS pandemic, and everyone on the frontline in the fight against the HIV/AIDS pandemic.

Contents

Abstract iv

List of Tables xii

List of Figures xiii

Acknowledgements xv

1. Introduction 1

1.1 HIV-1: A Brief History 1

1.2 Virology of HIV-1 3

1.2.1 HIV-1 Genome 3

1.2.2 HIV-1 Virion Structure 5

1.3 HIV-1 Infection 5

1.3.1 HIV-1 Transmission 5

1.3.2 Course of HIV-1 Infection 6

1.3.3 The Immune Response to HIV-1 Infection 7

1.3.3.1 Innate Immune Response to HIV-1 7

1.3.3.2 Cellular Adaptive Immune Response to HIV-1 10

1.3.3.3 Humoral Adaptive Immune Response to HIV-1 20

1.4 Non-Human Primate (NHP) Models 31

1.5 Human Model for HIV-1 Post-Infection Protection 34

1.5.1 Post-Treatment Controllers 35

1.5.2 Spontaneous Controllers 36

1.6 Dissertation Rationale 47

1.6.1 Research Objectives 50

1.6.1.1 Determine the Ontogeny and Functional Properties of HLA class II-restricted CD8+ T cells in HIV-1 VCs 51

1.6.1.2 Determine the Anti-viral Properties of Fab and Fc-mediated Antibody Effector Functions in HIV-1 VCs 52

2. Unconventional HLA class II-restricted CD8+ T cells in HIV-1 VCs 53

2.1 Introduction 53

2.2 Materials and Methods 57

2.3 Results 66

2.4 Discussion 85

3. Coordinated Fab and Fc-effector functions in HIV-1 VCs 94

3.1 Introduction 94

3.2 Materials and Methods 98

3.3 Results 117

3.4 Discussion 149

4. Discussion and Implications 157

4.1 Unconventional HLA class II-restricted CD8+ T cells in HIV-1 VCs 157

4.2 Coordinated Fab and Fc-effector Functions in HIV-1 VCs 165

5. Conclusions 170

Appendix A (Extended Data) 171

Extended Data 1 (related to Figures 1 and 2). HLA DRB1*0701 Gag Tetramer does not bind to HLA mismatched CD8+ T cells. 171

Extended Data 2 (related to Figures 1 and 2). Gag-specific HLA DRB1*0701-restricted CD8+ T cells are present in VC AA at different draw dates. 172

Extended Data 3 (related to Figures 1 and 2). Gag-specific HLA DRB1*0701-restricted CD8+ T cells in VC AA have predominant effector and central memory phenotypes. 173

Extended Data 4 (related to Figures 1 and 2). Gag-specific HLA DRB1*0701-restricted CD8+ T cells are present in VC AD at different draw dates. 174

Extended Data 5 (related to Figures 1 and 2). Gag-specific HLA DRB1*0701-restricted CD8+ T cells in VC AD have predominant effector and central memory phenotypes. 175

Extended Data 6 (related to Figures 3, 4, 5 and 6). Flow Cytometry bulk cell sorting gates for cells from VC AA and VC AD patients. 176

Extended Data 7 (related to Figures 11, 12 and 13). Comparable IgG binding magnitude, binding avidity and breadth against the global HIV-1 V1V2 Env breadth panel. 177

Extended Data 8 (related to Figures 11, 12 and 13). Comparable IgG1 binding magnitude, binding avidity and breadth against the global HIV-1 gp120 and V1V2 Env breadth panels. 178

Extended Data 9 (related to Figures 11, 12 and 13). Comparable to no IgG2 binding magnitude and breadth against the global HIV-1 gp140, gp120 and V1V2 Env breadth panels. 179

Extended Data 10 (related to Figures 11, 12 and 13). Comparable to no IgG3 binding magnitude and breadth against the global HIV-1 gp140, gp120 and V1V2 Env breadth panel in Citrate buffer treated samples for binding avidity measures (A) and PBS treated samples (B). 180

Extended Data 11 (related to Figure 14). Neutralization-guided down-selection of BG505gp140 T332N SOSIP.664 for use in structure-based studies. 181

Extended Data 12 (related to Figures 20 and 21). SEC purified VC AL, VC AP and VC AQ Fab-bound HIV-1 BG505gp140 T332N SOSIP.664 182

References 184

Biography 213

List of Tables

Table 1: Key Literature Highlighting the Presence of nAb and bNAbs in HIV-1 VCs..... 41

Table 2: Literature Highlighting the Presence of Antibody Fc-effector Functions in HIV-1 VCs..... 44

Table 3: HIV-1 Virus Controller (VC) Cohort..... 58

Table 4: HIV-1+ Chronic Patient Cohort. 59

Table 5: Seronegative (Healthy) Donor Cohort..... 59

Table 6: CD8 and CD4+ T cell-specific Genes. 76

Table 7: Genes Associated with CD8+ T Cell-mediated HIV-1 Replication Inhibition. 78

Table 8: T Cell Exhaustion-related Genes..... 79

Table 9: HIV-1 VC Patient Cohort..... 99

Table 10: HIV-1 EC Patient Cohort..... 100

Table 11: HIV-1 Env Pseudotyped Global Virus Panel..... 101

Table 12: Neutralization Fingerprinting (NFP) Virus Panel. 109

Table 13: HIV-1 Env gp120 Breadth Panel..... 127

Table 14: HIV-1 Env gp140 Breadth Panel..... 127

Table 15: HIV-1 Env V1V2 Breadth Panel..... 128

Table 16: HIV-1 VC High Responders Possess VRC01-like CD4bs Antibodies. 137

List of Figures

Figure 1: HLA DRB1-restricted Gag-specific CD8+ T cells in HIV-1 patients. 71

Figure 2: Gag-specific HLA DRB1*0701 restricted CD8+ T cells are present in multiple HIV-1 VC patients at different draw dates. 73

Figure 3: Gag-specific HLA DRB1*0701 restricted CD8+ T cells express both CD4+/CD8+ T cell lineage-specific genes. 75

Figure 4: Gag-specific HLA DRB1*0701 restricted CD8+ T cells have a unique anti-viral gene expression profile. 80

Figure 5: Gag-specific HLA DRB1*0701 restricted CD8+ T cells exhibit a less exhausted expression profile compared to Gag-specific HLA-A*0201 restricted CD8+ T cells. 81

Figure 6: TCR repertoire analysis of Gag-specific HLA DRB1*0701 restricted CD4+ T cells, CD8+ T cells and HLA-A*0201 restricted CD8+ T cells. 83

Figure 7: A subset of HIV-1 VCs develop bNAbs. 119

Figure 8: bNAb development in HIV-1 VCs is associated with infection duration. 120

Figure 9: Heterogenous multi-clade virion ADCP in HIV-1 VCs and ECs. 121

Figure 10: Heterogenous virion ADCP activity correlates with nAb breadth. 123

Figure 11: HIV-1 VCs and ECs cluster into distinct high and low responder groups. 124

Figure 12: IgG, IgG1 and IgG2 binding magnitude and breadth against global HIV-1 Env gp120 and gp140 antigen breadth panels is higher in high responders compared to low responders. 129

Figure 13: IgG and IgG1 binding avidity and breadth against HIV-1 Env gp120 and gp140 antigen breadth panels separates out high from low responders. .. 130

Figure 14: HIV-1 IgG and Fab binding to the trimeric native-like recombinant HIV-1 Env is only observed in the high responder group. 133

Figure 15: HIV-1 VC patients with bNAb activity bind to previously characterized vulnerable epitopes on the HIV-1 Envelope. 136

Figure 16: No dominant CD4bs or MPER epitopes that mediate neutralization by HIV-1 VC plasma. 139

Figure 17: The N332A V3 glycan mutation desensitizes the TRO.11 virus to neutralization by HIV-1 VC BA plasma. 140

Figure 18: CD4bs antibodies in HIV-1 VC AQ. 143

Figure 19: 45-46m2, 3BNC117 and CH235-like CD4bs potent bNAbs in HIV-1 VC AQ. 144

Figure 20: Predominant CD4bs antibodies in HIV-1 VCs with bNAbs. 147

Figure 21: A novel gp120-gp41 interface antibody in HIV-1 VC AL. 148

Acknowledgements

Mentor: Dr. Georgia Tomaras for being a patient and supportive advisor.

Committee members: Dr. Ferrari, Dr. Shinohara, Dr. Li and Dr. Tedder for their continuing support, helpful input and encouragements during my time at Duke.

Lab members: The Tomaras Lab for providing a welcoming and supportive environment, training and guidance for me to grow into an independent scientist; especially Alyse Frisbee, Tamika Payne, Matthew Tay, Derrick Goodman, Judith Lucas, Moses Sekaran, Michael Archibald, Jonathan Li, Lindsay Dahora, LaTonya Williams, Lu Zhang, Rachel Spreng, Sheetal Sawant and Glenn Overman who have provided input crucial to the completion of this thesis.

Collaborators: This thesis would not have been possible without the help, guidance, advice and reagents from collaborators: Moody Lab (Duke) for help with flow cytometry (notably Thad Gurley and Tarra Von Holle), Montefiori Lab (Duke) for help with neutralization assays (notably Celia LaBranche and Amanda Eaton), Haynes Lab (Duke) for help with reagents, Saunders Lab (Duke) for help with generating HIV SOSIP glycoproteins, Acharya Lab (Duke) for help with the negative stain electron microscopy experiments (notably RJ Edwards, Katayoun Mansouri, and Katarzyna Janowska), Yi Lab (Duke) for help with the T cell staining

assays, Hope Lab (Northwestern) for providing fluorescently labeled virus particles, Georgiev Lab (Vanderbilt) for help with the neutralization fingerprinting assay, NIH Tetramer Facility for providing tetramer reagents, NIH AIDS Reagent Program, Duke Human Vaccine Institute Flow Cytometry Core (notably Patrice McDermott), Duke Human Vaccine Institute Viral Genetic Analysis Core for help with RNA sequencing experiments (notably Todd Bradley, Kevin Wiehe, Yue Chen, Bhavna Hora and William Faison), the Duke Human Vaccine Institute Immunology Quality Assessment Core for HIV-1 viral load and CD4 T cell count testing services, and the Duke Center For AIDS Research Clinical Core (notably Stuart Carr and Kent Weinhold).

Funding Sources: Immunology Training Grant, Center for HIV-1/AIDS Vaccine Immunology and Immunogen Discovery (Grant UMI-AI100645), the R01/R56 National Institutes of Health (Grant AI-52779), NIH/NIAID MUC16 Grant (1R01AI125171), NIH/NIAID P01 (1P01A1120756) and Duke Center for AIDS Research (P30 AI 64518)

1. Introduction

Host pathogen interactions are crucial for our understanding of diseases, and how they can be treated or prevented. Thus, the development of effective therapies, vaccines and cures is heavily dependent on enhancing our understanding of the host-pathogen interactions.

The HIV-1/AIDS field has been an intriguing one given how it has been over 35 years since the discovery of HIV-1 as the causative agent of AIDS and yet a vaccine still eludes us. This highlights the complex nature of the host-HIV-1 interaction and why there is a need for more detailed studies and understanding of the virus and how it interacts with the host immune system so as to design more effective strategies of fighting this virus. Findings from this field will also have desirable wider reaching implications such as improving our understanding of basic virology or devising novel immunotherapeutic approaches that can enhance the host's response to various pathogens.

1.1 HIV-1: A Brief History

Two lentiviruses, human immunodeficiency viruses type 1 and 2 (HIV-1 and HIV-2), are the known causative agents of Acquired immunodeficiency syndrome (AIDS). HIV-1 originated from simian immunodeficiency virus (SIVcpz) that naturally infected chimpanzees in Cameroon and later gave rise to HIV-1 group M, which is now known to be the causative agent of the AIDS pandemic [1]. SIVcpz

is believed to have been transmitted from chimpanzees to human through contact with infected chimpanzee blood or meat, and SIV later adapted itself within the new human host to give rise to HIV-1 [1]. This is believed to have taken place around 1920 in Kinshasa, the Democratic Republic of Congo [2]. HIV-2, on the other hand, is believed to come from SIVsmm found in sooty mangabey monkeys rather than chimpanzees, and the cross-over into humans is also believed to have happened in the same manner as HIV-1 [3].

AIDS was reported as a new disease in 1981 that was first discovered in homosexual men and was characterized by unusual opportunistic infections and rare malignancies [4]. HIV-1 was then later identified as the retrovirus responsible AIDS by researchers at the Pasteur Institute in 1983 and was first referred to as Lymphadenopathy-Associated Virus or HTLV-III in 1984 by researchers at the National Cancer Institute [5, 6] . In 1986, a morphologically similar but antigenically distinct virus was identified as the causative agent of AIDS in western Africa, and this new retrovirus was called human immunodeficiency virus type 2 (HIV-2) [1].

HIV-1 is composed of four distinct lineages, referred to as groups M, N, O and P that all resulted from independent cross-species transmission event and have slightly different genetic make-up. The first to be discovered and the one that represents the pandemic form of HIV-1 is group M. Group M also turns out to be the most widely distributed as it is found in every country on the globe [7]. Group O which represents less than 1% of all global HIV-1 infections is mostly restricted to Cameroon, Gabon, and neighboring countries [8]. Group N, identified in 1998,

is even less prevalent than Group O, and is restricted to Cameroon. Group P, identified in 2009, is the most recently discovered and has only been documented in 2 patients from Cameroon[9]. HIV-1 groups N and M are believed to be of chimpanzee origin due to the close relation to SIVcpz*Ptt* from southern Cameroon. HIV-2 on the other hand is mostly restricted to West Africa, and its prevalence rate are on the decline as HIV-1 becomes more dominant in that region [10]. HIV-2 also has lower viral loads compared to HIV-1 which might explain the lower transmission rates of HIV-2 [11] , and HIV-2 infected individuals rarely progress to AIDS [12].

The last common ancestor of HIV-1 group M has been dated back to a period between 1910 and 1930 [13] in Kinshasa, the Democratic Republic of Congo, which is now widely believed to be the source of the AIDS pandemic [14].

HIV-1 group M is further classified into nine subtypes (clades) – A-D, F-H, J, K and more than 40 different circulating recombinant forms (CRF) generated when multiple subtypes infected the same population [15]. Subtypes A and D trace back to central Africa, subtype C predominates in southern Africa, India and other Asian countries, subtype is predominant in Europe and the Americas [16].

1.2 Virology of HIV-1

1.2.1 HIV-1 Genome

HIV is a member of the genus Lentivirus within the family of Retroviridae, subfamily Orthoretrovirinae. The genome of HIV-1 consists of two identical single-

stranded RNA molecules enclosed within the core of the virus particle. HIV-1 proviral DNA is generated by reverse transcription of the viral RNA genome into DNA, degradation of the RNA and integration of the double-stranded HIV-1 DNA into the human genome. Long terminal repeat (LTR) sequences flank the DNA genome on both ends, with a single promoter in the 5' LTR region mediating transcription of viral genes. HIV-1 genes are located in the central region of the proviral DNA and are known to encode at least nine proteins which are divided into three classes: 1). Major structural proteins – Gag, Pol and Env, 2). Regulatory proteins – Tat and Rev, and 3). Accessory proteins – Vpu (virus protein unique), Vpr (virus protein r), Vif (viral infectivity factor) and Nef (negative regulating factor) [17].

In a 5' – 3' direction, the 5' LTR region codes for the promoter for transcription of the viral genes, followed by the *Gag* gene reading frame that encodes outer core membrane proteins (MA, p17), capsid proteins (CA, p24), the nucleocapsid (NC, p7) and a smaller, nucleic acid-stabilizing protein. The *pol* reading frames comes next and it codes for the enzymes protease (PR, p12), reverse transcriptase (RT, p51) and RNase H (p15) or RT plus RNase H (together p66) and integrase (IN, p31). The *env* reading frame is adjacent to the *pol* reading frame and it is the source of the two envelope glycoproteins gp120 (surface protein, SU) and gp41 (transmembrane protein, TM). The regulatory proteins, Tat and Rev, are required for HIV replication initiation, while the accessory proteins are involved in viral replication, virus budding and pathogenesis [18]. It is important

to know the genetic make-up of HIV-1 as it helps us understand how the virus and its host cells interact, thus provide us with targets for therapeutic interventions and host immune responses.

1.2.2 HIV-1 Virion Structure

A mature HIV-1 particle is about 100nm in diameter and is covered by a lipid bilayer membrane envelope. The envelope has 72 knobs composed of trimers of gp120 surface protein anchored to the membrane by the trimers of the transmembrane protein gp41 [19]. The viral envelope encloses a layer called the matrix that surrounds the core of the virus which is held in the capsid. The capsid, a cone-shaped structure, contains RT and IN (both essential for HIV replication), and also houses the two identical single-stranded RNA molecules. The HIV-1 lipid bilayer membrane envelope gp120 and gp41 glycoproteins represent some of the major targets of the anti-HIV-1 humoral response and vaccine development [20].

1.3 HIV-1 Infection

1.3.1 HIV-1 Transmission

There are about 37 million people living with HIV/AIDS as of 2018, with an estimated 1.7 million new infections reported in 2018 [21]. In the United States, it is estimated that around 1.1 million people are living with HIV while about 38,000

new HIV infections occur each year. The southern states accounted for about 52% of new HIV diagnoses in the United States in 2018 [22].

HIV-1 transmission can occur by sexual contact across mucosal surfaces, maternal-infant exposure, or by percutaneous inoculation. Heterosexual transmission accounts for nearly 70% of HIV-1 infections worldwide, while the remainder is attributed to men who have sex with men (MSM), maternal-infant infection, and injection drug use [23]. Some of the factors that can modulate HIV-1 transmission include sexually transmitted diseases (STDs) [24] and pregnancy [25], which both can increase the HIV-1 acquisition risk, while circumcision has been shown to decrease transmission acquisition in males by about 60% [26]. Other factors that influence transmission include HIV-1 disease stage (risk of infection transmission higher from people with acute infection compared to middle or late infection) [27] and viral load, where viral loads less than 1000 copies/mL rarely result in transmission [28]. Socioeconomic factors have been shown to indirectly influence HIV-1 transmission, with transmission rates higher in low-income countries compared to high-income countries [29].

1.3.2 Course of HIV-1 Infection

The course of HIV-1 infection is usually patient-dependent, but there is a general sequence of events. Primary HIV-1 infection is associated with an acute mononucleosis-like clinical syndrome (3-6 weeks following infection) usually present in about 70% of infection cases [30]. Primary infection is usually followed

by the development of humoral and cellular immune responses to HIV-1, and then followed by a prolonged clinical latency period that has a median of 10 years and the patient is usually asymptomatic [31]. The end of this period is marked by the appearance of signs and symptoms, the development of clinically apparent disease referred to as AIDS (usually 8 -12 weeks from primary infection), with death usually expected within 2 years [32].

About up to 10^{10} new viral particles are generated per day during the acute phase of infection. It takes about 2-3 weeks for the viral RNA particles to become detectable, peaking up to several million copies/mL of plasma before declining to a steady-state level known as the viral set point which is a strong predictor of HIV-1 disease progression rate.

1.3.3 The Immune Response to HIV-1 Infection

1.3.3.1 Innate Immune Response to HIV-1

Pathogen sensing and innate immune signaling starts in the infected cell through the pathogen recognition receptors (PRRs) such as Toll-like receptors (TLRs) and RIG-I-like receptors that can detect pathogen-associated molecular patterns (PAMPs) in viral products (viral reverse transcriptase products). Sensing of PAMPs triggers a cell-intrinsic innate immune response that results in the production of cell-mediated and soluble antiviral factors that can also recruit and activate innate cells such as dendritic cells, NK cells and macrophages [33]. Thus,

the innate immune response results in triggering cell-intrinsic innate immune defense and innate-immune cell activation

Acute-phase proteins such as serum amyloid A are some of the first detectable innate immune responses during acute infection, and their production can be triggered by pro-inflammatory cytokines such as IL-15, type 1 interferons (IFNs), IL18, TNF, IFNγ, IL10 and CXCL10, whose plasma levels increase with viremia. The increase in cytokines/chemokines early on in infection is known as the cytokine storm. The cytokine storm can promote viral replication and mediate immunopathology, while some cytokines such as IFNs have anti-viral activity (inhibit HIV-1 replication) [34] and IL-15, IL-18 and IFNs can also enhance the innate and adaptive immune responses. Infected CD4+CCR5+ T cells, activated dendritic cells (DCs), monocytes, macrophages, natural killer (NK) cells, NKT cells and HIV-1 specific T cells are believed to be the sources of the acute-phase cytokines and chemokines [35, 36].

The role of DCs during acute HIV-1 infection is not quite clear. There is a rapid decline of circulating DCs during acute infection due to either migration of activated DCs to lymph nodes or activation-induced death of DCs [37]. There is also evidence that HIV-exposed conventional DCs fail to become fully activated as confirmed by low levels of IL-12 during acute HIV-1 infection [38], whereas HIV-exposed plasmacytoid DCs (pDCs) induce differentiation of CD4+ T cells into T_{reg} cells that might dampen the HIV-1-specific immune responses[39]. However, HIV-

1 exposed conventional DCs are also known to prime HIV-1 specific CD4+ and CD8+ T cells, thus promoting the cellular adaptive immune response to HIV-1 [40].

Natural Killer (NK) and Natural Killer T (NKT) cells can directly kill HIV-1 infected cells, and they can also produce anti-viral cytokines and chemokines. HIV-1 exposed NK and NKT cells have been shown to undergo proliferation and enhanced cytolytic activity during acute infection [41], and hence might be involved in the early control of HIV-1 replication. NK cells expressing the activating receptor KIR3DS1 have been shown to expand during acute infection in patients that express HLA-B Bw4 80Ile [42], and this was associated with slower disease progression [43]. Presentation of HIV-derived peptide epitopes by HLA-B57*01, a member of the HLA-B Bw4 80Ile family, to KIR3DS1 has been shown to result in activation of anti-viral NK cells [44].

The innate immune response primes and modulates the adaptive immune response [45], and this can be observed in the HIV-1 infection setting whereby early immune response during early acute infection can shape the course of disease progression and severity. Using an NHP model, significantly accelerated depletion of CD4+ T cells, increased SIV reservoir size and faster progression to AIDS was observed after blocking of the IFN receptor during acute SIV infection [46].

1.3.3.2 Cellular Adaptive Immune Response to HIV-1

Antigen Presentation and T-Cell Biology

Major Histocompatibility Complex (MHC) molecules (human leukocyte antigen, HLA, in humans) capture and present peptides to T cells, and they come in two forms (class I and class II). Class I molecules come in three different forms (HLA-A, -B and -C), while class II molecules come in four different forms (HLA-DR, -DP, -DQ and -Dra). Class II molecules are made up of an alpha- and a beta-chain that form an antigen-binding cleft that is open-ended and hence can accommodate longer peptides (more than 14 amino acids) compared to the class I molecule only composed of an alpha-chain that can only accommodate 8-9 amino acid long peptides [47].T cell receptors (TCRs) are preferentially restricted by either MHC class I or class II molecules with TCR-peptide-MHC recognition leading to T cell activation. The T cell epitope targeting paradigm states that CD4+ and CD8+ T cells recognize peptide antigens in the context of HLA (MHC) class II and class I molecules, respectively [48]

The TCR is responsible for the recognition of the peptide-MHC complex. It is comprised of two chains (alpha and beta), with the alpha chain composed of the TRAV (variable region) and TRAJ (joining region) gene segments, while the beta chain is made up of the TRBV (variable region), TRBD (diversity region) and TRBJ (joining region) gene segments. Humans can have 47 *TRAV* genes and 61 *TRAJ* genes in the alpha chain locus, while the beta chain locus can have 54 *TRBV*, 2 *TRBD* and *TRBJ* genes [49]. There are three complementarity-determining regions

(CDRs – CDR1, CDR2 and CDR3) from each alpha and beta chains of the TCR, and these form the recognition site for the peptide-MHC complex. Given the different combinations of the alpha and beta chain gene segments, it is believed that humans can in theory have up to 10^{15} – 10^{21} potential TCRs (actual repertoire is not this high since the body has an estimated 10^{13} cells [50]) and hence giving rise to a diverse TCR repertoire [51]. TCR diversity has been associated with effective control of viral infections such as HIV-1 infection [52, 53], and TCR repertoire analysis using techniques such as high-throughput sequencing (HTS) are key in deciphering the diversity of the TCR repertoires and their dynamics during immune responses. Given the extreme diversity of TCR repertoires, it is also key to keep in mind the limitations of TCR diversity analysis by HTS which can be influenced by parameters such as sequencing depth, sample sizes, and sample sources which might only represent a small fraction of the immune response [54].

Mature αβ T cells are divided into main lineages that are defined by the mutually exclusive expression of CD4 and CD8 coreceptor molecules. Thymocytes expressing a TCR consisting of an α and β chain (TCRαβ) can commit to either the cytotoxic (CD8+) or T-helper (CD4+) lineage fate during the thymic development stage. Lineage fate is controlled by key transcription factors such as the ThPOK (*Zbtb7b*) for the CD4αβ+ T-helper lineage or the Runt related transcription factor 3 (*Runx3*) for the CD8αβ+ cytolytic T lymphocytes [55]. ThPOK suppresses the cytolytic program in MHC class-II restricted CD4+ T cells, while

Runx3 counteracts ThPOK in MHC class I-restricted CD8+ T cells and hence promotes a cytolytic program.

HLA class I-restricted CD8+ T Cell Adaptive Immunity in HIV-1 Infection

CD8+ T cell antiviral activity has been shown to control viral replication in many chronic, persistent infections such as hepatitis B, hepatitis C, cytomegalovirus, and Epstein-Barr virus [56]. There is also evidence that HIV-specific CD8+ T cell responses can suppress HIV replication in vivo and hence control the rate of disease progression, although this protective effect is not effective in the majority of patients [57]. The HIV-specific CD8+ T cell response has been shown to appear shortly after infection, resulting in a temporal association between an increase in CD8+ T cell responses and a decrease in viral load [58]. The first T cell responses to HIV-1 infection arise as viremia approaches its peak, and the T cell response peaks 1-2 weeks later, as viremia declines [59]. Our group has shown that the broadest CD8+ T cell mediated virus inhibition activity occur at the earliest time points post-infection, and then became more narrowly focused on autologous virus later in infection [60]. CD8+ T cells have been shown to develop abnormally and become dysfunctional as HIV-1 infection progresses, but the early HIV-1 specific CD8+ T cell responses function normally [59], explaining their ability to control early viremia. Thus, the CD8+ T cell mediated immune response is critical for the resolution of acute viremia and exerts significant selective pressure on the virus resulting in fitness defects.

Multiple cohort studies of HIV-1 virus controllers (VCs), patients in whom plasma viremia is controlled to levels that are undetectable, have shown that virus-specific CD8+ T cell responses are a dominant feature of durable immune control [61]. HIV-1-specific T cells in VCs can effectively inhibit HIV-1 replication, unlike the responses observed in HIV-1 progressors [62]. Potent CD8+ T cell antiviral activity is one of the factors believed to mediate VC status [60], and in NHPs CD8+ T cells have also been reported to be the major factor mediating VC status [63]. CD8+ T cells from VCs have been shown to exhibit superior anti-viral capacity as compared to CD8+ T cells from HIV-1+ chronic patients due to their enhanced retention of functional qualities [64] and pro-survival phenotype [65]. Also, early CD8+ T cell depletion studies in SIV infected rhesus macaques that resulted in increased viral load after SIV challenge showed that CD8+ T cells are critical for controlling virus replication in vivo [66, 67].

CD8+ T cells with the ability to control viral replication display different physical, functional, phenotypic, and T-cell receptor (TCR)/epitope attributes, and these are usually effective in association with CD4+ T cell and B cell responses [56]. The physical attributes include the presence of high frequency HIV-1 specific CD8+ T cells at mucosal surfaces where the majority of HIV-1 transmission occurs. Functional attributes include poly-functionality (the ability to secrete multiple anti-viral cytokines), high proliferative capacity, *in-vivo* viral suppression and cytotoxicity abilities. The phenotype of these cells is characterized as either being effector memory or central memory with no exhaustion markers present. TCR

attributes such as high avidity with the peptide-MHC, TCR cross-reactivity allowing recognition of wild type and mutant HIV-1 epitopes, the ability to target conserved epitopes, public TCR, and the ability to target multiple antigens are all associated with potent anti-HIV activity [56].

The evident role of CD8+ T cells in controlling acute infection in humans and the variable reduction of viral load by T cell-based vaccines in macaques [68, 69] paved the way for clinical trials aimed at inducing HIV-1 specific T cell responses. The vaccines used in these clinical trials (HVTN 502, HVTN 503 and HVTN 505) did generate antigen-specific T cell responses but the responses did not result in vaccine efficacy at the population level [70]. Due to the lack of efficacy of traditional CD8+ T cell vaccines that target immune-dominant epitopes, there has now been increased interest in novel approaches targeting sub-dominant but highly conserved regions of the HIV-1 proteome [71, 72]. This approach is proving highly promising, as two separate human trials in the UK and Kenya have resulted in the generation of high frequencies of poly-functional CD8+ T cells with broad HIV-1 inhibition [71, 72]. Another promising novel CD8+ T cell vaccine approach using rhesus CMV vectored SIV vaccine was tested in macaques and resulted in the induction of a novel subset of MHC class II restricted CD8+ T cells and MHC E-restricted CD8+ T cells that were associated with the clearance of highly virulent SIV [73, 74]. These two new approaches have reinvigorated the CD8+ T cell-based vaccine field and suggest that there is hope for the development of a CD8+ T cell-

based vaccine that, either alone or in conjunction with B cell vaccines, will result in protection from HIV.

Unconventional CD8+ T cell responses

HLA class II-restricted CD8+ T cells: Despite the established strict association between class I MHC molecules and CD8+ T cells, there have been a number of reports in mice, rhesus macaques, and humans highlighting the existence of MHC class II restricted CD8+ T cells [73-77]. For most of the mouse studies, the unconventional class II-restricted CD8+ T cells were observed in the context of either bacterial and viral infections in CD4-deficient or MHC class II-deficient mice or in CD4-deficient mice with a transgenic class II-specific TCR [76, 78-80]. These studies indicate that in either CD4-deficient or MHC class II-deficient mice, there is a significant fraction of class II-restricted CD8+ T cells [76, 78-80]. It has also been suggested that these unconventional class II restricted CD8+ T cells might be present in normal B6 mice, but at a very low frequency (39). The presence of class II-restricted CD8+ T cells at high frequencies in CD4-deficient mice is thought to be due to misdirection during positive selection in the thymus whereby some immature thymocytes with TCRs selected by class II molecules later end up in the CD8 lineage due to the absence of CD4 [78, 80]. In MHC class II-deficient mice, it is thought that the absence of negative selection by class II molecules in the thymus results in the production of the class II-restricted CD8+ T cells, which

have been shown to react to class II molecules in a primary mixed lymphocyte reaction [79].

Interest in unconventional MHC class II-restricted CD8+ T cells was further heightened by findings from a NHP study on the protective effects of a rhesus CMV vectored SIV CD8+ T cell based vaccine in rhesus macaques that were challenged by a highly pathogenic SIV strain, SIVmac251 [73, 74]. 50% of the animals that received the CMV/SIV vaccine were completely protected from SIV infection, and these animals were able to clear the highly virulent SIV infection with no establishment of a viral reservoir, which is commonly formed after HIV or SIV infection [74]. Surprisingly, about 63% of the epitopes targeted by the CVM/SIV elicited CD8+ T cells were MHC class II restricted while the remainder were MHC-E restricted. The CMV vector used in this vaccine was designed so that it could suppress any responses to the conventional class I-restricted CD8+ T cells; thus, the protection from SIV observed in the vaccinated animals was primarily due to the presence of MHC class II-restricted and MHC E-restricted CD8+ T cells [74]. This was the first study to show the ability of unconventional CD8+ T cells to contain and clear SIV infection in rhesus macaques. However, the direct role of MHC class II-restricted CD8+ T cells in this protection model has not been tested yet, but there is now interest in investigating the protective role of these cells in an HIV-1 setting in humans.

HLA class II-restricted CD8+ T cells have been previously observed in human transplant recipients who generated allo-reactive CD8+ T cells [77, 81-83],

hence suggesting the possible role of these unconventional cells in allo-recognition. It has been suggested that the highly inflammatory and immunogenic conditions after transplantation might be involved in the misdirected lineage instruction of these class II-restricted CD8+ T cells [81]. Another notable feature of the HLA class II-restricted CD8+ T cells in transplant patients reported above is that they have a dual HLA class I and HLA class II restriction that was shown to be mediated by just one TCR complex, Vα1Vβ13 [77, 83]. HLA class II-restricted CD8+ T cells have also been detected in HIV-1 VCs, a rare subset of HIV-1 patients (<1%) who have the ability to maintain undetectable HIV RNA levels without therapy [75]. The HIV-1-specific class II-restricted CD8+ T cells displayed cytolytic capacity towards infected autologous CD4+ T cells and two different TCRs due to the presence of two variable alpha chains, Vα26 and Vα6. The Vα26Vβ2 TCR is believed to interact with HLA class I molecules during thymic development, while the Vα6Vβ2 TCR is responsible for interaction with HLA class II molecules in the periphery [75]. Given the MHC class II-restricted and MHC E-restricted CD8+ T cell-dependent protection against highly virulent SIV observed in the NHP CMV/SIV vaccine study, the presence of HLA class II-restricted CD8+ T cells during natural HIV-1 infection is an exciting discovery. More work is needed to further characterize the presence of these unconventional CD8+ T cells in different HIV-1 patient cohorts and determine how these cells affect infection status. These cells are present at very low frequencies in humans [75] and in wild type B6 mice [80], and a trigger event such as highly inflammatory conditions or a

vaccine that expands the frequency of these cells in the periphery may be required to induce this population of cells.

HLA-E-restricted CD8+ T cells: HLA-E (MHC-E) molecules are non-classical class I molecules (member of the non-classical Ib family) with limited genetic polymorphism that can also function as antigen presenting molecules to CD8+ T cells as previously reported in CMV [84] and Mycobacterium tuberculosis [85] infection settings. HLA-E mediated presentation of pathogen-derived peptides to CD8+ T cells was also reported in a CMV-vectored SIV vaccine that resulted in the clearance of SIV from 55% of the vaccinated of macaques whereby 35% of the CD8+ T cell response was restricted by Mamu-E (HLA-E version in macaques) [74, 86].

CD4+ T cell Adaptive Immunity in HIV-1 Infection

The T cell response to HIV-1 infection is usually dominated by CD8+ T cells as they mount a stronger response than CD4+ T cells [87]. However, CD4+ T cells are required for maintaining the CD8+ T cell response as demonstrated in a murine model whereby CD4+ T cell depletion results in an impaired CD8+ T cell response [88, 89]. CD4+ T cells are important in the development of durable functional antibody response to T cell-dependent antigens [90, 91], and they have also been shown to have a cytolytic effector function that correlates with slower disease progression [92].

The CD4+ T cell response peaks early during infection, but these cells are lost as the infection progresses [93]. Interestingly, there is evidence for a correlation between the strength of the CD4+ T cell response and slow disease progression, both in HIV-1 [94] and HIV-2 [95] infection. IL-21 producing CD4+ T cells have been shown to be crucial for maintaining a strong CD8+ T cell response in a chronic infection setting [96-98].

CD4+ T cells are capable of targeting most viral proteins, but there is preferential targeting of the Gag and Nef epitopes [99]. Unlike the conventional HLA class I presented peptides, HLA class II presented peptides tend to have rare to absent escape mutations that favor viral escape from the CD4+ T cell response [100]. There are also some studies that have shown an association between the expression of certain HLA class II alleles and the control of HIV-1 infection [101, 102], thus indicating a potential crucial role of the CD4+ T cell response in mediating virus control.

Mature CD4+ T cells are known to be plastic nature since there is evidence of antigen-stimulated CD4+ T cells undergoing transcriptional reprogramming characterized by the termination of ThPOK expression and gaining a cytolytic effector program and hence giving rise to cytolytic CD4+ T cells [103, 104]. HIV-1-specific cytolytic CD4+ T cells with similar features with HIV-1-specific cytolytic CD8+ T cells (reduce virus replication in virus-infected cells) have been shown to emerge early during acute HIV-1 infection [105].

An NHP study showed an association between longer survival and vaccine-induced SIV specific CD4+ T cell responses in rhesus macaques [106], while polyfunctional CD4+ T cells (CD40L, IL-2, IL-4, INFγ and TNFα) in response to HIV-1 *Env* stimulation were associated with decreased risk of HIV-1 acquisition in the HIV-1 RV144 Trial that showed a 31.2% decrease in HIV-1 acquisition risk 3 years post vaccination [107]. The idea of targeting the CD4+ T cell response has raised concerns of potentially further enhancing infection and disease progression by providing more activated target CD4+ T cells for the virus, but this phenomena seems to be only observed in the absence of a concomitant CD8+ T cell response [108].

1.3.3.3 Humoral Adaptive Immune Response to HIV-1

B Cell and Antibody Development

B cell development begins in the bone marrow where a pro-B cell develops into an immature B cell that expresses an immature B cell receptor (BCR) and IgM. Immature B cells transition into transitional B cells in the spleen where they then develop into mature B cells. Foreign antigen exposure results in activation of mature B cells and entry into the germinal center reactions that give rise to isotype-switched memory B cells and antibody-secreting plasma cells [109]. One B cell encodes a single antibody with a defined specificity, with the an individual estimated to make at least 10^8 different antibody specificities [110]

Antibodies are glycosylated protein molecules that can either be found on the surface of B cells or can be secreted into the extracellular space. A single antibody molecule is made up of two heavy (V_H and C_H) and two light chains (V_L and C_L) linked to each other by disulfide bonds. The identical heavy chains are encoded by the B cell variable heavy (V_H) and constant heavy (C_H) genes, while the identical light chains are encoded by the B cell variable light (V_L) and constant light (C_L) genes [111]. The heavy chain genes are found within a single gene locus (IGH), while the light chain genes are found as two separate gene loci – the lambda (λ) and the kappa (κ) loci. The N-terminus regions of the heavy and light chains make up the variable antigen binding site (Fragment antigen-binding, Fab) that contains the complementarity determining regions (CDRs) which determine antibody specificity. The Fab domain characteristics such as affinity for antigen and epitope specificity influence antibody function efficacy. The constant domains CH_2 and CH_3 of the heavy chain make up the crystallizable fragment, Fc, that mediates effector functions through binding to various forms of Fc receptors (FcRs) and complement [109]**.** Fab domain characteristics such as antigen affinity and epitope specificity, together with the Fc domain characteristics such as heavy-chain isotype, subclass, glycosylation profile and FcRs/complement receptor binding affinities define the activity profile of a given antibody [112].

There are five isotypes of antibodies (IgM, IgD, IgG, IgA and IgE) that are distinguished by their constant heavy chains (C_H) C-terminus regions that can be changed because of class switch recombination (CSR). Infection or immunization

triggers activated naïve B cells to switch from expressing IgM or IgD on their surface to expressing IgG, IgE or IgA. This class switching event changes the antibody effector function and improves its ability to fight off the pathogen that triggered the response[113]. IgG has four subclasses: IgG1 (65%), IgG2 (22%), IgG3 (7%) and IgG4 (4%). Distribution of the serum levels of the antibodies is as follows: IgM – 1.5mg/ml, IgG1 – 9mg/ml, IgG2 – 3mg/ml, IgG3 – 1mg/ml, IgG4 – 0.5mg/ml, IgA – 2.1mg/ml and IgE – $5x10^{-5}$mg/ml [109].

The earliest antibody responses against HIV-1 are gp41-specific IgM antibodies (8 days after first detectable plasma viral RNA) that later give rise to class-switched IgG and IgA antibodies [114]. HIV-1 envelope specific antibodies appear in sequential order, with gp41 (13 days after first detectable plasma viral RNA), gp120 (28 days after first detectable plasma viral RNA), CD4 binding site and membrane proximal external region (MPER) envelope epitopes targeted in that order. The gp41 immunodominant epitope is one of the earliest targeted epitopes by class switched IgG and IgA antibodies. HIV-1 gag epitopes are also targeted by IgG antibodies early on during primary infection, with the p24 and p55 epitopes targeted first (18 days after first detectable plasma viral RNA)and then followed by the p17 epitope (33 days after first detectable plasma viral RNA) [115]. These early antibody responses can form immune complexes (ICs) (with anti-gp41 antibodies predominating in acute infection ICs [116]), but they have been shown to have no neutralization activity. The first neutralizing antibodies are

usually detected around 13 weeks (clade B-infected patients) and 3-8 weeks (clade C-infected patients) post-infection [117].

Broadly Neutralizing Antibodies (bNAbs) in HIV-1 Infection

Given the ability of HIV to mutate and evolve into myriad quasi-species, a major key to controlling HIV-1 infection and disease progression is the induction of broadly neutralizing antibodies (bnAbs) that have the ability to bind diverse strains of cell-free virus and prevent infection of target cells [118]. bNAbs have been shown to have 1 or more of these unusual traits: restricted V_H usage, long heavy chain third complementarity-determining regions (HCDR3), high levels of somatic hypermutations (SHM), and autoreactivity with host non-HIV-1 antigens [119]. These traits likely help the bNAbs overcome the structural barriers present on the HIV-1 *Env* with the long HCDR3 enabling access to vulnerable epitopes shielded by glycans on the *Env* [120], while extensive SHM enables the antibody response to keep up with the constantly evolving virus [121]. These unusual traits also limit the production of such antibodies, and hence bNAbs are only found in a small subset of HIV-1 infected individuals (about 20%) [120]. Some of the known factors that drive bNAb development by providing persistent antigenic stimulation required to drive the extensive hypermutation often seen in bNAbs include high viral load, long infection length and virus (*Env*) diversity [122].

Despite HIV-1 variability, bNAbs target several conserved regions on the HIV-1 envelope (*Env*). The currently known distinct regions that are targeted by

bNAbs include: (1) V1V2 glycan site [123], (2) V3 glycan [123, 124], (3) membrane proximal external region (MPER) [125, 126], (4) CD4 binding site (CD4bs) [127, 128], (5) gp120-gp41 interface [129], (6) the gp41 fusion peptide [130, 131], and (7) silent face[132].

The HIV-1 Env has a glycan shield made of N-glycans attached to N-linked glycosylation sites which is meant to protect vulnerable sites on the *Env*. Even though the shield is generally non-immunogenic, some bNAbs have evolved to mediate neutralization by binding both the glycan and HIV-1 *Env* epitopes [133]. Some of these bNAbs include the bNAbs targeting the high mannose glycans at positions N301 and N332 on the variable loop 3 of the HIV-1 *Env* gp120 (V3) [134], and glycans in the V1V2 domain of the HIV-1 *Env* gp120 [134].

The CD4bs mediates viral entry into the host target cells by binding the CD4 receptor. CD4bs bNAbs represent of the most potent classes of bNAbs and have been of great interest because the CD4bs is functionally conserved (required for infectivity) and is mostly free of glycans that virus uses to mask most vulnerable epitopes [135]. Multiple potent Abs have been mapped to this region with the first described bNAb targeting the CD4bs being b12 bNAb which was first described in 1994 [127]. The second generation of CD4bs bNAbs is represented by VRC01 bNAb which was first reported in 2010 and represented a more potent class of bNAbs that neutralized about 90% of HIV strains compared to the 40% of b12 [128]. Other CD4bs bNAbs have been described that are relevant to my work include 3BNC117 bNAb, CH235 bNAb and 45-46m2 bNAb. 3BNC117, discovered

in 2011, is reported to have greater breadth compared to VRC01 [136] and reduced viremia for several weeks after passive infusion alone or in combination with another bNAb [137]). CH235 bNAb was first reported in 2014 [138] and have shown to neutralize 90% of HIV strains [139]). 45-46m2 bNAb is a more potent clonal variant of VRC01 that has been shown to neutralize about 96% of HIV strains [140]. The CD4bs is also targeted by non-neutralizing antibodies (Abs) which have now been shown to have different molecular contacts on the CD4bs compared to neutralizing Abs [141]. Non-neutralizing Abs also tend to bind more to the open-conformation of Env trimer and not to the closed conformation that is required to engage with the CD4 receptor [142].

The HIV-1 Env has a glycan shield made of N-glycans attached to N-linked glycosylation sites which is meant to protect vulnerable sites on the *Env*. Even though the shield is generally non-immunogenic, some bNAbs have evolved to mediate neutralization by binding both the glycan and HIV-1 *Env* epitopes [133]. Some of these bNAbs include the bNAbs targeting the high mannose glycans at positions N301 and N332 on the variable loop 3 of the HIV-1 *Env* gp120 (V3) [134], and glycans in the V1V2 domain of the HIV-1 *Env* gp120 [134].

The first described MPER bNAbs (2F5 and 4E10) [143] bind to a linear epitope in the *Env* gp41 subunit that is highly conserved across different HIV strains, and this bNAb class possesses great breadth. 10E8 bNAb [125], and DH511 bNAb [126]are also MPER bNAbs shown to possess both great breadth and potency [144].

Epitope Mapping of Polyclonal Antibody Responses

The continual discovery of new bNAb epitopes despite earlier comprehensive efforts and the advent of advanced techniques for epitope mapping suggests that more epitopes targeted by bNAbs remain to be identified. Thus, the use of novel approaches that do not rely on our knowledge of existing epitopes will be crucial in defining additional bNAb targets [145]. This will also help in designing probes that can be used to isolate the antigen-specific antibodies of interest that can be used for therapeutic purposes, and in the design of antigenic reagents that can be used in a vaccination strategy to drive the induction of specific antibodies of interest in vaccinated individuals.

Traditionally, serum neutralization assays and enzyme-linked immunosorbent assays (ELISAs) have been used for epitope mapping of the antibody responses in chronic patients or immunized individuals. Another recent epitope mapping approach is the computational neutralization fingerprinting (NFP) method that is used for predicting the epitope specificities of a polyclonal antibody response to HIV-1. NFP provides an efficient and accurate way of delineating bNAb specificities in polyclonal sera by using a set of reference set of monoclonal bNAb neutralization fingerprints (the potency pattern with which an antibody neutralizes a set of HIV-1 strains) so as to estimate the relative contribution of different types of known antibody specificities to the neutralization by a given polyclonal serum [146]. However, the major limitation of the above approaches is that they are restricted to previously characterized epitopes, and hence they might

not be ideal especially when trying to understand the polyclonal antibody response in unique HIV-1 patient cohorts whose antibody response is not well characterized and might involve targeting of novel and previously uncharacterized epitopes on the HIV-1 envelope. The traditional approaches are also limited to the detection of epitopes targeted by bNAbs, and hence miss out on the characterization targeted by non-bNAbs that might also be contributing to the immune response against HIV-1 [147].

A newly described approach for unbiased epitope mapping of polyclonal antibody responses involves the use of high-resolution microscopic approaches (negative-stain and cryo-electron microscopy) to directly image polyclonal antibodies in complex with the recombinant trimeric HIV-1 *Env* to map the specificities of polyclonal plasma responses [147]. The structure-guided approach is dependent on the use of recombinant, native-like trimeric HIV-1 envelope glycoproteins (SOSIPs) that expose bNAb epitopes while occluding epitopes targeted by non-neutralizing antibodies. Design of SOSIPs involve truncating the hydrophobic gp41 transmembrane region and the membrane-proximal external region (MPER), thus yielding soluble gp140 proteins made up of three gp120 and gp41 ectodomain subunits [148]. In some cases mutations that present known bNAb targets such as the N332 glycan in the HIV-1 *Env* V3 region are introduced, together with stabilizing mutations that result in a stable SOSIP [148] Examples of such SOSIPs include the widely used BG505 SOSIP.664 gp140 trimer that is based on the subtype A transmitted/founder virus, BG505. Negative-stain electron

microscopy (nsEM) has been shown to be capable of detecting different class of antibodies (antibodies targeting different regions on the SOSIP) in sera, and this involves detection of both bNAbs and non-neutralizing antibodies [147, 149]. Cryo-electron microscopy (cryoEM) provides a much more detailed analysis compared to nsEM since it has the capability to provide high resolution information about the targeted epitopes on the SOSIP (HIV-1 Envelope) and also high resolution paratope-epitope information [147]. Thus, structure-guided epitope mapping approaches coupled with the use of high resolution imaging techniques such as nsEM and cryoEM provide a more unbiased way of mapping the polyclonal antibody response (neutralizing and non-neutralizing) in an infection setting, and also provides high resolution insights into the molecular recognition of HIV-1 envelope epitopes by the anti-HIV-1 antibody response.

Antibody Fc-mediated Effector Functions

The antibody Fc domain binds to FcRs, with the widely studied FcRs being the IgG binding receptors known as FcγR that are expressed on most hematopoietic cells and some endothelial cells. FcγRs divided into three groups: FcγRI, FcγRII (A and B), and FcγRIII (A and B). FcγRI, FcγRIIA and FcγRIIIA are activating receptors, while FcγRIIB transduces an inhibitory signal. No signal has been associated with FcγRIIIB. Another type of FcR is the neonatal FcR (FcRn) that is responsible for mediating maternal IgG transcytosis to the neonate and regulating serum IgG levels [150]. Mucins such as MUC16 were recently identified

as another novel form of FcR targeted by IgG, whereby the antibody Fc domain interaction with the mucin (FcR) is also heavily modulated by the glycans in the Fc domain [151] which have been shown to affect antibody function, with the extent of glycosylation depending on antibody isotype [152].

Engagement of the antibody opsonized immune complexes with FcRs bridges the innate and adaptive immune systems that results in various innate immune effector functions. Several of these functions include antibody-dependent cellular cytotoxicity (ADCC), antibody-dependent cellular phagocytosis (ADCP), antibody-dependent complement deposition (ADCD) and antibody-dependent respiratory burst (ADRB) [153]. Due to the emerging role of antibody effector functions that engage monocytes in HIV-1 infected individuals, I focused on the Fc effector function ADCP.

Antibody-dependent cellular phagocytosis (ADCP)

ADCP is an Fc-mediated effector mechanism by which antibody-opsonized foreign particles or altered self-cells (pathogens, infected cells or their derivatives) bind to and activate FcγRs on a phagocyte (monocyte, neutrophil or macrophage) to induce phagocytosis and internalization of the immune complex. This internalization usually results in the degradation of the internalized target through phagolysosomal degradation [154], though there is also evidence of some pathogens surviving in phagosomes and hence using this process as an immune evasion strategy. Thus, there is need to investigate the fate of the internalized

target since most assays measuring ADCP activity only focus on measuring antigen uptake and not much is known regarding the fate of the internalized antigens [155].

ADCP activity, one of the Fc-effector functions enhanced in RV144 vaccine recipients [156], has been associated with protection as there are studies showing that FcγRIIa polymorphisms, major FcγR for IgG-mediated ADCP [157, 158], correlated with HIV-1 progression [159], while chronic HIV-1 infection is associated with impaired ADCP [160, 161]. ADCP was also recently identified as one of the immune factors associated with for decreased risk for HIV-1 acquisition in HVTN 505 clinical trial participants [162]. More interestingly, ADCP activity is present in patients naturally controlling HIV-1 infection and is directly correlated with IgG, IgG1 and IgG3 antibody subclasses that display strong binding to FcγRs [163]. When profiling ADCP activity across different HIV-1 patient groups, ADCP activity was demonstrated to be higher in naturally controlling patients compared to viremic chronic progressors and healthy donors [163], and FcγRIIa engagement and activation was also shown to be higher in the controller patient group [158, 164]. ADCP is also part of the polyfunctional coordinated Fc effector profile (ADCC, NK cell activation and ADCD) only observed in patients controlling HIV-1 infection [163].

Thus, ADCP might not only contribute to protection from HIV-1 infection but might also be involved in controlling infection and disease severity in already infected individuals. There is already evidence for ADCP working in tandem with

other Fc effector functions, but not much is known about the potential relationship between ADCP and the Fab-mediated neutralization response. Given that ADCP is also involved in modulating the adaptive immune response by facilitating antigen presentation of the degraded internalized targets to lymphocytes, there is a likely potential of ADCP working in tandem with and/or driving the development of the nAb response in an HIV-1 infection setting, thus further bridging the Fc- and Fab-mediated effector functions in an HIV-1 infection setting. Other Fc effector functions such as ADCD and ADCT have recently been associated with driving bNAb development by enhancing antigen delivery to germinal centers (GCs) and promoting antigen presentation by follicular dendritic cells (DCs) to B cells [165, 166], thus providing evidence for the potential role of Fc effector functions in shaping the adaptive immune response. Shifting focus to ADCP and elucidating its potential relationship with the bNAb response will not only further support the role of a coordinated neutralizing and non-neutralizing antibody response to HIV-1 infection, but also help further enhance our understanding of the link between the antibody Fc domain and bNAb development.

1.4 Non-Human Primate (NHP) Models

Macaques have been the most widely used NHP pre-clinical model for HIV/AIDS research mostly because of their relevance and also because of their greater availability [167]. Some of the advantages of using NHP models in HIV/AIDS research include the ability to control for parameters that might be

difficult to assess in humans, the ability for extensive analysis of cells and tissues, and also the ability to perform proof-of-concept studies that are not allowed in humans [168]. There are also some key similarities between HIV and pathogenic SIV infection in rhesus macaques: (1) viremic kinetics with acute peak and post-peak decline, (2) presence of cases that can naturally control infection characterized by low viral loads and enrichment of ‘protective HLA (MHC) alleles, (3) emergence of robust early innate and adaptive immune response to the virus whose magnitude and quality decline with time, (4) chronic progression to AIDS (simian AIDS) associated with opportunistic infections, (5) presence of key events such as chronic immune activation, mucosal immune dysfunction, microbial translocation, and high infection rate of central memory CD4+ T cells, and (6) ART suppression of virus replication plus presence of a persistent latent HIV/SIV reservoir [168].

Some of the major successful/impactful findings from the NHP models include understanding of the early events of virus transmission and dissemination, disease pathogenesis, roles of the host immune response, and preclinical testing of vaccine candidates and ART/PrEP strategies [168].

However, there are some fundamental differences in the infectious agents used (SIV/SHIV vs HIV) and also the nature of the immune response (host genetics/polymorphisms) that can act as barriers in translating NHP findings into humans. SIVmac is more virulent than HIV and hence achieves a 10-100-fold higher viral set point, while progression to AIDS also tends to be faster in

macaques compared to humans [169]. In an effort to compensate for the differences in the biology of SIV and HIV, chimeric HIV-SIV viruses (SHIVs) made up of an SIV backbone genome containing an inserted HIV-1 *Env* gene are now being used [170].

FcR polymorphisms and IgG subclasses [171] are known to alter the IgG-FcR interaction, and can also alter the balance of activation and inhibition signals in response to HIV-1 infection [158, 172]. Some of the IgG subclasses differences between humans and NHPs include: (1) no analog of the human IgG3 with an elongated hinge region in macaques that has been shown to contribute to enhanced ADCP activity [112], (2) the inability of NHP IgG4 to perform Fab arm exchange which has been linked with the decreased effector function of IgG4 in humans by prevent target cross-linking [173], and (3) NHP IgG2 and IgG4 have stronger ADCC activity compared to their human counterparts [174]. NHPs and human also have differences in FcγR expression patterns and allelic variations: (1) NHP neutrophils do not express FcγRIIIb (role not clearly defined in humans), (2) NHPs have more allelic variants of the FcγRIIa compared to just the two (H131 and R131) known in humans, (3) humans express more of the low affinity FcγRIIIa F158 allele (IgG1 and IgG3 binding affinity) resulting in less robust ADCC responses in humans compared to NHPs [175], (4) NHP FcγRIIb has allelic variant (131H) that results in higher affinity binding to IgG2 compared to its human counterpart, and (5) NHP neutrophils have expression levels of FcγRII compared to human neutrophils [174, 175].

These and other known/unknown interspecies differences in IgG subclasses and activity [174, 175], FcR polymorphisms/allelic variations, FcR expression patterns, IgG-FcR interactions that can alter downstream antibody Fc-effector functions and complicate interpretation of some preclinical studies [172]. Thus, a better understanding of some of these differences will help in the efforts of achieving a fluent translation of observations between NHP models such as macaques and humans.

1.5 Human Model for HIV-1 Post-Infection Protection

HIV-1 is different from other vaccine-preventable diseases because of its ability to rapidly invade and hide in host cells and evade detection by the host immune responses, while its ability to rapidly mutate and evolve, and targeting of and destruction of critical host immune system cells makes it challenging for immunotherapeutic approaches. Developing an HIV-1 vaccine has also been hampered by other factors such as the lack of clear correlates of protective immunity, and challenges in accurately translating NHP findings to humans highlighted in section 1.5. Thus, individuals who are infected with HIV but do not progress to AIDS in the absence of ART can provide key insights into the mechanisms by which the immune system can control viral infection [176].

Vaccines are based off the ability of the host to contain and sometimes clear infection, and hence individuals exhibiting spontaneous natural or post-treatment (after interrupting therapy) control HIV-1 infection hold the key to providing the

blueprint for a successful and effective HIV-1 vaccine that can mimic and enhance the natural response to HIV-1 infection [177].

1.5.1 Post-Treatment Controllers

There is a rare clinical phenotype of HIV-1 infection control that is observed in treated HIV-1 infected patients who undergo treatment interruption and are still capable of maintaining very low viral loads post-treatment. This unique patient group is defined as having a viral load of less than 400 copies/mL at least 24 weeks after cessation of therapy [178].

Post-treatment controllers (PTCs) are believed to be distinct from spontaneous HIV-1 controllers, and hence are not capable of achieving control status without prior ART. PTCs, unlike spontaneous HIV-1 controllers, have weaker CD8+ T cell responses, lack enrichment of protective HLA alleles, frequently present with symptomatic acute retroviral syndrome and have pre-ART viral loads comparable to that of non-controllers [179].

Early ART initiation [178], low frequency of HIV infection within naïve and central memory CD4+ T cells [180], and a restricted HIV reservoir [181] are some of the factors that are thought to significantly increases the chances of achieving post-treatment control. While interrupting or stopping therapy is not recommended, these rare post-treatment controllers provide evidence of sustained HIV remission and hence understanding of this phenomenon, especially some of the mechanisms

and predictors of post-treatment control, could further aid vaccine and cure development efforts.

1.5.2 Spontaneous Controllers

Most people with untreated HIV-infection have ongoing viral replication and progressive CD4+ T cell depletion that usually culminates into disease progression to AIDS. However, a rare small group of infected individuals (5-15%) are known remain clinically and/or immunologically stable in the absence of treatment for at least 5 years with low viral loads and normal CD4+ T cell counts [182]. These patients naturally maintain viral replication under control and do not progress to AIDS and are collectively referred to as HIV-1 Controllers. HIV-1 Controllers can be further sub-divided into Virus Controllers (VCs) or Elite Controllers (ECs) based on viral load, and these definitions are not equally defined since there is no universal consensus on the viral load definition and duration of viral load control. For the purposes of this document, HIV-1 Virus Controllers are defined as having a viral load of less than 5,000 copies/mL of plasma and a CDC4+ T cell count of greater 400 cells/µL of blood, while HIV-1 Elite Controllers have a viral load of less than 50 copies/mL of plasma and a CD4+ T cell count of greater 400 cells/µL of blood [183].

The mechanisms for viral containment in HIV-1 Controllers are largely unknown, and hence there is no clear correlate or determinant of virus control. Several studies have highlighted multiple host and virus factors that are thought to

be behind the virus control phenotype, even though the precise mechanisms or combinations of mechanisms remain still unknown [182]. Infection by attenuated/defective viruses has been thought to be one of the factors that leads to HIV-1 infection control [184, 185], but this seems to be patient dependent since there is also evidence of normal, replication-competent viruses in HIV-1 controllers [186].

Host genetic factors have also been attributed to the HIV-1 controller phenotype. Specific HLA allotypes have been associated with differential rates of HIV-1 disease progression, with mainly HLA class I allele linked with virus control [187]. HLA-B5701 and HLA-B27 have been found to be enriched in North American and European cohorts of HIV-1 controllers [188, 189], while the HLA-B5703 allele (the prevalent B57 subtype in Africans) is enriched in the African cohorts of HIV-1 controllers [190]. The role of the B57 allele in virus control is not clearly defined, however some observations that might explain the controller phenotype include: evidence showing that B5701-selected escape mutations are not associated with viral rebound [188], B5701 positive patients that lack clear evidence of T cell escape mutations [191], the direct interaction between the B5701 molecule with certain killer immunoglobulin-like receptors (KIR3DL1) involved in anti-HIV-1 innate immunity [192], and the strong linkage of the B5701 allele with the *HCP5* gene strongly associated with HIV-1 control [193]. Despite the association of these HLA class I alleles with virus control, not all HIV-1 Controllers possess these so-called ‘protective HLA alleles [194]’ while disease

progression is also observed in some patients with ‘protective HLA alleles [52, 195]. This suggests that specific HLA-B alleles are neither a necessary nor a sufficient genetic co-factor for HIV-1 control, and also highlights the genetic variability within this unique patient cohort.

Even though the role of the innate immune response is not widely appreciated in an HIV-1 infection setting, some unique properties of the innate immune system have been identified in HIV-1 controllers. HIV-1 Controller myeloid dendritic cells (mDCs) have been shown to have an enhanced ability to generate potent effector cell responses against HIV-1 without enhancing the overall levels of immune activation [196]. Plasmacytoid DCs with anti-viral properties (secretion of high levels of IFNα) are enriched in HIV-1 controllers compared to viremic chronic progressors [197]. Another interesting observation in HIV-1 controllers is the upregulation of an innate T cell subset, γδ T cells. γδ T cell levels usually decrease with disease progression, but HIV-1 controllers have been shown to maintain higher than normal levels of γδ T cells. However, their role in HIV-1 infection control is still not clear [198].

The CD8+ T cell response is believed to be the backbone of the anti-viral immune activity in HIV-1 controllers. CD8+ T cells from HIV-1 controllers have been shown to have superior ability to inhibit HIV-1 replication in *ex-vivo*-infected autologous CD4+ T cells. This enhanced anti-viral efficacy is thought to be partly mediated by factors such as the ability of protective HLA class I alleles to present a broad number of HIV peptides for T cell recognition, the ability to generate high

magnitude CD8+ T cell responses, and the ability to preferentially target highly conserved proteins [199]. HIV-1 specific CD8+ T cells have also been shown to have a superior proliferative capacity upon encounter with HIV antigens [200], enhanced ability to produce the cytolytic protein perforin [200], and the ability to produce multiple anti-viral cytokines [201]. Despite the enrichment of polyfunctional and anti-viral CD8+ T cells in HIV-1 controllers, it is also still not clear whether these cells are sufficient or even required for HIV-1 control since there are many HIV-1 controllers that lack these potent HIV-1 specific CD8+ T cell responses. This again highlights the immune heterogeneity present in this unique patient cohort, and also suggest the broader involvement of other host and/or virus factors in mediating HIV-1 infection control.

The involvement of the humoral antibody response in mediating HIV-1 infection control is still not clear, with most studies arguing against the role humoral immunity in viral control [182]. Several studies have shown that HIV-1 controllers have lower frequencies of neutralizing antibodies compared to viremic progressors [202], which is also supported by the observation that neutralizing antibodies are more readily detected in patients with high viral loads. However, there is evidence that a small group of HIV-1 controllers can develop bNAbs [203, 204], and there are also a few recent studies that are supporting the potential involvement of not only neutralizing, but also non-neutralizing antibodies in mediating HIV-1 infection control [163, 203]. Some of the more recent literature highlighting the presence of

nAbs (Table 1) and non-neutralizing antibody Fc-effector functions (Table 2) in HIV-1 VCs are summarized in the tables below.

Table 1: Key Literature Highlighting the Presence of nAb and bNAbs in HIV-1 VCs

GROUP	KEY FINDINGS
Xu Yu [205] (2020) – USA (Boston) Patient Cohort	1). Distinct transcriptional profile pattern of mDCs, CD4+ T cells, and monocytes, coupled with a higher antigen presenting cell function of mDCs (T cell co-stimulation, improved B cell receptor signaling, activation of cytokine signaling) to induce Tfh cells in vitro and facilitates bNAb development in HIV-1 VCs. 2). Slightly increased viral antigen exposure leads to higher levels of immune activation of monocytes, B cells, CD4 T cells and mDCs, and may facilitate evolution of nAb breadth
Ronald Desrosiers [206] (2019) – USA (Miami) Cohort	1). An autologous HIV-1 isolate from an HIV-1 EC had a usually long V1 domain (49 amino acids – top 1% of length of Env sequences in LANL HIV Database) with two additional N-glycosylation sites and a pair of cysteines 2). These unusual features did not affect viral infectivity and replication capacity 3). Potential role of the unusual V1 region in shielding virus from V3-glycan targeting antibodies
Philip Berman [207] (2019) – USA (San Francisco) Cohort	1). Proviral HIV-1 Env sequences from an HIV-1 EC had low genetic diversity 2). The Env sequences had an elongated V1 region (37 – 39 amino acids) and two extra cysteines 3). The V1 unusual features (extra pair of cysteines, extra glycosylation site and longer V1) did not affect binding or sensitivity to neutralization by PG9, PG16, PGT121, PGT128, PGT130, 35022 or 4E10 bNAbs
Jose Alcami [208] (2018) – Spanish Patient Cohort	1). Preferential targeting of the viral envelope V3-glycan region in HIV-1 Controllers (11 of 12 HIV-1 VCs with bNAb activity targeted the V3-glycan epitope) – no VRC01-like bNAb activity was detected (ELISA and NFP approach) 2). Slightly higher bNAb frequencies in VCs compared to ECs

Michel Nussenzweig [203] (2017) – USA (Boston/ New York) Cohort	1). bNAb sensitive strains of HIV-1 co-exist with potent neutralizing Abs – a combination of bNAbs (recognition of non-overlapping epitopes) resulted in sustained control of viremia in mice (YU2 virus for 3 weeks) 2). Preferential targeting of the viral envelope V3-glycan region in HIV-1 Controllers
Xu Yu [209] (2017 – USA (Boston) Patient Cohort	1). nAb breadth associated with the enrichment of CXCR3+PD-1^{Lo} Tfh-like cells that are preferentially induced in vitro by functionally superior DCs from HIV-1 VCs 2). CXCR3+PD-1^{Lo} Tfh-like cells are efficiently primed by myeloid DCs from HIV-1 VCs
Galit Alter [210] (2017) – USA (Boston) Patient Cohort	1). Unique inflammatory signature (CXCL13, sCD40L, IP10, RANTES and TNFα) observed in plasma from HIV-1 VCs who developed bNAbs 2). Low antigenic diversity, antigen persistence and a unique inflammatory profile may be linked to the development of nAb breadth
Vincent Vieillard [211] (2017) – France (Paris) Patient Cohort	1). The presence of W614A-3S (3S gp41 Env motif) nAbs was associated with lower viral loads (at least one log difference with LTNPs without the 3S nAbs) and higher CD4+ T cell counts and IFNγ producing CD4s 2). nAb response increased over a 5-year period (antibody durability)

Barton Haynes [212] (2014) – USA Patient	1). A CD4bs bNAb (CH98) isolated from an HIV-1 VC individual with lupus that neutralized 62.8% of HIV-1 viruses in a panel of Tier 1 and 2 viruses, and behaves more like CH103 compared to VRC01 in how it binds to the CD4bs
Michel Nussenzweig [204] (2009) – USA (New York) Patient Cohort	1). 50 independent clones expressing high affinity nAbs targeting the gp120 variable loop (gp120I420R) – 27%, CD4bs (D368R) – 9%, co-receptor binding site, and a new neutralizing epitope in the same region of gp120 as the CD4bs isolated from HIV-1 VCs
Jean-Francois Delfraissy [213] (2009) – France (Paris) Cohort	1). Magnitude and breadth of nAbs were heterogenous in HIV-1 VCs, but lower than in chronic viremic individuals 2). No correlation between humoral responses and CD8+ T cell responses 3). No clear correlate of immunity in controllers
Lucile Musset [214] (2009) – France (Paris) Cohort	1). Anti-cardiolipin antibodies associated with the level of 2F5-like and MPER peptide-targeting antibodies in HIV-1 Long-term Nonprogressors
Francis Barin [215] (2006) – France	1). 2G12-like, 2F5-like and 4E10-like Abs enriched in HIV-1 Long-term Nonprogressors with nAb breadth

(Paris) Patient Cohort	

Table 2: Literature Highlighting the Presence of Antibody Fc-effector Functions in HIV-1 VCs

GROUP	KEY FINDINGS
Galit Alter [165] (2018) – USA (Boston) Patient Cohort	1). ADCP, together with the presence of sialylated glycans in the Fc domain are among some of the factors that can separate out neutralizers from non-neutralizer HIV-1 VCs 2). The potential role of Fc domain sialylation on antigen deposition in GCs and B cell maturation that might drive the evolution of high affinity-matured bNAb responses
Ivan Stratov [216] (2017) – Australia (Melbourne) Cohort	1). HIV-1 ECs have higher levels of Env-specific (gp140) and Vpu epitope-specific Abs capable of binding FcyRIIIa and inducing ADCC
Andres Finzi [217] (2017) – USA (Boston) Patient Cohort	1). Increased expression of NKG2D (this receptor positively influences ADCC) ligands on cells infected with viruses coding for *Nef* from HIV-1 ECs – downregulation of NKG2D ligands by HIV-1 *Nef* from HIV-1 ECs is inefficient

	2). NKG2D ligand expression levels correlated with enhanced susceptibility of HIV-1 infected cells to ADCC
Galit Alter [163] (2016) – USA (Boston) Patient Cohort	1). HIV-1 ECs produce a highly polyfunctional Fc-mediated humoral response (ADCC, ADCD, ADCP and NK cell activation) marked by elevated IgG3/IgG1 levels
Andres Finzi [218] (2016) – USA (Boston) Patient Cohort	1). *Nef* isolates from HIV-1 ECs poorly downregulate CD4 from surface of infected cells and results in increased exposure of CD4i epitopes targeted by ADCC mediating Abs
Margaret Ackerman [219] (2014) – USA (Boston) Cohort	1). HLA status not associated with divergent humoral responses 2). Ab subclass (IgG1) and specificity profiles (gp120 and p24) associated with divergent effector function 3). gp120-specific and p24-specific IgG1 levels correlates with ADCP
Ivan Stratov [220] (2014) – Australia (Melbourne) Cohort	1). Broader and higher magnitude NK cell mediated ADCC in HIV-1 VCs compared to chronic viremic progressors 2). More ADCC cross-reactivity to HIV-1 subtypes B and E Envs compared to A and C 3). Glycosylation of HIV-1 *Env* important for recognition of ADCC epitopes
Stephen Kent [221] (2013) – Australia (Melbourne) Cohort	1). Broader ADCC responses observed in long-term slow-progressors (LTSP) 2). Predominant targeting of Vpu epitopes in the LTSP patients

Galit Alter [158] (2013) – USA (Boston) Cohort	1). Antibodies (Abs) from HIV-1 VCs have superior phagocytic activity compared to abs from viremic individuals 2). Abs from HIV-1 VCs are biased toward interactions with the activating FcγRIIa receptor over interactions with the inhibitory FcγRIIb
Guido Ferrari [222] (2013) – France (Paris) Patient Cohort	1). Higher ADCC Ab titers in HIV-1 VCs compared to non-controllers 2). Higher ADCC titers in B57- controllers compared to B57+ controllers
Jean-Francois Delfraissy [213] (2009) – French Patient Cohort	1). ADCC activity higher in HIV-1 VCs compared to progressors

1.6 Dissertation Rationale

The association of the presence of unconventional CD8+ T cell responses and SIV infection clearance in macaques [73, 74], together with the detection of these cells in HIV-1 VCs [75] has generated interest in these unconventional CD8+ T cell responses and their possible role in an HIV-1 infection setting. The NHP SIV study only showed an association between class II- and E-restricted CD8+ T cells with SIV clearance, but there was no direct investigation of the functional properties of these cells. The use of a reprogrammable CMV vector was responsible for the induction of the class II-restricted CD8+ T cells in the NHP study since the delivery of the same vaccine regimen using a different viral vector (adenovirus) did not result in the induction of these unconventional class II-restricted CD8+ T cells. Thus, it is not known where these cells come from since they do not fit into the classical paradigm of antigen presentation, and also whether natural HIV-1 infection can result in the induction and/or expansion of an already existing pool of class II-restricted CD8+ T cells in humans. It is also not clear whether the class II-restricted CD8+ T cells have anti-viral properties that enable them to mediate suppression of viral replication and killing of infected cells, and how that anti-viral activity compares to that of classical class I-restricted CD8+ T cells. Another outstanding question is whether the induction and/or maintenance of these cells is the same in all HIV-1 infected patient groups or they are enriched in some groups such as HIV-1 VCs that usually possess a strong CD8+ T cell response. Understanding the factors involved in the induction of these cells, their

ontogeny, functional properties and distribution in different patient groups will help highlight whether these cells represent a novel potent CD8+ T cell subset that further improves our understanding of what constitutes an effective immune response to HIV-1 and also help provide a target for vaccine design.

The detection and isolation of bNAbs from patients with very low viral loads such as HIV-1 VCs and ECs has raised questions regarding the factors key for bNAb development especially in a low viral load and low viral diversity setting. Despite a few recent studies (summarized in Table I) highlighting the potential involvement of functionally superior mDCs, enhanced Tfh priming and preserved B cell function in inducing bNAb development in a low viral load and viral diversity environment [205, 209], we still do not have a complete understanding of the factors and processes that induce bNAb development in HIV-1 VCs. The presence of bNAbs in patients naturally controlling virus replication has also raised the question of whether these bNAbs are capable of neutralizing autologous viruses and hence whether they involved in mediating the virus controller status observed in these individuals. Given the possibility of the presence of a more potent bNAb response in HIV-1 VCs, there is a need to investigate whether HIV-1 VC bNAb response is capable of targeting novel, previously uncharacterized vulnerable epitopes on the HIV-1 *Env.* This investigation will highlight any differences between HIV-1 VC and chronic viremic bNAb responses and could also potentially lead to the characterization of a new class of potent bNAbs.

Studies looking at humoral responses in an HIV-1 infection setting have mostly looked at Fab and Fc-effector humoral responses separately. However, there is data highlighting the importance of the antibody Fc domain for enhancing the neutralization in-vivo effect of bNAbs [223, 224], together with recent studies showing how the Fc-effector profile (ADCD and ADCT) can distinguish chronic viremic [166] and HIV-1 VC [165] patients with and without bNAb activity. Another recent finding showed correlations between IgG3 V2-specific bNAbs neutralization potency with ADCP and ADCT [225]. These findings highlight the potential role of the Fc domain/Fc-mediated effector functions in modulating the bNAb response. Thus, there is need to identify other Fc effector functions/profile that are linked with the bNAb response so as to better understand the nature of a potent polyclonal humoral response to natural HIV-1 infection. This will also not only allow us to gain a more complete mechanistic link the Fc effector functions and the nAb response but will also allow us to better identify features that could be used to induce or develop more potent bNAbs.

With ADCP being one of the Fc effector functions enriched in HIV-1 VCs compared to non-controllers (chronic viremics), there is a need to better characterize and understand the ADCP response in HIV-1 VCs and also investigate the association with the nAb response. Accurate assessment of ADCP activity is affected by the limitations of the current experimental set-ups used to measure ADCP activity in HIV-1 VCs (summarized in Table 2). Some of the limitations include the use of monomeric HIV-1 antigens instead of infectious HIV-

1 virions, and the absence of an ADCP assay that uses infected cells. There is a need for novel approaches that will give a more accurate insight into the ability of the antibody response and effector cells to clear infected cells. The use of autologous immune effector cells (monocytes and neutrophils) will also provide a better representation of ADCP activity in vivo since this will also account the FcγR expression pattern (including activating FcγRIIa and inhibitory FcγRIIb) and distribution of different FcγR allelic variants since that also affects ADCP activity. There is also a need to start investigating the breadth of ADCP activity in patients using multi-clade difficult to neutralize (Tier 2) viruses (which is what is done when assessing nAb breadth) that represent common circulating strains. This approach will provide a more accurate assessment of the potency and breadth of patient's ADCP response, and how that could relate with and nAb breadth.

1.6.1 Research Objectives

Utilizing the HIV-1 VC/EC patient cohort as a human model for natural HIV-1 protection, my objectives were to: 1). Determine the ontogeny and functional properties of HLA class II-restricted CD8+ T cells in an HIV-1 infection setting (this work has been published [226], and 2). Investigate the relationship between multi-clade virus ADCP activity and nAb breadth in HIV-1 VCs (Nyanhete *et al*. In prep 2020).

Our long-term goal is to define immune mechanisms of virus control and how they can be induced. This will have broader impact for vaccine design and immunotherapeutic strategies by informing what key immune responses to target.

The experiments, data, and conclusions for each of these goals are covered in Chapters 2 and 3, while the implications of the findings presented in this dissertation will be collectively discussed in Chapter 4.

1.6.1.1 Determine the Ontogeny and Functional Properties of HLA class II-restricted CD8+ T cells in HIV-1 VCs

I hypothesized that unconventional HLA class II-restricted CD8+ T cells were present in HIV-1 VCs. I also hypothesized that HLA class II-restricted CD8+ T cells capable of suppressing viral replication in autologous CD4+ T cells are 'ex-CD4+ T cells' that have CD8-like anti-viral effector functions. RNA-seq and TCR repertoire analysis were used to resolve the ontogeny of HIV-1-specific HLA class II-restricted CD8+ T cells, while anti-viral activity of these cells was measured in a modified CD8+ T cell viral inhibition assay. Flow cytometry was used to measure the frequencies of these cells in different HIV-1 patient cohorts (HIV-1 VCs and Chronic Viremics) and healthy donors. The findings from study aim are highlighted in Chapter 2 and they have been published in a journal (Nature Scientific Reports) [226] that grants authors the right to post accepted manuscripts in appropriate institutional repositories.

1.6.1.2 Determine the Anti-viral Properties of Fab and Fc-mediated Antibody Effector Functions in HIV-1 VCs

The three main hypotheses were:

1) HIV-1 VCs developed nAb breadth coordinated with virion ADCP activity.

2) HIV-1 VC bNAb polyclonal response targeted both known bNAb epitopes and previously unidentified vulnerable HIV-1 *Env* regions.

3) Polyclonal antibody responses to natural HIV-1 infection can be mapped by direct electron microscopy.

The TZMbl neutralization and THP-1 ADCP assays using multi-clade Tier 2 viruses were used to measure nAb and ADCP magnitude and breadth responses. Investigation of binding to known epitopes by the polyclonal antibody response was done using a multiplexed antibody binding assay, biolayer interferometry, neutralization fingerprinting (NFP) assay and the TZMbl neutralization assay using viruses with mutations in known epitopes. Negative-stain electron microscopy of antibody-*Env* trimer complexes was done to map both known and potential novel specificities of the polyclonal antibody response. The findings from this study are highlighted in Chapter 3 and are in a paper “Predominant CD4bs antibodies in HIV-1 VCs with coordinated bNAb and virion ADCP activity” that is ready for submission (Nyanhete *et al*).

2. Unconventional HLA class II-restricted CD8+ T cells in HIV-1 VCs

2.1 Introduction

The hallmark of an effective viral vaccine is to elicit robust, effective and extensive humoral and cellular immune responses against the virus. Within the context of HIV-1, broadly neutralizing antibodies (bNabs) that prevent infectivity, non-neutralizing antibodies with Fc-mediated antiviral activity, and cytotoxic CD8+ T cells that eliminate virus-infected cells have emerged as three major elements that regulate viral clearance [70, 227-231]. Optimism for T cell-based vaccines received a major boost with the report of a non-human primate (NHP) T cell-based vaccine study that resulted in the induction of a novel subset of MHC class II and class E-restricted CD8+ T cells [74, 86]. These novel subsets of CD8+ T cells were associated with complete clearance of SIV in 50% of animals [73, 232]. Surprisingly, the majority of the epitopes targeted by these protective CD8+ T cells were MHC Class II-restricted and the remainder were MHC-E restricted; challenging the conventional MHC-I restricted CD8+ T cell paradigm [74, 233]. These findings were remarkable because natural infection with HIV-1 or SIV usually induces T cell responses that decrease virus replication in acute infection but fail to eradicate the virus [60, 233]. This work highlights a potential role for unconventional MHC class II-restricted CD8+ T cells in controlling viremia. Further analysis of elicitation of these atypical CD8+ T cells in humans by other pathogens

will elucidate whether they are an attractive target for induction by vaccine strategies.

Although rarely reported, the presence of unconventional MHC class II-restricted CD8+ T cells has been reported in mice and human studies [76-83, 234]. CD4-deficient, MHC class II-deficient mice or CD4-deficient mice with a transgenic class II-specific T Cell Receptor (TCR) provide the most evidence for unconventional MHC class II-restricted CD8+ T cells elicited by either bacterial or viral infections in mice [76, 78-80, 234], although there is some evidence for very low frequency unconventional CD8+ T cells in wild-type B6 mice [80]. In humans, HLA class II-restricted CD8+ T cells were previously observed in human transplant recipients who generated allo-reactive CD8+ T cells [77, 81-83], indicating a possible role of these unconventional cells in allo-recognition. It has been suggested that the highly inflammatory and immunogenic conditions following transplantations might be involved in the misdirected lineage instruction of these HLA class II-restricted CD8+ T cells [81]. In the context of viral infection, cytolytic effector memory HIV-1specific class II-restricted CD8+ T cells have also recently been observed in a small subset of HIV-1 virus controller (VC) patients who naturally control viremia in the absence of any form of therapy [75]. However, it is still not clear whether this unique cell population is present in any other cohorts. Given these infrequent observations of HLA class II-restricted CD8+ T cells in humans, it is important to identify other cohorts with these cellular subsets, to elucidate their functional role and investigate the factors responsible for the

induction of these cells. Given their association with HIV-1 clearance in non-human primates, it is especially important to further investigate the functional role of HLA class II-restricted CD8+ T cells in the setting of HIV-1 infection.

HIV-1 VCs represent a rare subset of HIV-1-infected individuals (<1%) that can maintain undetectable HIV-1 RNA levels without therapy [182]. We and others have previously shown that CD8+ T cells from VCs have an enhanced ability to inhibit HIV-1 replication in infected autologous CD4+ T cells through both soluble anti-viral factors and contact dependent, target cell killing [60, 64, 65, 235-238]. We have also shown that this potent VC CD8+ T cell antiviral activity is augmented by enhanced mRNA stability and transcription of antiviral cytokines [237, 238], and also the presence of multifunctional and highly proliferative HIV-1 specific CD4+CD8+ double positive T cells [239]. Thus, the VC patient cohort provides us with a human model of HIV-1 virus replication suppression that we can use to study CD8+ T cell mediated suppression of HIV-1 and also investigate the presence and functional role of HLA class II-restricted CD8+ T cells in HIV-1+ patients.

The aim of this study was to determine the presence of unconventional class II-restricted CD8+ T cells in a southern U.S. HIV-1 virus controller cohort and to define their anti-viral gene expression signature and relationship to the CD4+ T cell lineage. We first determined the frequency, memory phenotype and viral suppressive ability of these HLA class II-restricted CD8+ T cells in different cohorts (seronegative healthy donors, VCs and chronic patients) to understand whether different disease states affected induction/maintenance, frequency and memory

phenotype of these cells. Using ex vivo cells from HIV-1 VCs with a consistent presence of class II-restricted CD8+ T cells at multiple time points during the course of infection, we examined the nature of these rare cells through analysis of their anti-viral gene expression signature, TCR repertoire diversity, and expression of T cell lineage-specific transcription factors representative of ontogeny. These findings define the presence of unconventional anti-viral HIV-1 Gag-specific class II-restricted CD8+ T cells with a distinct transcriptional profile characterized by the expression of both CD4 and CD8-lineage specific genes.

2.2 Materials and Methods

Patient cohorts.

Eleven antiretroviral therapy (ART)-naïve HIV-1-infected virus controllers (Table 3) (maintaining plasma HIV-1 loads of <5,000 RNA copies/ml and CD4+ T cell counts of >400 cells/µl) were enrolled through the Infectious Diseases Clinic at Duke University Medical Center. The specimens utilized in this study were restricted to those patients that met this virus controller definition. Although the precise time of infection for these patients is unknown, the minimum length of infection (ranges from >2 to >14 years) is based on when these patients first reported to the clinic (VC M - 8 years, VC O -3 years, VC V – 3 years, VC X – 2 years, VC AA – 12 years, VC AD – 3 years, VC AF – 14 years, VC AG – 4 years, VC AH – 13 years, VC AJ – 4 years and VC AX – 11 years). Four HIV-1+ chronic patients (Table 4) and five healthy uninfected donors (Table 5) were enrolled through the Center for HIV/AIDS Vaccine Immunology and Immunogen Discovery (CHAVI-ID). All patients were HLA typed using the next generation sequencing typing method. PBMC genomic DNA underwent PCR amplification and cDNA library preparation before allelic-level 3rd generation sequencing typing of full-length HLA genes was performed using the Illumina platform (ProImmune Ltd, Oxford, UK). Nine VCs were evaluated in the Viral Inhibition Assays (VIA) measuring the ability of CD8+ T cells to mediate suppression of multiple HIV-1 virus strains, while seven of the nine VCs from the VIA (based on sample availability) were tested for the contribution of HLA II-restriction in CD8+ T cell-

mediated anti-viral activity. Sample availability and HLA haplotype (DRB1*0701) determined which samples (VCs, chronic viremics and healthy donors) were further characterized with HLA tetramers by flow cytometry. Frequency of class II-restricted CD8+ T cells and their presence at multiple time points in one patient determined which patient samples were evaluated by RNA-seq analysis. The studies were reviewed and approved by the Duke University Medical Center Institutional Review Board, and all participants provided written informed consent. All research was performed in accordance with the Duke University School of Medicine guidelines and regulations.

Table 3: HIV-1 Virus Controller (VC) Cohort.

List of HIV-1 VC patients used in the study. VC AA went onto ART after enrollment into the study, and hence the time points before and after ART enrollment were used when determining the frequency and memory phenotype of class II-restricted CD8+ T cells.

PATIENT	**HLA ALLELE**	**CD4 CELL COUNT (cells/µL)**	**VIRAL LOAD (copies/mL)**	**ART**
VC M	DRB1*0701	719 – 966	1020 – 1035	Naïve
VC O	DRB1*0701	834	1320	Naïve
VC V	DRB1*0701	1269	67	Naïve
VC X	DRB1*0701	565 – 717	601 – 2660	Naïve
VC AA	DRB1*0701	462 – 581	<20 – 547	08/2013
VC AD	DRB1*0701	407 – 524	716 – 1040	Naïve
VC AF	DRB1*0701	729 – 1102	<20 – 47	Naïve
VC AG	DQB1*0501	1420	47	Naïve

VC AH	DRB1*0301	1182 – 1899	<20 – 392	Naïve
VC AJ	DQB1*0501	493	108	Naïve
VC AX	DRB1*0701	1281	<20	Naive

Table 4: HIV-1+ Chronic Patient Cohort.

List of HIV-1+ chronic patients used in the tetramer staining assay.

PATIENT	HLA ALLELE	CD4 CELL COUNT (cells/µL)	VIRAL LOAD	GEOGRAPHIC REGION
425	DRB1*0701	485	17010 – 367500	Malawi
153	DRB1*0701	823	21665 – 58573	USA
830	DRB1*0701	424	16108 – 27075	South Africa
432	DRB1*0701	253	17010	Malawi

Table 5: Seronegative (Healthy) Donor Cohort.

List of healthy donors (seronegatives) used for tetramer staining assays in this study.

PATIENT	HLA ALLELE	GEOGRAPHIC REGION
091	DRB1*0701	USA
242	DRB1*0701	USA
653	DRB1*0701	USA
736	DRB1*0701	USA
918	DRB1*0701	USA

PBMC isolation and storage.

Peripheral blood mononucleated cells (PBMCs) were isolated from whole blood using the Ficoll-Plaque Plus (GE Healthcare) density gradient centrifugation. PBMC were frozen (90% fetal bovine serum [FBS]-10% dimethyl sulfoxide) and stored in liquid nitrogen until analyzed.

Cell culture and cell subset preparation.

Cryopreserved PBMCs were thawed in a 37°C water bath, transferred to prewarmed RPMI 1640 (Gibco/Invitrogen) supplemented with 10% heat-inactivated FBS and 1% penicillin/streptomycin (Invitrogen) and then washed 2 times before they were examined for recovery and viability. 1 million cells per mL were activated by 50 ng/mL anti-CD3 (eBioscience) and 100 ng/mL anti-CD28 antibodies for 7 days in media containing RPMI 1640 supplemented with 20% heat-inactivated FBS, 1% penicillin-streptomycin, and 20 U/ml recombinant human interleukin-2 (IL-2) (PeproTech). For generating effectors and targets for the virus inhibition assay (VIA), activated PBMCs were separated into CD8+ and CD8- subsets after 3 days in culture using a CD8+ T cell isolation kit and CD8+ depletion beads, respectively (Miltenyi Biotech).

MHC class II and MHC Class I tetramers.

HLA DRB1*0701 $Gag_{293-312}$ tetramers (FRDYVDRFYKTLRAEQASQE), HLA DRB1*0701 Human $CLIP_{87-101}$ tetramers (PVSKMRMATPLLMQA), and HLA-

A*02:01 SL9 Gag_{77-85} tetramers conjugated to either PE or BV421 were obtained from the NIH Tetramer Facility (Atlanta, GA). The tetramers were used at a final concentration of 10 µg/ml.

Cell staining and flow cytometry.

On day 7 of cell culture, activated PBMCs were enriched for CD8+ T cells using a CD8+ T cell isolation kit (Miltenyi Biotech) and then examined for viability. $8x10^6$ CD8+T cells were stained with a combination of either 10µg/ml HLA DRB1*0701 $Gag_{293-312}$-PE and 10µg/ml HLA DRB1*0701 $Gag_{293-312}$-BV421 tetramer or 10µg/ml HLA DRB1*0701 Human $CLIP_{87-101}$-PE and 10µg/ml HLA DRB1*0701 Human $CLIP_{87-101}$-BV421 tetramers (NIH Tetramer Facility) for 1hr at room temperature (or 30 minutes at 37°C for the HLA-A*02:01 SL9 Gag_{77-85} tetramers). The cells were then washed once with PBS/2% FBS and then resuspended. The expression of surface molecules was assessed using the following antibodies: CD3-APC-H7 (BD Biosciences), CCR7-BV605 (Biolegend), CD8-FITC (Biolegend), CD56-APC (eBiosciences), CD16-BV711 (BD Biosciences), CD4-AF700 (Biolegend), CD19-PercP-Cy5.5 (BD Biosciences), CD45RA-ECD (Beckman Coulter). The tetramer stained CD8+ T cells were then incubated with the surface marker antibodies for 30 minutes at 4°C in PBS/2% FBS. The cells were washed once with PBS/2% FBS and then stained with Live/Dead Fixable Aqua-Dead Cell Stain (ThermoFisher Scientific, Waltham, MA) for 30 minutes at 4°C in PBS (Invitrogen). The cells were washed once with PBS,

and then once with PBS/2% FBS before being fixed in PBS/2% paraformaldehyde. Samples were acquired and analyzed using the LSRII flow cytometer (BD Biosciences) and analyzed using FlowJo software (Tree Star, Ashland, OR). For RNA-sequencing, BD FACS ARIA II (BD Biosciences) was used to sort tetramer stained PBMCs into 350µL of RLT lysis buffer (Qiagen).

RNA Sequencing.

PBMC-extracted RNA from class II-restricted CD8+ T cells, class I-restricted CD8+ T cells, class II-restricted CD4+ T cells, bulk CD8 and CD4+ T cells from VC AA and VC AD were subjected to reverse transcription and amplification using the Smartseq ultra-low v4 kit (Takara Bio, Mountain View, CA). 200 pg of amplified cDNA was prepared for Illumina sequencing using the Nextera XT library preparation kit (Illumina, San Diego, CA). Libraries were quantified using qPCR (Kapa Biosystems, Wilmington, MA) and sequenced to a minimum depth of 25 million reads per sample (2x75bp reads) on the Illumina NextSeq (NCBI Sequence Read Archive Accession number: PRJNA542922). Raw FASTQ files were merged and then trimmed using the default settings of the cutadapt Python module (http://cutadapt.readthedocs.io/en/stable/index.html). The trimmed reads were aligned to the human genome GRCh38 using STAR [240]. After reference alignment read counts on each gene were quantified by HTSeq [241], significantly differentially expressed transcripts were determined by DESeq2 R package [242], and filtering for adjusted p values of less than 0.05 as seen in Fig 5A. For Fig 5B

through 7, heat maps were generated by comparing the Reads Per Kilobase of transcript per Million mapped reads (RPKM) using lists of known associated genes and calculating the z-scores by row.

Gene Network analysis was done using GeneMania [243] and pathway analysis was performed using Ingenuity Pathway Analysis (QIAGEN Inc., https://www.qiagenbioinformatics.com/products/ingenuity-pathway-analysis). MiXCR, an open source immune repertoire analysis package (https://github.com/milaboratory.mixcr), was used for paired-end read merging and extraction of TCR sequences from bulk RNA-seq data [244]. TCR repertoire analysis was then performed using the open source software tool tcR (https://github.com/imminfo/tcr)[245].

Transmitted/founder virus.

Replication-competent virus stocks from full-length infectious molecular clones (IMCs) expressing transmitted/founder viruses (CH058.c, WITO, WEAU3, CH040 and CH077) and lab-adapted NL4.3 were generated as described [60, 246]. Briefly, proviral DNA was transfected into 293T cells by using Fugene HD (Roche). Working stocks were amplified by passaging virus in human PBMC (American Red Cross). PBMC-derived virus supernatants were collected every 2 to 3 days and filtered through a 0.45µm syringe filter, and titers were determined on TZM-bl cells (obtained through the NIH AIDS Research and Reference Reagent

Program, Division of AIDS, NIAID, NIH, from J C. Kappes, Xiaoyun Wu, and Tranzyme, Inc.)[60].

Viral Inhibition Assay

This assay to measure the ability of CD8+ T cells to suppress HIV-1 replication in infected target CD4+ T cells has been previously described [60]. Briefly, CD4+ enriched target cells were infected with HIV-1 infectious molecular clones (MOI=0.1) via 2-hour spinoculation at 1200 RPM. Following spinoculation, infected target cells were plated at $2.25x10^4$ cells/well and CD8+ effector T cells were added to cultures at varying Effector:Target ratios (0.25:1, 0.5:1, 1:1, 2:1). Co-cultures were incubated at 37°C and 5% CO2 for three days and virus production was measured by TZM-bl assay [60] with a readout of relative light units (RLU).

Blocking assays.

This assay was adapted from the previously described virus inhibition assay [60] to measure the ability of CD8+ T cells to suppress HIV-1infection by MHC Class I and/or Class II recognition of infected target cells. Briefly, CD4+ enriched target cells were infected with HIV-1 infectious molecular clones (MOI=0.1) via 2-hour spinoculation at 1200 RPM. Following spinoculation, infected target cells were plated at $2.25x10^4$ cells/well and incubated for 30 minutes in the presence or absence of monoclonal antibodies targeting MHC Class I (3F10), MHC Class II

(L243), or a negative isotype control (P3x63). Following the incubation, CD8+ effector T cells were added to cultures at varying Effector:Target ratios (0.125:1, 0.25:1, 0.5:1, 1:1). Co-cultures were incubated at 37°C and 5% CO2 for three days and virus production was measured by TZMbl assay [60] with a readout of relative light units (RLU).

Statistical Analyses

Statistical significance of results was determined by the non-parametric Sign test performed using SAS (r) Proprietary Software 9.4 (TS1M2), Copyright (c) 2002-2012 by SAS Institute Inc., Cary, NC, USA, and the graphs were generated using GraphPad Prism 8.

2.3 Results

Primary human CD8+ T cells can inhibit virus replication through both HLA Class I and Class II recognition.

In an effort to investigate the possible functional role of HLA class II-restricted CD8+ T cells in HIV-1 viral control, we chose to look at the nature of the potent anti-HIV-1 CD8+ T cell responses in HIV-1 VCs with broad CD8+ T cell mediated anti-HIV-1 inhibitory activity [60, 235, 237, 238]. VC patients with a viral load below 5,000 copies/mL and a CD4+ T cell count above 400 cells/µL (Table 3) were enrolled for this study. The potency and breadth of CD8+ T cell-mediated virus inhibition was first assessed using a contact-mediated viral inhibition assay (VIA) against a panel of lab-adapted (NL4-3) and full-length subtype B (WITO, WEAU3, CH040.c, CH058.c and CH077) transmitted/founder virus strains [247]. Primary CD8+ T cells isolated from the peripheral blood of the VC patients were tested for HIV-1 inhibition in HLA-matched primary autologous CD4+ enriched T cells. While the magnitude of inhibitory activity varied, all the VCs tested possessed broad CD8+ mediated viral inhibitory activity against the panel of HIV-1 viruses (refer to Figure 1A in [226]). We next tested whether CD8+ T cell mediated HIV-1 antiviral activity was dependent on the concentration of CD8+ T cells. Anti-viral activity increased with increasing effector (CD8+): target (CD4+) ratios with a subtype B T/F virus CH058.c (refer to Figure 1B in [226]). The primary CD8+T cells isolated from seronegative donors lacked antiviral activity (refer to

Figure 1B in [226]). These results confirmed the potent HIV-1 specific antiviral response within the CD8+T cell population of HIV-1 VC patients.

To determine whether HLA class II-restricted CD8+ T cells are part of the anti-HIV-1 cellular repertoire in chronic virus controllers, we interrogated a VC cohort (Table 3) for the presence of HLA class II-restricted CD8+ T cell antiviral activity capable of suppressing T/F virus CH058.c replication in autologous CD4+ T cells. An MHC blocking virus inhibition assay (VIA) was used in which infected primary CD4+ T cells were treated with either 3F10 (anti-MHC class I monoclonal antibody) (refer to Supplementary Figure 1 in [226]) or L243 (anti-MHC class II monoclonal antibody) prior to incubation with autologous primary CD8+ T cells. Infection of CD4+ T cells resulted in a ~15% drop in their viability. Infected CD4+ T cell viability was not affected by the addition of the L243 and 3F10 monoclonal antibodies **(**refer to Supplementary Figure 2A in [226]). We found that HLA class II-restricted CD8+ T cells, capable of suppressing T/F virus CH058.c replication, were present in five out of the seven HIV-1 VC patients tested (refer to Figure 2 in [226]). In addition to HLA class II-restricted antiviral CD8+ T cell activity, all VC subjects possessed HLA class I-restricted antiviral activity, as expected.

To test whether contact was required for the MHC blocking activity, the targets and effector cells from VC AH were separated in a trans-well MHC blocking VIA (refer to Supplementary Figure 2B in [226]). Class II-blocking was abrogated, consistent with a contact dependent mechanism (refer to Supplementary Figure 2B in [226]). These data indicated that human HIV-1 VC subjects possessed HIV-

1 specific HLA class II-restricted specific CD8+ T cells capable of suppressing HIV-1 replication in autologous CD4+ T cells.

Detectable low frequency of memory HLA DRB1*0701 restricted $Gag_{293-312}$–specific CD8+ T cells in HIV-1 VC patients

I next sought to determine the frequency and memory phenotype of the HLA class II-restricted CD8+ T cells in HIV-1 VCs (Table 3) and also in chronic patients (Table 4) and seronegative healthy donors (Table 5).

We, and others, have previously shown that VCs and chronically infected HIV-1 donors (chronic patients) with anti-viral CD8+ activity contain predominantly Gag-specific effector CD8+ T cells [98, 237, 248-253]. Within the HIV-1 Gag-p24 region is the immune-dominant, HLA class II-restricted epitope spanning from amino acid position 293-312, $Gag_{293-312}$, that is targeted in more than 90% of HIV-1 VCs and treated patients [254]. Thus, given the importance of Gag-specific antiviral activity, I utilized the available DRB1*0701 $Gag_{293-312}$ -specific class II tetramer in those patients who were HLA DRB1*0701 positive to assess the prevalence of Gag-specific class II-restricted CD8+ T cells in HIV-1 infected subjects. Tetramer staining specificity was first confirmed using HLA DRB1*0701 mismatched patients (Extended Data 1).

In this VC cohort, four of the seven VC patients tested in the MHC blocking experiment (VC V, VC AA, VC AD and VC AF) HLA matched the available HLA class II $Gag_{293-312}$ tetramer (DRB1*0701), and of these four patients only two (VC

AA and VC AD) demonstrated blockable HLA class II-restricted CD8+ T cell activity (refer to Figure 2 in [226]). Two VCs (VC M and VC X) that had demonstrated CD8+ T cell-mediated antiviral activity against a panel of viruses (refer to Figure 1A in [226]) and one additional VC within the cohort (VC AX) that had not been previously screened for CD8+ T cell mediated antiviral activity were also DRB1*0701 tetramer matched and thus included in the tetramer analysis (Table 3). The seven DRB1*0701 tetramer matched VC patients (VC M, VC V, VC X, VC AA, VC AD, VC AF and VC AX) had PBMC samples from at least 2 time-points, while the available chronic viremics and seronegative donors had PBMC samples from only one time-point due to limited sample availability.

Since memory HIV-1-specific CD8+ T cells are known to be important for controlling viral replication [56, 255], I examined the frequency and memory phenotype of HLA DRB1-restricted CD8+ T cells. CCR7+ CD45RA+ cells define naïve T cells, CCR7+CD45RA- define a central memory phenotype, CCR7-CD45RA+ define a terminally differentiated effector memory phenotype, and CCR7-CD45RA- cells define an effector memory phenotype [256]. To increase specificity of the class II staining, I utilized a dual staining approach (Figure 1A) with different fluorophores for HIV-1 Gag and negative control tetramer presenting the invariant peptide, CLIP [257].

Using tetramer staining of cryopreserved PBMCs, the five available HIV-1 seronegative donors did not have detectable HLA DRB1-restricted $Gag_{293-312}$–specific CD8+ T cells (Figures 1B & 2). Two of the four available HIV-1+ chronic

patients had a very low frequency of HLA DRB1-restricted $Gag_{293-312}$–specific CD8+ T cells while the remaining two patients did not have any detectable HLA DRB1-restricted $Gag_{293-312}$–specific CD8+ T cells (Figures 1C and 2). The HLA DRB1-restricted $Gag_{293-312}$–specific CD8+ T cells in the chronic patients were predominantly effector memory cells, 62.5% of the HLA class II-restricted CD8+ T cells for patient 425 and 93.3% for patient 830 (Figure 1D). Of the seven VC patients tested, only two, VC AA and VC AD, had consistent detectable HLA DRB1-restricted $Gag_{293-312}$-specific CD8+ T cells across multiple visit dates during the course of their infection (Figures 1E and 2, Extended Data 2 and Extended Data 4). These HLA DRB1-restricted $Gag_{293-312}$–specific CD8+ T cells were predominantly central memory (CM) and effector memory (EM) phenotypes (VCAA = CM: 15.3-40.5%, EM: 43.6-67.2%) (VCAD = CM: 34.3-43.9%, EM: 22-44.4%) (Figure 1F, Extended Data 3 and Extended Data 5). We did not see any correlation between the estimated length of infection and frequency of class II-restricted CD8+ T cells or correlation between CD4+ T cell count and frequency of class II-restricted CD8+ T cells. In summary, two natural HIV-1 virus controllers had HLA DRB1-restricted $Gag_{293-312}$–specific central and effector memory CD8+ T cells consistently present at low frequencies (0.0011% - 0.018%).

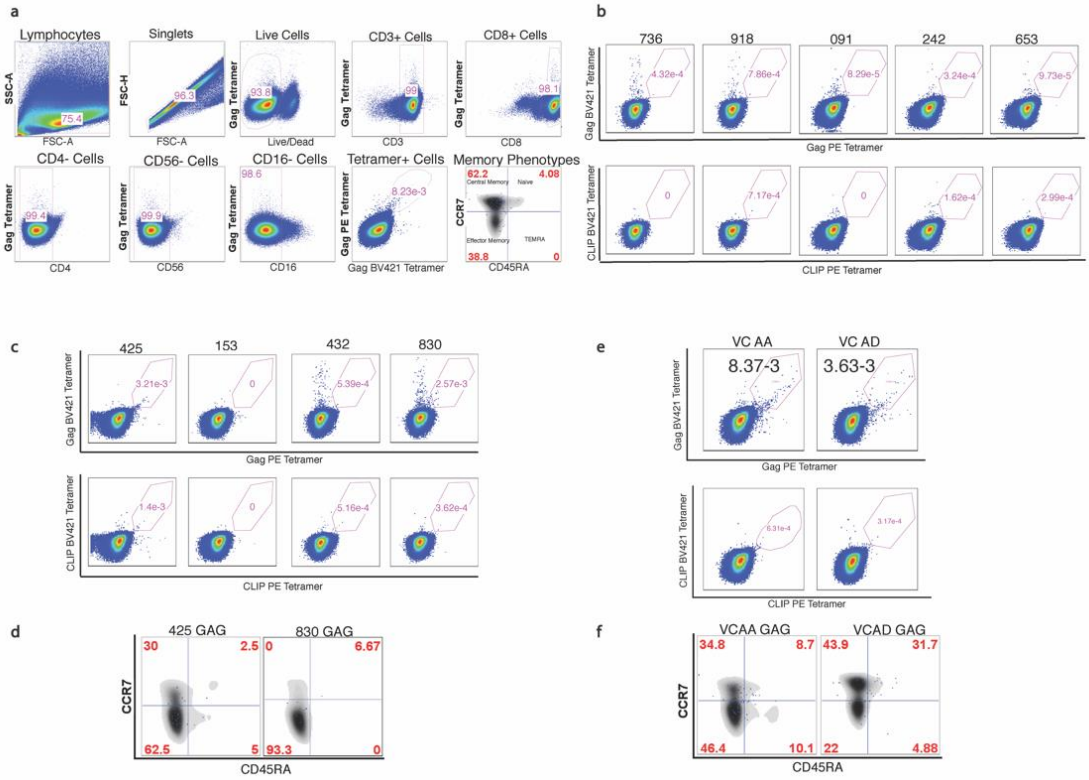

Figure 1: HLA DRB1-restricted Gag-specific CD8+ T cells in HIV-1 patients.

A. Gating strategy for flow cytometry analysis of tetramer-positive HLA DRB1-restricted Gag-specific CD8+ T cells in HIV-1 in our patient cohorts. Cells were first gated for lymphocytes (SSC-A vs. FSC-A) and singlets (FSC-H vs. FSC-A). The single cell lymphocytes were then stained with Live/Dead Aqua stain to isolate the live cells. The live cells were further analyzed for expression of CD3 and CD8 while gating out CD4+ cells, CD56+ and CD16+ cells (Natural Killer cells) so as to narrow down the target population to live, healthy CD8+ T cells (CD3+, CD8+, CD4-, CD56-, CD16-). Gag or CLIP tetramer positive cells were then analyzed from the pure CD8+ T cell fraction by double fluorochrome verification (PE and BV421) to ensure discrimination of true tetramer binding events. Only events that were double positive for the PE and BV421 tetramers were considered to be the tetramer positive events. The memory phenotypes of the tetramer positive events were defined by the surface expression of CCR7 and CD45RA. Naïve tetramer positive events were double positive for CCR7 and CD45RA. Central Memory tetramer positive events were CCR7+ and CD45RA-. Effector Memory tetramer positive events were CCR7- and CD45RA-. Terminally differentiated effector memory (TEMRA) tetramer positive events were CCR7- and CD45RA+ [256]. B. Gag-specific HLA DRB1*0701 restricted CD8+T cells are absent in HLA-matched seronegative healthy individuals. Anti-CD3/CD28 activated PBMCs were enriched for CD8+ T cells by negative selection after seven days in culture and subsequently stained with PE and BV421-labeled $Gag_{293\text{-}312}$ tetramers and analyzed by flow cytometry. The human $CLIP_{87\text{-}101}$ –DRB1

tetramer served as the negative control. Results are presented as a percentage of the CD8+ T cells in the PBMC pool. DRB1-restricted HIV-1 $Gag_{293-312}$ –reactive CD8+ T cells are absent in activated PBMCs from healthy donors. C. Gag-specific HLA DRB1*0701 restricted CD8+T cells are rarely detectable in HLA-matched HIV-1 Chronic patients. Anti-CD3/CD28 activated PBMCs were enriched for CD8+ T cells by negative selection after seven days in culture and subsequently stained with PE and BV421-labeled $Gag_{293-312}$ tetramers and analyzed by flow cytometry. The human $CLIP_{87-101}$ –DRB1 tetramer served as the negative control. Results are presented as a percentage of the CD8+ T cells in the PBMC pool. DRB1-restricted HIV-1 $Gag_{293-312}$ –reactive CD8+ T cells are barely detectable in activated PBMCs from HIV-1+ Chronic patients. D. The majority of DRB1-restricted $Gag_{293-312}$ specific CD8+ T cells reside in the effector memory ($CCR7^{-}CD45RA^{-}$) subsets in PBMC in the HIV-1+ Chronic patients. DRB1-restricted $Gag_{293-312}$ specific CD8+ T cells from chronic patients 425 and 830 (2 chronic patients with barely detectable DRB1-restricted $Gag_{293-312}$ specific CD8+ T cells) were separated into four subsets (Naïve, Central Memory, Effector Memory and Terminally-differentiated Effector Memory) based on CD45RA and CCR7 surface expression levels. E. $Gag_{293-312}$ tetramer detection of $Gag_{293-312}$ -specific HLA-DRB1-restricted CD8+ T cells in VCAA and VCAD. Anti-CD3/CD28 activated PBMCs were enriched for CD8+ T cells by negative selection after seven days in culture and subsequently stained with PE and BV421-labeled $Gag_{293-312}$ tetramers and analyzed by flow cytometry. The human $CLIP_{87-101}$ –DRB1 tetramer served as the negative control. Results are presented as a percentage of the CD8+ T cells in the PBMC pool. DRB1-restricted HIV-1 $Gag_{293-312}$ –reactive CD8+ T cells can be readily detected in activated PBMCs from anHIV-1virus controller individuals. F. The majority of the DRB1-restricted $Gag_{293-312}$ specific CD8+ T cells in VC AA and AD reside in the effector memory ($CCR7^{-}CD45RA^{-}$) and central memory ($CCR7^{+}CD45RA^{-}$) subsets in PBMCs. DRB1-restricted $Gag_{293-312}$ specific CD8+ T cells from VC AA and VC AD were separated into four subsets (Naïve, Central Memory, Effector Memory and Terminally-differentiated Effectors) based on CD45RA and CCR7 surface expression levels. T. Nyanhete designed, performed, analyzed and interpreted the experiment data.

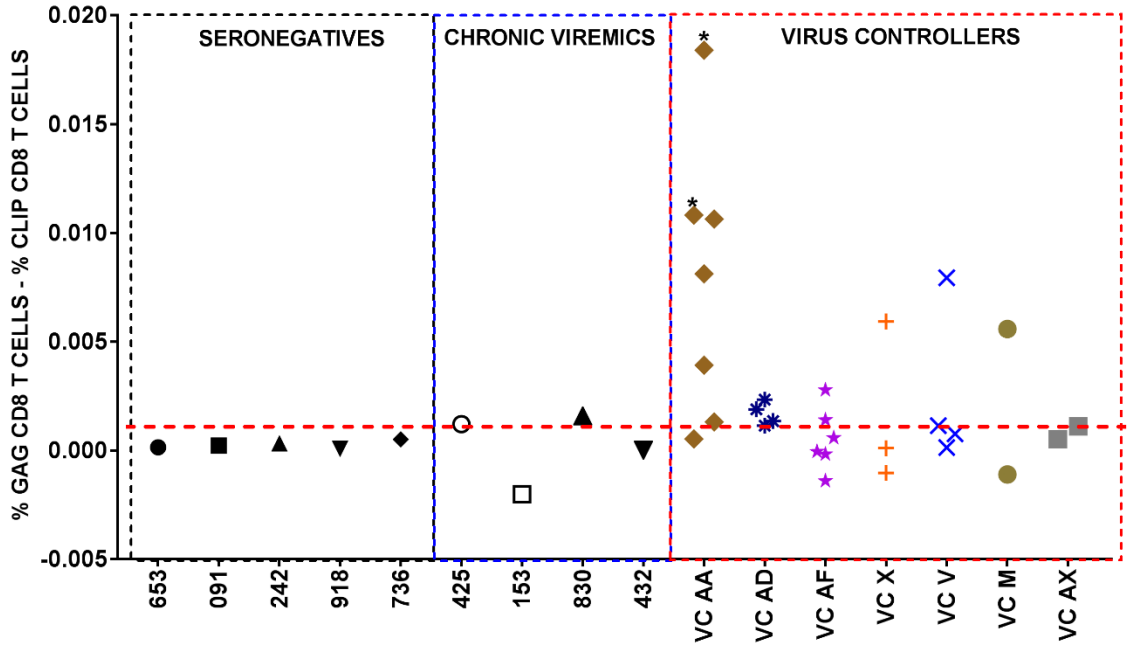

Figure 2: Gag-specific HLA DRB1*0701 restricted CD8+ T cells are present in multiple HIV-1 VC patients at different draw dates.

PBMCs obtained from VC patients at different draw dates were screened for the presence of Gag-specific HLA class II-restricted CD8+ T cells using tetramer staining. The frequency of CLIP+ CD8+ T cells was subtracted from the frequency of Gag+ CD8+ T cells so as to get a positive signal detection of Gag specific CD8+ T cells. The positivity cut-off, shown as the red horizontal line, was set at 0.001% which was double the highest frequency of the HIV-1 seronegative donors. Of the seven VCs we assayed, six had detectable Gag-specific class II-restricted CD8+ T cells on at least one draw date while only VCs AA, AD and AF had detectable class II-restricted CD8+ T cells at more than one draw date. VC AA and VC AD had the most detectable class II-restricted CD8+ T cells on most of the draw dates we tested. Two of the four patients enrolled into the study as chronic patients, had detectable class II-restricted CD8+ T cells. The frequency of the Gag-specific class II-restricted CD8+ T cells observed in the chronic patients was much lower than the frequency observed in the VC patient cohort. Notably, no class II-restricted CD8+ T cell were detected in all our five HLA-matched seronegative donors. Single time points were assayed for the chronic viremics and seronegative donors due to limited longitudinal sample availability. * Two draw dates when the patient VCAA was on ART. T. Nyanhete designed, performed, analyzed and interpreted the experiment data.

HLA DRB1*0701 restricted $Gag_{293-312}$–specific CD8+ T cells are a unique T cell subset that expresses both CD4+ and CD8+ T cell-specific genes

I next asked whether these unconventional HIV-1 class II CD8+ T cells have a unique transcriptional profile compared to conventional class I CD8+ T cells and conventional class II CD4+ T cells. The very low frequency of class II- CD8+ T cells (barely at the limit of quantitation) in two of the four chronic patients tested and their absence in the healthy donors (Figure 2) limited our gene expression analysis to the two VC patients, VCAA and VCAD, that had the highest frequencies and most consistent (across multiple time points) class II- CD8+ T cells. Gag-specific class II-restricted CD4+ T cells, Gag-specific class II-restricted CD8+ T cells and Gag-specific class I-restricted CD8+ T cells were stained, and flow sorted with class I or class II fluorophore-labeled tetramers (Extended Data 6) and RNA-sequencing performed on bulk sorted tetramer positive cell populations. The purity of the sorted CD4 and CD8 T cell subsets ranged from 97.1 – 98.9%.

HLA class II-restricted CD8+ T cells (GagIICD8) in both patients had a unique gene expression profile compared to HLA class I-restricted CD8+ T cells (SL9CD8) and HLA class II-restricted CD4+ T cells (GagIICD4) (Figure 3A). Given the unique gene expression profile of HLA class II-restricted CD8+ T cells, we then evaluated the expression of known human CD4+ and CD8+ specific genes and lineage-specific transcription factors (Table 6), [258-260]). Conventional CD4+ T cells are known to be $Runx3^{Low}ThPOK^{High}$, while conventional CD8+ T cells are known to be $ThPOK^{Low}Runx3^{High}$ [55, 261, 262].

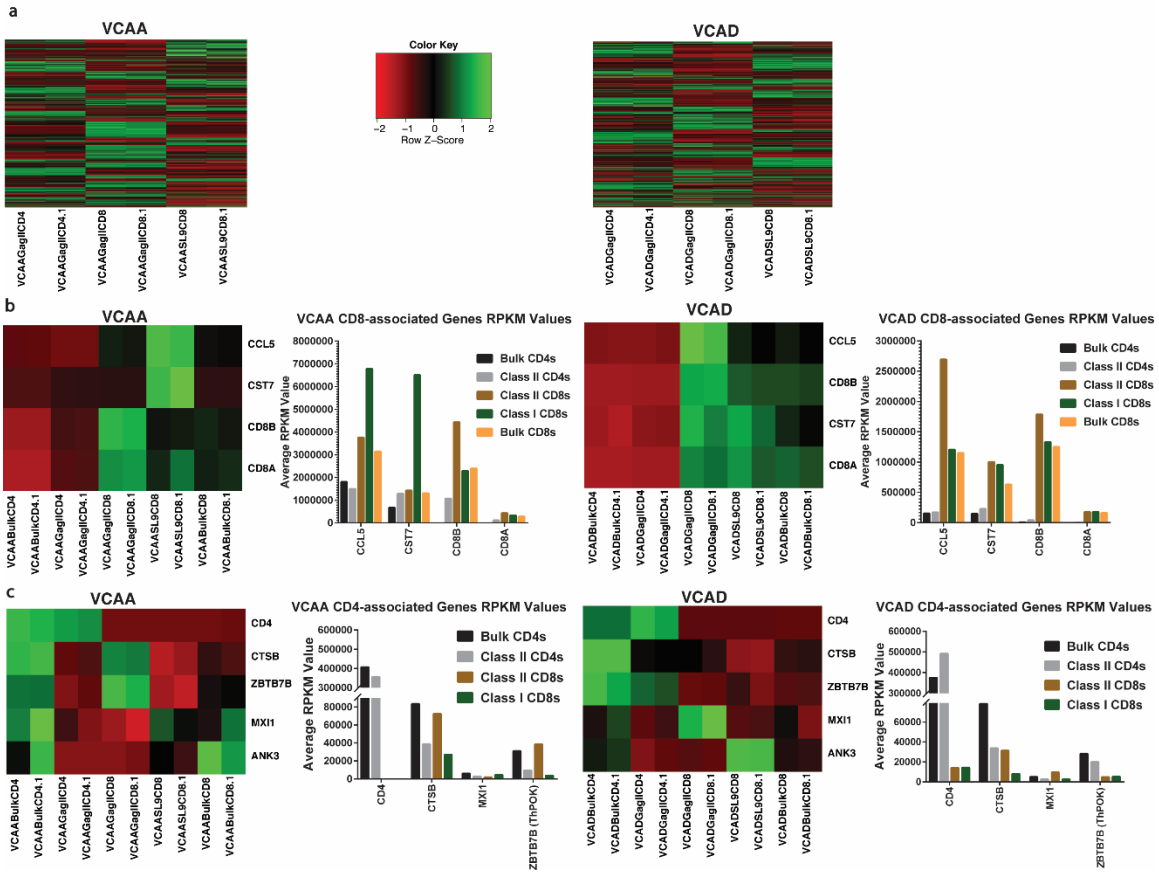

Figure 3: Gag-specific HLA DRB1*0701 restricted CD8+ T cells express both CD4+/CD8+ T cell lineage-specific genes.

A. Gag-specific HLA DRB1*0701 restricted CD8+ T cells have a unique gene expression profile. Heatmap and hierarchical clustering of significant differentially expressed genes in tetramer sorted Gag-specific class II-restricted CD4+ T cells (GagIICD4), class II-restricted CD8+ T cells (GagIICD8), and class I-restricted CD8+ T cells (SL9CD8) from VCAA (5100 genes) and VCAD (4886 genes). Two replicates are shown for each subset. Green represents high expression, while red represents low expression. B. Gag-specific HLA DRB1*0701 restricted CD8+ T cells express CD8+ T cell lineage-specific genes. Heatmap comparing gene expression levels of CD8+ T cell lineage specific genes *CCL5, CST7, CD8A* and *CD8B* in bulk sorted CD4+ T cells (BulkCD4), tetramer sorted Gag-specific class II-restricted CD4+ T cells (GagIICD4), class II-restricted CD8+ T cells (GagIICD8), class I-restricted CD8+ T cells (SL9CD8) and bulk sorted CD8+ T cells (BulkCD8) from VCAA and VCAD. Two replicates are shown for each subset. Green represents high expression, while red represents low expression. The bar plot shows the average reads per kilobase million (RPKM) values of the target genes. C. Gag-specific HLA DRB1*0701 restricted CD8+ T cells express CD4+ T cell lineage-specific genes. Heatmap comparing gene expression levels of CD4+ T cell lineage specific genes *CD4, CTSB* (Cathepsin B), *ZBTB7B* (ThPOK), *MXI1* and *ANK3* in bulk sorted CD4+

T cells (BulkCD4), tetramer sorted Gag-specific class II-restricted CD4+ T cells (GagIICD4), class II-restricted CD8+ T cells (GagIICD8), class I-restricted CD8+ T cells (SL9CD8) and bulk sorted CD8+ T cells (BulkCD8) from VCAA and VCAD. Two replicates are shown for each subset. Green represents high expression, while red represents low expression. The bar plot shows the average reads per kilobase million (RPKM) values of the target genes. T. Nyanhete designed the experiment, sort purified the cell subsets used for RNA seq, analyzed and interpreted the RNA seq results. RNA-seq experiments performed by Yue Chen. Heatmaps generated by T. Bradley, K. Wiehe and W. Faison under the direction of T. Nyanhete.

Table 6: CD8 and CD4+ T cell-specific Genes.

Gene Signatures used to Differentiate Human CD4 and CD8+ T cells [258, 259]

CD8+ T Cell Gene Signature	CD4+ T Cell Gene Signature
CD8a, CD8b, CCL5, TBX21, CST7	*CD4, ANK3, MXI1, CTSB*, ThPOK (*ZBTB7B*)

CD8+ T cell subsets (BulkCD8 - CD8+ T fraction composed of both Gag tetramer-specific and Gag tetramer-nonspecific CD8+ T cells, SL9CD8 - Gag p17-specific class I-restricted CD8+ T cells and GagIICD8 - Gag p24-specific class II-restricted CD8+ T cells) all expressed CD8-specific genes (*CD8B, CD8A, CST7 and CCL5*), which were all absent in the CD4+ T cell subsets (Figure 3B). Bulk CD4+ T cells and tetramer specific CD4+ T cells (GagIICD4) all expressed *CD4*, while VCAD tetramer specific CD4+ T cells also expressed *ZBTB7B* (ThPOK) and *CTSB* (Figure 3C). Interestingly, we observed that HLA class II-restricted CD8+ T cells (GagIICD8) also expressed multiple CD4-associated genes, with VCAA class II CD8s expressing *ZBTB7B* (ThPOK) and *CTSB*, while VCAD class II CD8s expressed *MXI1* (Figure 3C). Additionally, Gag tetramer-specific CD4+ T cells

(GagIICD4) had reduced expression levels of multiple CD4-associated genes *ThPOK, MXI1* and *CTSB* compared to the CD4+ T cell fraction composed of both Gag tetramer-specific and Gag tetramer-nonspecific CD4+ T cells (BulkCD4) (Figure 3C).

The results from the transcriptomics analysis suggests that HLA class II-restricted CD8+ T cells from patients VCAA and VCAD, while sharing some features from both conventional CD4 and CD8+ T cells, possess some distinct features that make them a unique T cell subset that might possess distinct functional properties that could be harnessed to complement conventional CD8+ T cell-mediated HIV-1 control.

DRB1*0701 restricted $Gag_{293-312}$–specific CD8+ and CD4+ T cells have distinct TCR repertoires

To test the hypothesis that Gag-specific HLA class II-restricted CD8+ T cells have a unique transcriptional profile with evidence of anti-viral gene expression, I profiled expression of known cytolytic molecules and anti-viral genes associated with CD8+ T cell-mediated anti-HIV-1 activity [238, 263-266] (Table 7) in HIV-1 Gag-specific HLA class II-restricted CD8+ T cells, HLA class I-restricted CD8+ T cells and HLA class II-restricted CD4+ T cells from VCAA and VCAD.

Table 7: Genes Associated with CD8+ T Cell-mediated HIV-1 Replication Inhibition.

CLASS	GENES [238, 263-266]
Anti-viral cytokines	*CCL3, CCL4, CCL5, CCL3L1, CCL22, XCL1, CSF2, TNFRSF9, TNFRSF4, IFNy, IL2*
Effector molecules	*Perforin, GZMA, GZMB, GZMH, GNLY, CD107a, GZMK, SPON2, ITGAL*
Other anti-viral genes	*EOMES, TBX21, IL21R, IL7R, IL2RG, ID2, GATA3, IL2RA*

HLA class II-restricted CD8+ T cells (GagIICD8) in VCAA and VCAD had unique anti-viral gene expression profiles compared to the conventional HLA class I-restricted CD8+ T cells (SL9CD8) **(**Figure 6**)**. VCAA HLA class II-restricted CD8+ T cells highly expressed *CCL22, IL21R, GATA3, GNLY, IL2RA* and *SPON2* (Figure 4A), while VCAD HLA class II-restricted CD8+ T cells highly expressed *XCL1, ITGAL, IL7R, LAMP1, IL2RA* and *SPON2* (Figure 4B) compared to their respective HLA class I-restricted CD8+ T cells. *SPON2* and *IL2RA* genes were highly expressed in HLA class II-restricted CD8+ T cells compared to HLA class I-restricted CD8+ T cells in both patients (Figure 4). We also observed that HLA class II-restricted CD8+ T cells had lower expression of T cell activation and exhaustion markers (Table 8) compared to HLA class I-restricted CD8+ T cells (Figure 5). VCAA HLA class I-restricted CD8+ T cells highly expressed *CD160, TIGIT, FASLG* and *KLRG1* transcripts associated with chronic activation and

exhaustion (Figure 5A), while VCAD HLA class I-restricted CD8+ T cells highly expressed *PDCD1* (PD1), *CD160, TIGIT* and *KLRG1* transcripts associated with chronic activation and exhaustion (Figure 5B) compared to their respective HLA class II-restricted CD8+ T cells. *CD160, TIGIT* and *KLRG1* were highly expressed in HLA class I-restricted CD8+ T cells in both patients, while *CTLA4* was highly expressed in HLA class II-restricted CD8+ T cells in both patients (Figure 5). VCAA and VCAD patient-specific variations in anti-viral and exhaustion gene expression profiles were also observed.

Table 8: T Cell Exhaustion-related Genes.

CLASS	GENES [266]
Negative Regulators/Exhaustion Markers	*HAVCR2, CTLA4, PD1 (PDCD1), TIGIT, LAG3, CD160, FASLG, KLRG1*

These results demonstrate that HLA class II-restricted CD8+ T cells in VCs had lower expression of T cell activation and exhaustion markers, and a unique anti-viral gene signature compared to conventional HLA class I-restricted CD8+ T cells.

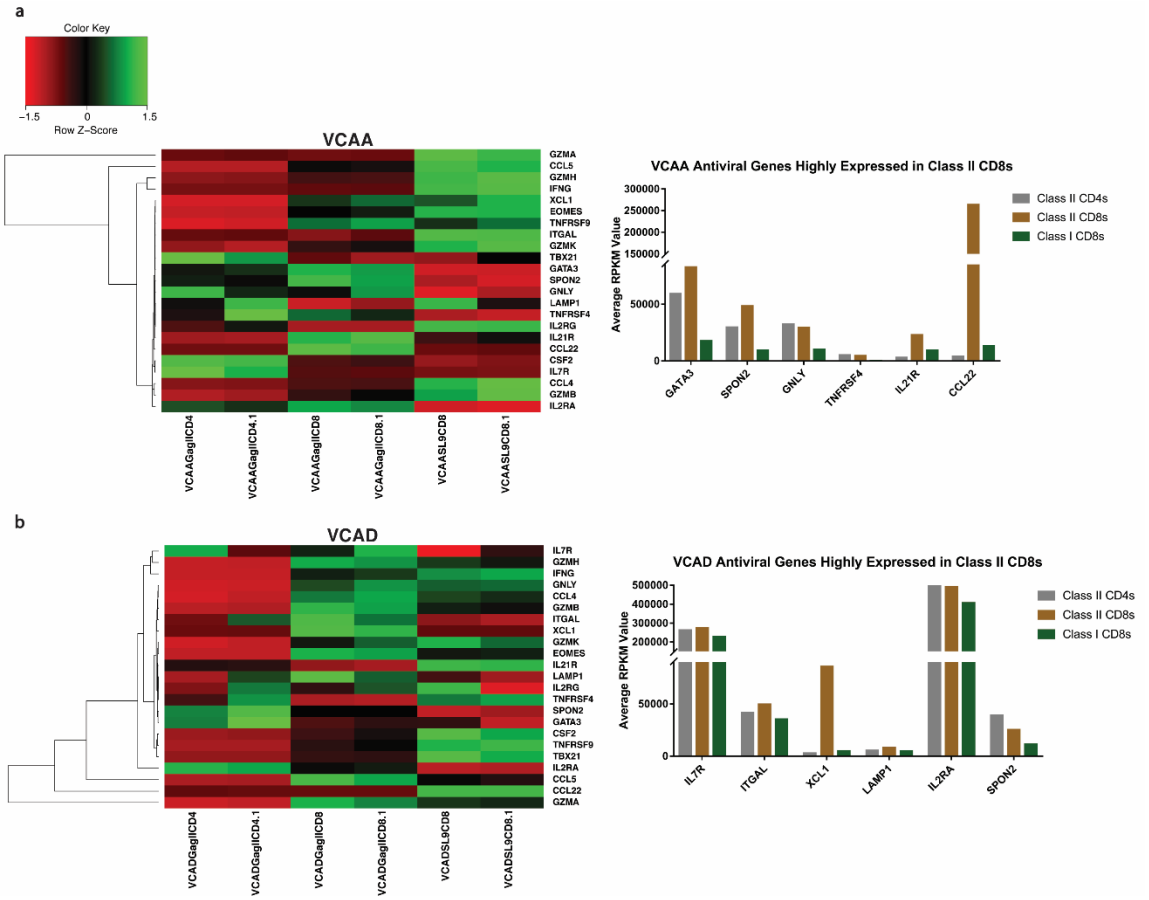

Figure 4: Gag-specific HLA DRB1*0701 restricted CD8+ T cells have a unique anti-viral gene expression profile.

Heatmap and hierarchical clustering of anti-viral genes (Table 7) based on expression levels in tetramer sorted Gag-specific class II-restricted CD4+ T cells (GagIICD4), class II-restricted CD8+ T cells (GagIICD8) and class I-restricted CD8+ T cells (SL9CD8) from VCAA (A) and VCAD (B). Two replicates are shown for each subset. Green represents high expression, while red represents low expression. The bar plot shows the average reads per kilobase million (RPKM) values of anti-viral genes of interest highly expressed in class II-restricted CD8+ T cells compared to class I-restricted CD8+ T cells. T. Nyanhete designed the experiment, sort purified the cell subsets used for RNA seq, analyzed and interpreted the RNA seq results. RNA-seq experiments performed by Yue Chen. Heatmaps generated by T. Bradley, K. Wiehe and W. Faison under the direction of T. Nyanhete.

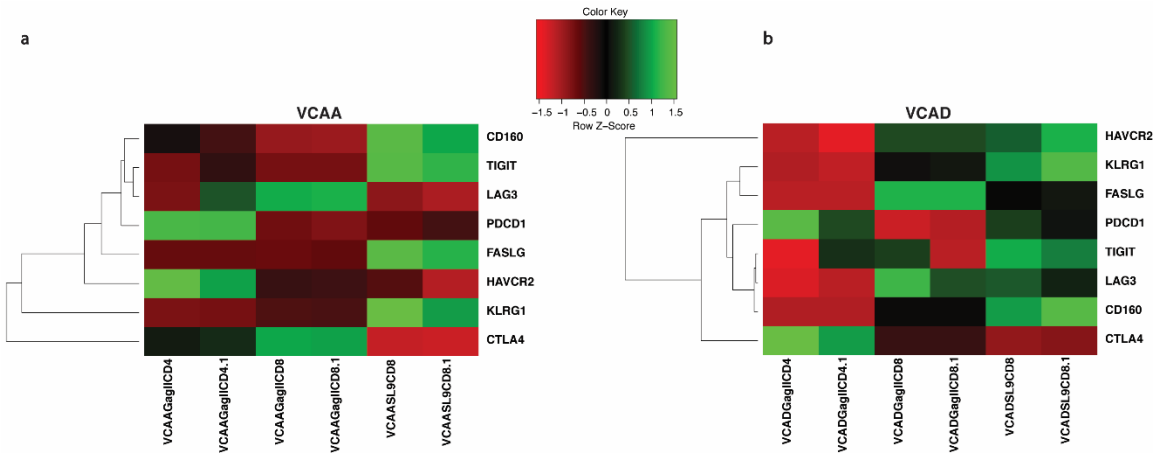

Figure 5: Gag-specific HLA DRB1*0701 restricted CD8+ T cells exhibit a less exhausted expression profile compared to Gag-specific HLA-A*0201 restricted CD8+ T cells.

Heatmap and hierarchical clustering of selected T cell exhaustion/activation-related genes (Table 8) based on expression levels in tetramer sorted Gag-specific class II-restricted CD4+ T cells (GagIICD4), class II-restricted CD8+ T cells (GagIICD8) and class I-restricted CD8+ T cells (SL9CD8) from VCAA (A) and VCAD (B). Two replicates are shown for each subset. Green represents high expression, while red represents low expression. T. Nyanhete designed the experiment, sort purified the cell subsets used for RNA seq, analyzed and interpreted the RNA seq results. RNA-seq experiments performed by Yue Chen. Heatmaps generated by T. Bradley, K. Wiehe and W. Faison under the direction of T. Nyanhete.

DRB1*0701 restricted $Gag_{293-312}$–specific CD8+ and CD4+ T cells have distinct TCR repertoires

To gain an insight into how HLA class II-restricted CD8+ T cells respond to a given antigen, I examined the clonal diversity of HIV-1 Gag-specific HLA class II-restricted CD8+ T cells. Given that we also had HLA class II-restricted CD4+ T cells targeting the same $Gag_{293-312}$ epitope, TCR repertoire analysis enabled

measurement of antigen-specific T cell diversity in both HLA class II-restricted CD4 and CD8+ T cells.

Based on the Gini index which measures the skewness of the clonal distribution (with a low score associated with an equal clonal distribution while a high score is associated with repertoire skewing) from the tcR package [245], analysis of the top 100 clones in VCAA and VCAD [226] shows that the HLA class I-restricted CD8+ TCR repertoire was consistently narrow and biased in both patients (Figure 6A), suggesting an oligoclonal expansion of class I-restricted CD8+ T cells in response to Gag p17. For VCAA (no protective alleles), the HLA class II-restricted CD8+ TCR repertoire was broad and diverse while the HLA class II-restricted CD4+ TCR repertoire was narrow and biased (Figure 6A). VCAD (HLA B57*01 protective allele) had a narrow and biased HLA class II-restricted CD8+ TCR repertoire while the HLA class II-restricted CD4+ TCR repertoire was broad and diverse (Figure 6A). These findings indicate that there is a polyclonal expansion of HLA class II-restricted CD8+ T cells compared to HLA class II-restricted CD4+ T cells in response to $Gag_{293-312}$ in VCAA, while an oligoclonal expansion of HLA class II-restricted CD8+ T cells compared to HLA class II-restricted CD4+ T cells is observed in VCAD (Figure 6A).

Given the observed clonal diversity differences between HLA class II-restricted CD8+ and CD4+ T cells targeting the same epitope, I further interrogated the clonal composition of these two subsets by comparing the highly variable Complementarity Determining Region 3 (CDR3) nucleotide sequence overlap. Vβ

CDR3 nucleotide sequence overlap across the different T cell subsets, expressed as a similarity Jaccard Index score ranging from zero to one, showed low CDR3 sequence sharing and TCR repertoire similarity between HLA class II-restricted CD8+ and CD4+ T cell subsets (Figure 6B).

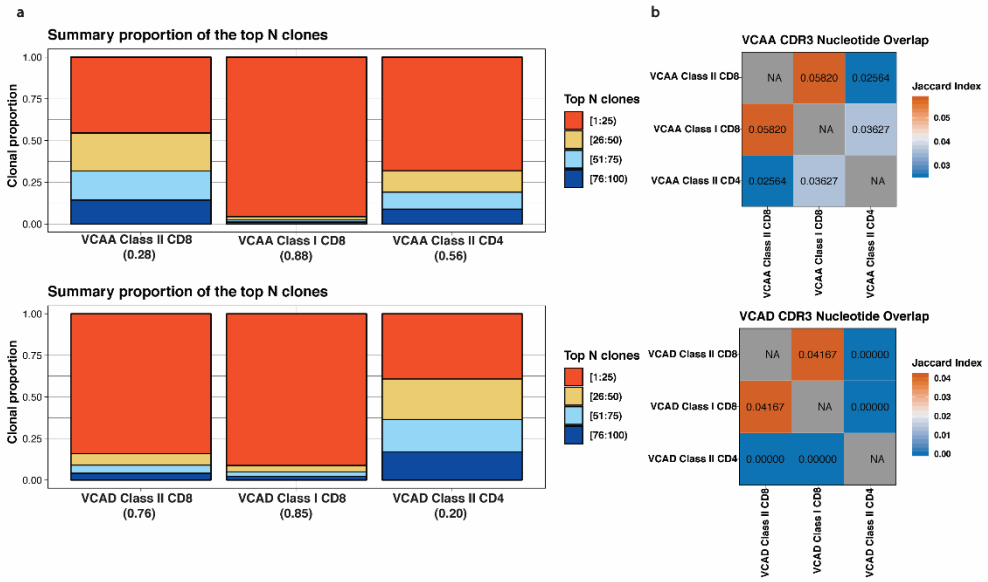

Figure 6: TCR repertoire analysis of Gag-specific HLA DRB1*0701 restricted CD4+ T cells, CD8+ T cells and HLA-A*0201 restricted CD8+ T cells.

A. TCR repertoire diversity of Gag-specific HLA DRB1*0701 restricted CD4+ T cells, CD8+ T cells and HLA-A*0201 restricted CD8+ T cells in VCAA and VCAD. Top proportions bar plot showing the proportions of the top 100 most abundant clonotypes in repertoires from tetramer sorted Gag-specific class II-restricted CD4+ T cells (GagIICD4), class II-restricted CD8+ T cells (GagIICD8) and class I-restricted CD8+ T cells (SL9CD8) from VCAA and VCAD. The GINI Index calculated by tCR is listed in parentheses below each bar. B. Tetramer sorted Gag-specific HLA DRB1*0701 restricted CD4+ T cells and CD8+ T cells targeting the same epitope have distinct TCR repertoires. Heatmap showing the Jaccard Index evaluating relatedness of TCR repertoires from tetramer sorted Gag-specific class II-restricted CD4+ T cells (GagIICD4), class II-restricted CD8+ T cells (GagIICD8) and class I-restricted CD8+ T cells (SL9CD8) using the TRBV CDR3 nucleotide sequence overlap. The Jaccard Index ranges from 0 (dissimilar) to 1 (similar). T. Nyanhete designed the experiment, sort purified the cell subsets used for RNA seq,

analyzed and interpreted the MiXCR results. RNA-seq experiments performed by Yue Chen. MiXCR extraction of TCR sequences from RNA-seq data performed by W. Faison.

In summary, these results demonstrate that HLA class II-restricted CD4+ T cells and HLA class II-restricted CD8+ T cells with shared epitope specificity have distinct TCR repertoires.

2.4 Discussion

CMV-vectored SIV vaccine studies reported control of infection associated with induction of unconventional MHC class E- or II-restricted CD8+ T cells in NHPs [73, 74, 232]. Studies are ongoing to analyze the specific contribution of MHC-II vs. MHC-Ia vs. MHC-E restricted CD8+ T cell responses to protection in the setting of RhCMV/SIV-mediated prophylactic vaccine protection (Louis Picker, personal communication). Ranasinghe *et al.* first reported that HIV-1-specific cytolytic class II-restricted CD8+ T cells are present in HIV-1 infection [75]. These findings have resulted in increased interest in elucidating the properties of these unconventional class II-restricted CD8+ T cells and their possible role in mediating control of HIV-1 infection. In this study, we assessed the distribution of class II-restricted CD8+ T cells in different HIV-1 patient cohorts, their relative contribution towards CD8+ T cell mediated suppression of HIV-1 replication, ontogeny, functional properties and determined TCR repertoire composition in selected individuals.

To further expand on the work done by Ranasinghe *et al* and investigate whether atypical class II-restricted CD8+ T cells are only present in HIV-1 VCs, the presence of class II-restricted CD8+ T cells was interrogated in HIV-1 chronic patients, HIV-1 VCs and healthy donors. Among the three HIV-1+ patient cohorts interrogated, we observed that HIV-1+ VC patients had detectable MHC class II-restricted CD8+ T cells, while the frequency of class II-restricted CD8+ T cells were undetectable in the healthy donors and barely at the limit of quantitation in the

chronic patients. The majority of VC patients exhibited contact-dependent, non-lytic, anti-viral activity which was abrogated by the addition of anti-MHC monoclonal antibodies, while one patient, VC V, exhibited contact independent non-lytic virus inhibition that was not blocked by the addition of anti-MHC antibodies. We and others have shown that CD8 T cells can mediate contact independent nonlytic virus inhibition [60, 237, 267, 268], thus potentially explaining why the high CD8+ T cell-mediated viral inhibition activity displayed by VC V was not blocked by the anti-MHC antibodies. Alternatively, VC V CTL activity could be mediated by other non-classical HLA restriction such as HLA-E which has also been reported to mediate CTL activity in humans [84, 269] and non- human primates [86].

Thus, given our finding and that of others [75], we believe that natural HIV-1 infection can induce these cells. One hypothesis is that the CD4+ T cell depletion, high viremia and inflammatory cytokine storm present during acute HIV-1 infection creates a CD4 deficient, pro-inflammatory environment [59, 270] that might be conducive for the expansion of these rare class II-restricted CD8+ T cells or their conversion from CD4+ T cells. This possibility is also supported by the observation that CD4-deficient mice mount strong MHC class II-restricted CD8+ T cell responses after primary bacterial or viral infection [76, 78-80, 234]. Additionally, reports from the transplant patients with class II-restricted CD8+ T cells suggested that the highly inflammatory and immunogenic environment might be involved in the induction of these atypical class II-restricted CD8+ T cells [81]. However, more

studies are needed to understand the relationship between HIV-1 infection and MHC class II-restricted CD8+ T cells, and further our understanding of additional factors driving or restricting induction and detection of these cells. Moreover, we also observed that the MHC class II-restricted CD8+ T cells present during natural HIV-1 infection had predominant effector and central memory phenotypes. This finding was striking as canonically, CD8+ T cells associated with lower viral loads in chronic HIV-1 infection possess either a central memory [271] or effector memory phenotype [272, 273] with low PD-1 expression [274, 275].

The presence of a class II-blockable CD8+ T cell mediated anti-viral activity was further supported by the presence of a unique anti-viral gene expression profile in Gag-specific class II-restricted CD8+ T cells. Two anti-viral genes from our down-selected list, *SPON2* and *IL2RA*, were highly expressed in HLA class II-restricted CD8+ T cells compared to HLA class I-restricted CD8+ T cells in both patients. *SPON2* is highly expressed in CD8+ T cells primed to exert effector activities [266, 276, 277], while *IL2RA* expression is also required for IL-2 dependent CD8+ T cell effector responses [278, 279]. *XCL1*, which was highly expressed in VCAD HLA class II-restricted CD8+ T cells inhibits a broad range of HIV-1 isolates, independent of viral co-receptor usage and genetic subtype [264], while *CCL22* which is highly expressed in VCAA class II-restricted CD8+ T cells is a known anti-viral β-chemokine secreted by both CD8+ and CD4+ T cells during HIV-1 infection [280].

Potent CD8+ T cell antiviral activity is one of the factors thought to mediate VC status [60, 65, 235, 238, 239, 281]. Given these findings, it is plausible that the presence of unconventional HLA class II-restricted CD8+ T cells may contribute to the CD8-mediated anti-viral activity present in VCs. MHC class II and E-restricted CD8+ T cells have been reported in the NHP model to have desirable features for potent CD8+ T cell mediated anti-viral activity. Some of these features include a broader antigen epitope recognition profile, unique targeting of supertopes and the ability to target conserved, subdominant epitopes [74]. Thus, it will be interesting to probe whether the HLA class II-restricted CD8+ T cells in VCs and chronic patients have some of the above unique features, and also whether the higher frequency of HLA class II-restricted CD8+ T cells observed in the VC patients might be involved in mediating their superior protective capacity.

Highlighting the ontogeny of these atypical CD8+ T cells is critical for understanding the factors that trigger induction of these cells and hence will provide valuable insight into how these cells can be targeted by vaccines and harnessed to provide protection from HIV-1 or other viral infections. In the NHP study, the rhesus CMV vector was responsible for the induction of MHC class II-restricted CD8+ T cells and not natural infection. However, the observation of unconventional CD8+ T cells in humans in our study and others [75, 81, 82], suggests that they might also be induced without the aid of a CMV vector. Preliminary transcriptomic findings from two VC patients, VCAA and VCAD, suggest that HLA class II-restricted CD8+ T cells have a unique transcriptome and

express both CD8-associated (*CD8α/β, CST7* and *CCL5*) and CD4-associated genes (ThPOK and *CTSB* for VCAA, and *MXI1* for VCAD). This initial observation suggests the possibility that HLA class II-restricted CD8+ T cells could be 'ex-CD4+ T cells' that undergo re-programming to adopt CD8+ T cell like features and hence explaining the presence of CD8-specific genes, an anti-viral gene signature usually associated with CD8+ T cells, CD4-specific genes and HLA class II-restriction.

HIV-1 infection has been reported to disrupt CD4+ T cell lineage-defining transcriptional profile [282]. Furthermore, the presence of peripheral lineage-intermediate T cell subsets with CD4 and CD8 surface markers/effector molecule expression patterns in numerous disease settings is not entirely unheard of [283]. Non-traditional CD4+ T cells with cytolytic functions [92, 105, 284], and lineage intermediate CD4+/CD8+ double positive T cell subsets have been previously reported in HIV-1 infection [285, 286]. We have also previously reported the presence of anti-viral and cytolytic CD4+/CD8+ double positive T cells in our HIV-1 Virus Controller patient cohort which included patients VCAA and VCAD used in this study [239]. However, the transcriptomics findings are not conclusive due to the limited sample size and also the need for lineage-tracing experiments in murine models to clearly define the relationship between CD4+ T cells and HLA class II-restricted CD8+ T cells. HLA class II-restricted CD8+ T cells exhibit patient-specific transcriptomic features that might be linked to the differences in viral loads, CD4+ T cell counts and other biological differences between patient VCAA and VCAD. It

is also possible that these differences might be due to different induction mechanisms of HLA class II-restricted CD8+ T cells in patients VCAA and VCAD.

TCR repertoire clonal diversity analysis highlights repertoire richness and gives an indication of how different T cell subsets respond to a given antigen [287]. TCR diversity enables T cells to respond to multiple foreign antigens [287] and in the context of HIV-1 infection this will endow the immune system with the ability to recognize circulating epitope variants. However, in the HIV-1 setting, it is not clear whether having a dominant protective CD8+ T cell clonotype or multiple subdominant clonotypes is better for HIV-1 replication control. TCR repertoire diversity of antigen-specific T cells was shown to be comparable between HIV-1-infected and HIV-1-uninfected subjects [288], while clonal diversity could not distinguish elite controllers from chronic patients with the HLA-B5701 protective allele [289]. However, there are studies showing that HLA class I-restricted CD8+ T cells [289-291] have narrow and biased repertoires with dominant clonotypes. Narrow and biased repertoires were also recently reported for HLA class II-restricted CD8+ and CD4+ T cells responding to the same HIV-1 Gag antigen in one VC patient [75].

In our study, HLA class I-restricted CD8+ T cells from both individuals had narrow and biased TCR repertoires suggesting an oligoclonal expansion in response to the Gag p27 antigen. However, the HLA class II-restricted CD8+ and CD4+ TCR repertoires were different in the two individuals even though both T cell subsets were $Gag_{293-312}$-specific and DRB1*0701-restricted. It is interesting to

highlight that the one VC patient, VCAD, with a narrow and biased HLA class II-restricted CD8+ TCR repertoire (similar to that of the class I-restricted TCR repertoire) had the protective HLA-B57*01. VCAA, without protective HLA alleles, had a broad and diverse HLA class II-restricted CD8+ TCR repertoire. It is still unclear how the presence/absence of protective HLA alleles would influence HLA class II-restricted CD8+ TCR repertoire diversity as more patients need to be examined to confirm the relationship we observed in our two patients. Despite having different HLA class II-restricted CD8+ TCR repertoires, both patients still met the prespecified VC cohort criteria for enrollment. It remains to be seen how clonal diversity might affect HIV-1 replication control by both HLA class I- and HLA class II-restricted CD8+ T cells.

Even though we were able to detect the rare HLA class II-restricted CD8+ T cells in some of the HIV-1 infected individuals, this study still had a number of limitations. This study utilized the available HLA DRB1*0701 class II-restricted $Gag_{293-312}$ tetramer and is therefore limited to the detection of a small fraction of the entire HIV-1-specific HLA class II-restricted CD8+ T cell subset within each individual and only for those individuals with this matching HLA haplotype. Further studies with more sensitive multimers such as dodecamers instead of tetramers, autologous optimal class II-restricted HIV-1 epitopes (other than the Gag epitope used in this study) within each individual and with other HLA alleles may detect higher frequencies of HLA class II-restricted CD8+ T cells. Further studies to characterize these cells ex vivo or through the generation of T cell lines and clones

will enable characterization of this cellular subset by probing the class II-restricted breadth (other than $Gag_{293-312}$) and function (functional reactivity to the target HIV-1 peptides, and ability to mediate viral suppression). Limited patient sample availability and very low to no detection of class II-restricted CD8+ T cells in chronic viremics and healthy patients limited investigating the presence of unconventional class II-restricted CD8+ T cells in a larger patient cohort and the comparative RNA seq analysis of patient samples with different disease outcomes. Future studies investigating the frequency and gene expression profile of class II-restricted CD8+ T cells in large HIV-1 patient cohorts with different disease outcomes (acute patients who later progress to become chronic viremics or acute patients who later become virus controllers, and also patients on ART-therapy (treatment-induced controllers) will help assess the importance of these cells in viremic control and also highlight any distinguishing features of these cells in different disease conditions. Additionally, due to the low frequency directly *ex vivo*, we examined expanded CD8 T cells for HLA class II activity. Thus, the expansion process may have impacted the phenotypes of the HLA class II-restricted $Gag_{293-312}$–specific CD8+ T cells. Further studies with more sensitive multimers such as dodecamers instead of tetramers may result in the detection of a larger subset of these cells without prior expansion of the CD8+ T cell subset. However, given these limitations, it is remarkable that HLA class II-restricted CD8+ T cells were detected in these HIV-1 positive individuals and suggests that there might even be a larger subset of these atypical cells that were missed in this study. For the TCR diversity

measurements, we were not able to measure the total body TCR diversity due to the complexity of this approach, but we only focused on the TCR diversity of a defined peripheral blood T cell subpopulation at one given time-point during the course of infection. Future studies will focus on utilizing T cells from lymph nodes and blood at multiple time points during course of infection so as get better snapshot of the HLA class II-restricted CD8+ T cells repertoires.

In summary, we have demonstrated the presence of atypical anti-viral memory HLA class II-restricted $Gag_{293-312}$–specific CD8+ T cells with a unique transcriptional profile that includes expression of both CD4 and CD8+ T cell lineage-specific genes in HIV-1 virus controllers (VCs). The presence of these unconventional HLA class II-restricted CD8+ T cells was associated with natural HIV-1 infection since these cells were not present in HIV-1 seronegative individuals. The finding that functional HLA class II-restricted CD8+ T cells are present in HIV-1+ individuals highlights that elucidation of the ontogeny of this activity in humans can lead to a better understanding of how to induce protective CD8+ T cell immunity by vaccination.

3. Coordinated Fab and Fc-effector functions in HIV-1 VCs

3.1 Introduction

Despite the emerging data illustrating the role of the humoral response in conferring protection against HIV-1 infection as well as promoting viral control and clearance [292], there is still a lot of skepticism over the post-infection protective role of the humoral response in HIV-1 Virus Controllers (VCs) [202, 213, 293-295]. bNAbs, typically observed in non-controllers (viremic chronic progressors) with high viral loads and higher virus sequence diversity [296], are not associated with control of autologous virus and hence the perceived lack of association with protection against spontaneous HIV-1 disease progression in HIV-1 VCs [202, 297, 298]. However, there are a few isolated studies that have highlighted the presence of bNAbs in patients with very low to undetectable viremia [203, 206-208, 299-301]. Most importantly and unlike in chronic progressors, there is evidence from studies by Freund et al [203] and Pilgrim et al [301] that show that viruses from HIV-1 VCs are sensitive to neutralization by autologous bNAbs or plasma samples. Epitope mapping of the HIV-1 VC bNAb response indicates predominant targeting of the V3 glycan [203, 208]. However, epitope mapping of HIV-1 VC bNAb responses were done using approaches that limit the findings to already known bNAb targets defined using chronic viremic bNAb responses. The previous epitope mapping approaches have also largely overlooked the poorly neutralizing or non-neutralizing antibody response which together with the

neutralizing response is part of the HIV-1 Env-directed immune response. Thus, there is a need for an epitope mapping approach that maps the polyclonal antibody response (neutralizing and non-neutralizing) so as to provide a more complete picture of the HIV-1 *Env*-directed immune response in the patient. This approach will also help identify a potential novel HIV-1 VC bNAb response capable of targeting novel, previously unidentified epitopes that could also partly explain the ability to neutralize autologous viruses.

Non-neutralizing antibody effector functions have also been implicated in controlling viremia [223, 302], with some studies showing a correlation between Fc-mediated effector functions and slow HIV-1 disease progression [213, 221, 303]. One study highlighted the enrichment of functionally coordinated humoral Fc-mediated effector functions (ADCC, ADCP, NK cell activation and complement activation) in patients that control infection compared to viremic chronic progressors[163], and another demonstrated enhanced Fcγ receptor (FcγR2A and FcγR3A) signaling by HIV-1 VC IgG compared to IgG from non-controllers [164]. Thus, even though most HIV-1 VCs are known for developing efficient antiviral T-cell responses with cytotoxic CD8+ T cells, especially in patients expressing protective human leukocyte antigen (HLA) alleles such as HLA-B*57 and B*27, recent evidence suggest that the antibody responses might also be involved in HIV-1 control.

Studies looking at humoral responses in an HIV-1 infection setting have mostly looked at Fab and Fc-effector humoral responses separately. However,

there is now data suggesting the potential role of the Fc domain [223, 224]/Fc-mediated effector functions in modulating the bNAb response in chronic viremic [166] and HIV-1 VCs [165]. Thus, there is need to identify other Fc effector functions/profile that are linked with the bNAb response so as to better understand the nature of a potent polyclonal humoral response to natural HIV-1 infection. This will also not only allow us to gain a more complete mechanistic link the Fc effector functions and the nAb response but will also allow us to better identify features that could be used to induce or develop more potent bNAbs.

Given the enrichment of ADCP activity in HIV-1 VCs compared to chronic viremics, together with the evidence for bNAb development in patients with very low viral loads, I hypothesized that HIV-1 VCs developed nAb breadth that correlated with ADCP activity and targeted known and previously uncharacterized vulnerable HIV-1 *Env* regions.

Our findings show the presence of bNAbs in patients with low viral loads (VCs) that correlates with multi clade virion ADCP activity resulting in clusters of patients with either high or low nAb/ADCP breadth independent of HLA protective allele status. IgG binding magnitude and breadth to either monomeric or trimeric native-like HIV-1 *Env* antigens distinguished HIV-1 VCs with high or low nAb/ADCP breadth. A subset of the high responder patients with bNAb activity had a polyclonal antibody response targeting known multiple vulnerable bNAb epitopes (V3 glycan, MPER and CD4 binding site) that act in concert to mediate the observed neutralization breadth. Negative-stain electron microscopy of the

polyclonal IgG complexed with the HIV-1 Env further confirmed the predominance of CD4bs antibodies that have similar approach angles to some of the most potent CD4bs bNAbs (45-46m2, 3BNC117 and CH235) capable of neutralizing about 90% of circulating HIV-1 strains.

This work highlights the novel association between virion ADCP breadth and nAb breadth in HIV-1 VCs, and also provides the first evidence for the presence an antibody response that is similar to a class of highly potent CD4bs bNAbs in a low viremia setting in the absence of autoimmunity. This work also adds to the recently growing literature supporting the role of the Fc effector functions in modulating bNAb development.

3.2 Materials and Methods

HIV-1 Virus Controller Patient Cohort and Plasma samples

30 antiretroviral therapy (ART)-naïve HIV-1-infected virus and elite controllers (Table 9 and Table 10) (maintaining plasma HIV-1 loads of <5,000 RNA copies/ml and CD4+ T cell counts of >400 cells/µl) were enrolled through the Infectious Diseases Clinic at Duke University Medical Center. The specimens utilized in this study were restricted to those patients that met this virus controller definition. Although the precise time of infection for these patients is unknown, the minimum length of infection (ranges from >2 to <14 years) is based on when these patients first reported to the clinic. All patients were HLA typed using the next generation sequencing typing method. PBMC genomic DNA underwent PCR amplification and cDNA library preparation before allelic-level 3rd generation sequencing typing of full-length HLA genes was performed using the Illumina platform (ProImmune Ltd, Oxford, UK). Plasma samples were collected from 30 HIV-1 Virus Controller patients at multiple time points from the date of diagnosis, stored at -80°C and thawed at 4°C prior to use.

Table 9: HIV-1 VC Patient Cohort.

Male and Female HIV-1 Infected Patients with a Viral Load above 50 and less than 5000 copies/mL of plasma and a CD4+ T cell count greater than 400 cells/µL of blood enrolled in the HIV-1 VC Cohort (* - CD4 Count was not done for that draw date and an average of two counts from draws date within a year of that draw date is used)

Patient	**Estimated Years Infected**	**Virus Load**	**CD4 T Cell Count**	**Protective HLA allele Status**
VC N	~10	2170	821	None
VC O	~3	312	924	B57*03
VC Q	~7	2970	795	None
VC T	~3	519	601*	None
VC X	~2	601	627	B57*01
VC AA	~12	547	463	None
VC AB	~5	894	643	None
VC AC	~21	2060	997	B57*01
VC AD	~3	1040	449	B57*01
VC AH	~13	138	981	B57*03
VC AJ	~4	108	493	None
VC AK	~23	67	1825	B57*03
VC AL	~12	158	762*	None
VC AM	~16	494	470	Missing
VC AO	~12	299	379*	None
VC AP	~21	3496	776	B57*03
VC AQ	~24	300	1307	B27*05
VC AR	~20	Not Done	316	B57*01
VC AT	~8	785	716	B57*03

VC AY	~10	Not Done	Not Done	None
VC BA	~11	Not Done	Not Done	B57*03
VC BB	<1	487	466	B57*01

Table 10: HIV-1 EC Patient Cohort.

Male and Female HIV-1 Infected Patients with a Viral Load less than 50 copies/mL of plasma and a CD4+ T cell count greater than 400 cells/µL of blood enrolled in the HIV-1 EC Cohort

Patient	**Years Infected**	**Virus Load**	**CD4 T Cell Count**	**Protective HLA Status**
VC G	~8	47	1887	B57*03
VC V	~3	48	1847	B27*05
VC AF	~14	47	729	A32*01
VC AG	~4	47	1420	None
VC AI	~20	<20	1159	B57*03
VC AS	~3	<20	1093	None
VC AW	~10	<20	337	Missing
VC AX	~11	<20	910	B57*01

Cell Lines

THP-1 monocytic cells were purchased from ATCC and grown in supplemented RPMI-1640 (10% FBS, 1% Penicillin/Streptomycin). TZM-bl cells were obtained from the NIH AIDS Research and Reference Reagent and were grown in Dulbecco's modified Eagle's medium (HyClone) containing 10% heat-inactivated fetal bovine serum (Hyclone) and 50µg gentamicin/mL (Sigma).

Env-pseudotyped viruses

Molecularly cloned full-length gp160 were used for HIV-1 Env pseudovirus production by co-transfecting 293T/17 cells with an Env-deficient HIV-1 backbone plasmid (pSG3ΔEnv) as previously described [304]. The Env-pseudotyped virus stocks (Table 11) were titrated in TZM-bl cells as described in Hu X et al [304].

Table 11: HIV-1 Env Pseudotyped Global Virus Panel.

Pseudotyped HIV-1 Viruses Representative of the Global Circulating HIV-1 Strains used in the TZMbl Neutralization Assay [305].

HIV Envelope	Subtype	Tier	Country of Origin
TRO11	B	2	Italy
25710	C	2	India
X2278	B	1B	Spain
BJOX2000	CRF07_BC	2	China
X1632	G	2	Spain
CE1176	C	2	Malawi
246F3	AC	2	Tanzania
CH119	CRF07_BC	2	China
CE0217	C	2	Malawi
CNE55	CRF01_AE	2	China
MN.3	B	1A	United State

TZM-bl Neutralization Assay

Neutralization, using heat inactivated (56°C for 30 minutes) plasma samples from HIV-1 Virus Controllers, was measured in a previously validated format by using Tat-regulated Luc reporter gene expression to quantify reductions in Env-pseudotyped virus infection in TZM-bl cells [306]. TZM-bl is a genetically engineered HeLa cell line that expresses CD4, CCR5, and CXCR4 and carries Tat-regulated reporter genes for firefly Luc and Escherichia coli β-galactosidase under regulatory control of an HIV-1 long-terminal-repeat sequence[307]. Briefly, 50μl of the Env-pseudotyped virus was incubated with serial 3-fold dilutions of plasma or IgG in a total volume of 150μl for 1hr at 37°C in 96 well flat bottom culture plates. Freshly trypsinized TZM-bl cells were then added (1x10^{4}/well in a 100μl volume) in 10% DMEM growth medium containing DEAE-dextran (Sigma, St. Louis, MO) to achieve a final concentration of 10μg/ml. Control wells had either cells + pseudovirus (virus control) or cells only (background control). After a 48hr incubation, 150μl of culture medium was removed from each well, and 100μl of a luciferase reporter gene assay system reagent (Bright-Glo, Promega) was added. After a short incubation of at least 2 minutes, 150μl of lysate from each well was transferred to 96-well black solid plates (PerkinElmer Life Sciences) for measurement of luminescence in a luminometer (PerkinElmer Life Sciences, Victor X3). The 50% inhibitory dose (ID_{50}) or 50% inhibitory concentration (IC_{50}) was defined as the reciprocal of the plasma reagent dilution or IgG concentration

that resulted in a 50% reduction in relative luminescence units (RLU) compared to virus control wells after subtraction of background RLU [308].

HIV-1-specific binding antibody assay (BAMA)

HIV-1 Virus Controller plasma HIV-1-specific antibodies were measured using the standardized HIV-1 binding antibody multiplex assay (BAMA) as previously described [309]. HIV-1-specific antibody isotypes were detected with mouse-anti human IgG (Southern Biotech, Birmingham, AL), conjugated to phycoerythrin, at 4μg/ml. Antibody measurements were acquired on a Bio-Plex instrument (Bio-Rad, Hercules, CA), and the readout is in mean fluorescent intensity (MFI). All assays were run under good clinical laboratory practice (GCLP)-compliant conditions, including tracking of positive controls by Levey-Jennings Charts.

Antibody Avidity

Antibody binding avidity was measured by BAMA with the following modifications as previously described [310]: a 15-minute dissociation step using the Na-Citrate buffer (pH 3.0, Teknova) was performed at room temperature after the formation of antigen-antibody immune complexes prior to the addition of the secondary detection antibody. The avidity measurement was the retained binding magnitude measured as mean fluorescence intensity (MFI) in the presence of the dissociation buffer.

Plasma IgG extraction

Polyclonal IgG was purified from the HIV-1 Virus Controller patient plasma by using protein G affinity chromatography (GE Healthcare) according to the manufacturer's instructions. Briefly, plasma was 2-fold diluted with Tris-buffered saline (TBS) at pH 7.5, and 200μl of diluted plasma was incubated in each well of the protein G HP Multitrap 96-well plate (GE Healthcare, Inc.) for 1 hour. Unbound fractions were removed by centrifugation at 1,500g for 3 minutes. Wells were then washed 3 times with 200μl of TBS. IgG was eluted with 2.5% glacial Acetic Acid, and immediately neutralized with 120μl of 1M Tris-HCl (pH 9.0). The eluted IgG fractions were pooled, concentrated and desalted using Amicon Ultra Centrifugal filters (Millipore) with a 30 kDa cutoff at 14,000g for 12 mins. The IgG was concentrated to the desired volume, assayed for protein concentration using a NanoDrop 1000 spectrophotometer (Thermo Fisher Scientific) and storage at 4°C.

Fluorescently Labelled HIV-1 Virions

Fluorescently labelled HIV-1_{BAL}-Tomato, HIV-1_{CM235}-mcherry, HIV-$1_{92TH023}$-Tomato and HIV-1_{1086C}-mcherry were generated as previously described [311, 312]. Briefly, labelled virus was generated by co-transfecting 293T cells with an HIV-1 proviral plasmid encoding Gag protein fused with a C-terminal fluorescent tag and virus stocks were purified from cell supernatant. HIV-1_{BAL} proviral plasmid was made up of the R9BaL coding sequence cloned into a NL4-3 backbone, while the HIV-$1_{92Th023}$ proviral plasmid consisted of the 92Th023 gp160 coding sequence

cloned into a CRF01_AE backbone, the HIV-1_{CM235} proviral plasmid was made of the CM235 sequence cloned into a backbone, and the HIV-1_{1086C} proviral plasmid consisted of the 1086C sequence cloned into a backbone.

Fluorescently Labelled recombinant HIV-1 trimeric Envelope coated beads

Biotinylated trimeric recombinant HIV-1 Envelope (BG505gp140 T332N and CH505TF SOSIPs) were conjugated to Neutravidin fluorescent beads (Invitrogen) as previously described [313]. Briefly, 10μl of 0.1% BSA/PBS-washed beads were incubated with 10μg biotinylated antigen overnight at 4°C on a rotator. Unbound antigen was removed by washing three times with 1ml 0.1% BSA/PBS.

THP-1 Antibody-dependent cellular phagocytosis (ADCP) Assay

ADCP assay was performed as previously described[228]. Briefly, 9x10^5 beads or 10μl of diluted fluorescence labelled HIV-1_{BAL}, HIV-1_{1086C}, HIV-$1_{92Th023}$, or HIV-1_{1086C} were mixed with 10μl (25μg/ml final concentration) purified HIV-1 Virus Controller IgG in a 96-well round bottom plate. Control wells had monoclonal antibody plus antigen plus cells (positive control), non-HIV-1 specific antibody plus antigen plus cells (negative control), PBS plus antigen plus cells (background control), and just cells only. After a 2-hour incubation at 37°C, 100μl of 5x10^4 of CD4-blocked THP-1 cells were added to each well and then spinoculated at 1200g for 1 hour at 4°C. After the 1hour spinoculation, the antigens/viruses and cells were incubated at 37°C for 1 hour for phagocytosis/virion internalization. Following

incubation, the cells were fixed in 2% paraformaldehyde prior to acquisition on the flow cytometer. For phagocytosis score calculation, a cutoff was first assigned based on the 95th percentile of the no-antibody control. For each sample, the % of cells above this cutoff was multiplied by their mean fluorescence intensity (MFI), and then normalized to the corresponding result for the no-antibody control to give the final phagocytosis (ADCP) score. A background level of phagocytosis was determined based on the mean + 3 standard deviations of the non-HIV-1 specific antibody (CH65).

Infectious Virion Capture Assay

The infectious virion capture assay was performed as previously described [314] . Briefly, 100μl of 20μg/ml of monoclonal IgG was mixed with 100μl of diluted HIV-1_{BaL}, HIV-1_{CM235} or HIV-1_{1086C} fluorescent virus in 96-well 1.1ml plate and centrifuge the plate at 450g for 90 minutes at room temperature to generate IgG-HIV-1 virion immune complex (IC). Transfer 150μl of the immune complex onto a protein G plate attached to a new 96-well 1.1 ml receiving plate and shake plate at 800rpm for 1 hour at room temperature. After the incubation, centrifuge the protein G for 3 minutes at 700g at room temperature followed by 2 washes with 200μl 1X TBS to collect all the uncaptured immune complexes (flow-through) in the receiving plate. Qualitative measurement of the number of virions in the flow-through (un-captured virions) was done using the TZM-bl infection assay. 25μl of virus from the receiving plate (flow-through plate) was used to infect 100μl of 16x10^4 cells/ml of

freshly trypsinized TZM-bl cells. Controls included RPMI only (no-antibody) plus cells, virus plus cells Infection was measured by firefly luciferase assay at 48 hours post-infection (at 37°C) as previously described[116]. The percentage of infectious captured virus from the TZM-bl infection was calculated as follows: % of un-captured infectious virus (flow-through) = [(mean relative light units of sample)/(mean relative light units of no-antibody (RPMI) only)] * 100. % captured infectious virus = 100 - % of un-captured infectious virus. The positivity cut-off was calculated as 3 times the no-antibody (RPMI) % captured infectious virus.

Bio-Layer Interferometry Assay

Bio-layer interferometry (BLI) measurements were done with the ForteBio Octet RED 384 instrument and ForteBio streptavidin biosensors using the previously described protocol [315]. Kinetics assays were performed at 25°C using settings using settings of Standard Kinetics Acquisition rate (5.0 Hz, averaging by 20) at a sample plate shake speed of 1000rpm. The biotinylated RSC3, BG505gp140 T332N SOSIP and BSA proteins were loaded onto streptavidin (SA) sensors which were then dipped in kinetics buffer (ForteBio) to establish a baseline time course and then dipped into wells containing HIV-1 Virus Controller IgG or IgG Fabs (diluted in kinetics buffer to 200μg/ml) to monitor antibody association. The dissociation step was monitored by dipping antibody-bound sensors back into the wells used to collect the baseline time course. To subtract binding due to non-specific interactions of antibodes with the sensors, biotinylated RSC3Δ371/P363N

– loaded SA sensors and biotinylated BSA-loaded SA sensors were used as controls for the RSC3 and the BG505gp140 T332N SOSIP, respectively.

Neutralization Fingerprinting Analysis

Neutralization fingerprinting of the polyclonal antibody response in HIV-1 Virus Controllers N, AA, AL, AP, AQ and BA was done using an optimized panel of 30 diverse strains (Table 12) as previously described [146]. Briefly, the neutralization fingerprint of a plasma sample is represented as a combination of the neutralization fingerprints of a reference set of bNAbs, grouped in ten epitope-specific clusters. Thus, the prevalence of each of the ten antibody groups can be estimated for the given plasma sample, with prevalence scores ranging between 0 (low) and 1 (high), with the positivity cut-off set at 0.25. Additionally, two measures (Residual score and Median of scores) are computed as a way to estimate prediction confidence for the prevalence scores[146]

Table 12: Neutralization Fingerprinting (NFP) Virus Panel.

A 30-strain HIV-1 Virus Optimized for Sequence Diversity, Ability to Correctly Cluster the Neutralization Fingerprints of the Reference bNAbs According to Epitope Specificity and High Minimum bNAb Neutralization Breadth [146].

Virus Name	Clade
7165.18	B
16845-2.22	C
231965.c01	D
T235-47	AG
26191-2.48	C
T235-8	AG
3168_V4_C10	C
620345.c01	AE
6785_V5_C14	C
C1080.c03	AE
CH038.12	BC
CH181.12	BC
CNE5	AE
CNE55	AE
DU123.6	C
DU422.1	C
Q259.d2.17	A
Q461.e2	AD
QH0515.1	B
QH0692.42	B
R1166.c01	AE

R2184.c04	AE
RHPA4259.7	B
T257-31	AG
TRO.11	B
WITO4160.33	B
X2088_c9	G
ZM135M.PL10a	C
ZM249M.PL1	C
ZM53M.PB12	C

Binding Antibody Multiplex Assay (BAMA) Epitope mapping

BAMA was performed as previously described [309]. IgG binding to the following protein probes: Antigenically resurfaced gp120 glycoprotein RSC3 containing the CD4bs and RSC3Δ371I/P363N mutant (AIDS Research and Reference Reagent Program), which has the isoleucine at position 371 of RSC3 removed so as to reduce b12 and VRC01 binding[128], which is further reduced by the P363N mutation[316]. Samples with IgG that showed a loss of reactivity to the CD4bs mutant (RSC3Δ371/P363N) and reacted to RSC3 were classified as containing CD4bs antibodies (IgG RSC3/ RSC3Δ371/P363N binding ratios greater than 2.5 represented a positive signal for VRC01-like activity).

TZM-bl Neutralization Assay Epitope mapping

Mapping of the epitopes targeted by neutralizing antibodies in HIV-1 Virus Controller plasma samples that neutralize the parent virus with an ID_{50} titer > 100 was done using an optimized panel of 4 viruses (TRO.11, COT6.15, JRFL and CH505TF) with targeted mutations in the CD4bs, V2 glycan, V3 glycan, 2G12 and MPER epitopes (Table) that are known to be targeted by bNAbs. A 3-fold decrease in the neutralization titer (ID_{50}) for the mutant virus compared to the wild type virus indicated the involvement of that specific epitope in mediating neutralization of the wild type (parent) virus

IgG Fab Preparation

IgG Fabs were prepared by digesting purified 4mg of IgG with 0.125ml papain-agarose resin (Thermo Fisher Scientific) for 6 hours at 37°C as outlined in the Thermo Fisher Scientific protocol. Fc and non-digested IgG were removed by 10-minute incubation with shaking at room temperature with protein A plus spin column (Thermo Fisher Scientific). Fc and non-digested IgG were captured by the protein A, and the purified IgG Fab fraction was collected after centrifuging the protein A spin column for 1 min at 300g. Optimal recovery of purified IgG Fab was done by washing the protein A spin columns twice with 1ml of 1X PBS (pH 7.4). The collected IgG Fab was concentrated to a desired volume by ultracentrifugation using Amicon Ultra Centrifugal filters (Millipore) with a 10 kDa cutoff.

IgG Fab Quality Control by SDS-PAGE and SEC

Fab size and homogeneity were assessed by Sodium Dodecyl Sulfate – PolyAcrylamide Gel Electrophoresis (SDS-PAGE) and SEC. For SDS-PAGE, 1μg protein/lane was loaded on a Novex Tris-Glycine 4% - 20% Gel (Thermo Fisher Scientific) in reducing vs non-reducing conditions and run at 225V for 45 minutes in 1X Novex Tris-Glycine SDS Running Buffer. Bands were visualized with SimplyBlue Safe Stain (Thermo Fisher Scientific), and the size of the fragments evaluated by running a protein standard ladder (Thermo Fisher Scientific). For SEC, about 750μg protein was loaded on a Superdex 200 increase 10/300 column using a 500μl loop and run at 0.5ml/min using an Akta Pure System (GE Healthcare). Fab peaks were analyzed with the provided Unicorn 7.0.2 software.

Fab-Env complexes for electron microscopy (EM)

BG505 trimers were incubated with purified HIV-1 Virus Controller Fab at ratios of 1: 84 (VC AL), 1:59.7 (VC AP) and 1:49 (VC AQ) overnight at room temperature. After overnight incubation, the complexes were cross-linked with 7.5mM glutaraldehyde for 5 minutes at room temperature and the excess glutaraldehyde was quenched with 75mM Tris buffer (pH 7.4) for 5 minutes at room temperature. The cross-linked Fab-Env complexes were then purified by loading them on a Superdex 6 increase 10/300 column using a 500μl loop and run at 0.5ml/min using an Akta Pure System (GE Healthcare). The fractions containing the complexes (peak 1 on the SEC profile) were pooled in 10kDa cut-off tubes

(Millipore Sigma) and concentrated down to about 50μl final volume. Quality check of the purified complexes (peak 1 from the SEC profile) was done using SDS-PAGE as previously described in this paper.

Negative-Stain EM (nsEM)

SEC-purifed complexes were diluted to 80-100µg/ml in 5% glycerol in 20mM HEPES, 150mM NaCl (HBS) pH 7.4. A 5µl drop loaded on 400 mesh carbon coated copper grid (EMS, cat#G400-Cu) for 10-15sec and then rinsed with 3 drops of aquoues 2% (w/v) uranyl formate (EMS, cat#22450). The grid was incubated in the last drop for 1min, then excess stain blotted and gird air dried. Images collected with Philips EM420 transition electron microscope at 120kV at 4.02Å/pixel.

3D reconstructions were generated using standard methods within the Relion 3.0 pipeline and as described here. Approximately 100 micrographs per dataset were imported and corrected for the contrast transfer function. Typical defocus ranged from 0.5 - 1 µm underfocus, and any overfocused images were discarded. From the CTF-corrected images, particles were template-picked using 2D class averages from a previous unliganded SOSIP sample as templates, and then extracted as a stack of 96-pixel (~386 Å) boxes. One to three rounds of 2D classification and class averaging were used to discard bad particle picks, and select a subset of SOSIP particles, both liganded and unliganded. An initial 3D model of a bare, unliganded, SOSIP was generated from PDB structure 5UM8, by removing the Fab chains from this model and generating a map at 4.02 Å/pixel

using UCSF Chimera's molmap function, low-pass filtered to 15 Å. This initial model, further low-pass filtered to 60 Å within Relion, was used with the selected particle stack for 3D classification into three classes, typically yielding one unliganded class and two classes representing SOSIP trimer with bound Fabs. These Fab-bound classes were subjected to a final homogenous refinement, typically yielding reconstructions with resolutions from 17-20 Å. The models used for fitting the NSEM maps were PDB 6MYY, chains A, B and E only, for the SOSIP trimer, and PDB 4LST, chains H and L only, for the Fab. Models were manually docked into the NSEM maps, and fitting was refined as a rigid-body using Chimera's fitmap function. All figures of maps and models generated with UCSF Chimera.

Recombinant Soluble HIV-1 envelope SOSIP gp140 production

Recombinant SOSIP Env production was performed with Freestyle293 cells as previously described [317]. Briefly, Freestyle293 cells were diluted to 1.25 x 10^6 cells/mL with fresh Freestyle293 media to a volume of 1L on the day of transfection. The cells were then co-transfected with 650ug of SOSIP expressing plasmid DNA and 150ug of furin expressing plasmid DNA complexed with 293Fectin (ThermoFisher). Cell culture supernatants were harvested by centrifugation for 30 min at 3500 rpm on day 6 of culture. The collected filtered (0.8um filter) cell-free supernatant was concentrated to <100ml with a single-use tangential flow filtration cassette and 0.8um filtered again. PGT145 affinity

chromatography was used to purify the trimeric Env protein. PGT145-coupled resin was packed into Tricorn column (GE Healthcare) and stored in PBS with 0,05% sodium azide. Cell-free supernatant was applied to the column at 2mL/min using an AKTA Pure (GE Healthcare), washed, and protein was eluted off of the column with 3M $MgCl_2$. 10mM Tris pH8 was used to dilute the elute which was then 0.2um filtered and concentrated down to 2mL for size exclusion chromatography (SEC). SEC was performed with a Superose6 16/600 column (GE Healthcare) in 10mM Tris pH8, 500mM NaCl. Fractions containing the trimeric HIV-1 Env protein were pooled together, sterile filtered, snap frozen, and stored at -80°C.

Statistical Methods

Statistical analyses were performed using R statistical software (R Foundation for Statistical Computing, Vienna, Austria). All p-values are two-sided and considered significant at the 0.05 level.

A magnitude-breadth (M-B) curve describes the magnitude (neutralization titer) and breadth (proportion of isolates neutralized) of an individual sample against a panel of HIV-1 isolates, while the area under the curve (AUC) provides a summary value of the M-B profile. A partial M-B curve was used to illustrate binding antibody response magnitude (MFI) and breadth (the number of antigens with MFI > 100) of given HIV-1 *Env* breadth panels, its AUC-MB is the area under the M-B curve over the entire MFI range [318]. The AUC values between Virus Controllers and Elite Controllers and between high responders and low responders

were compared using the Mann-Whitney U test. FDR correction was applied to raw p-values to account for multiple testing.

For correlation with ADCP scores, neutralization breadth was defined as the number of isolates neutralized. ADCP breadth was defined as the average ADCP score across 3 viruses: BaL, CM235, and 1086C. Spearman's rank correlation coefficients and associated p-values were obtained using the *cor.test* function in R. Clustering of subjects was performed using the R function *kmeans* with default parameters.

Hierarchical clustering analysis was performed in R Studio using the pvclust package as previously described (https://github.com/shimo-lab/pvclust). Hierarchical clustering was done using the Euclidean distance measure and the Ward's minimum variance method. 10,000 bootstraps were performed, and rectangles were drawn around branches with approximately unbiased $p<0.05$. Two p-values were reported: Approximately Unbiased (AU) and Bootstrap Probability (BP) p-values, with the AU p-value computed by multiscale bootstrap resampling providing a better approximation to the unbiased p-value compared to the BP p-value computed by normal bootstrap resampling.

3.3 Results

A subset of HIV-1 VCs develops broadly neutralizing antibodies.

To determine the presence of nAb activity and better understand the breadth and magnitude of the nAb response in HIV-1 VCs and ECs (Tables 9 and 10) against HIV-1, plasma samples from HIV-1 Virus Controllers were tested using a standardized TZM-bl Nab assay against a standardized panel of 2 tier 1 and 9 tier 2 multi-subtype Env-pseudotyped HIV-1 viruses that represent the major global circulating strains of HIV-1 [305] (Table 11).

29 of the 30 patients neutralized the tier 1 strains (MN.3 – Tier 1 and X2278_C2_B6 – Tier 1B), while neutralization of the more difficult-to-neutralize tier 2 strains was limited to only a subset of the HIV-1 VC and EC patient cohort (Figure 7A). No neutralization against the negative control murine leukemia virus (MLV) confirms specificity of the HIV-1 Nab assay. 35% of the VC patients neutralized 80% of the strains, while 58% of the patients neutralize 50% of the strains, and 4 patients (VC N, VC AL, VC AP and VC AQ) neutralize all of the strains in the panel (Table 12).

Neutralization breadth was defined as the fraction of Env-pseudotyped HIV-1 viruses (tier 1 and tier 2 strains) neutralized with an infectious dose 50 (ID_{50}) titer greater than 30 (cut-off for positivity), while neutralization magnitude was defined as the natural logarithm of infectious dose 50 (ID_{50}) titer. Quantification of the neutralization magnitude and breadth in the HIV-1 VC cohort using the magnitude-breadth curve (M-B curve) [318, 319] showed that patients with a higher HIV-1

plasma viral load had a higher neutralization magnitude and breadth response compared to patients with undetectable HIV-1 plasma viral load (elite controllers), which was more pronounced for tier 1 viruses (Figure 7B).

A subset of the HIV-1 VC patients with Nab activity against both tier 1 and 2 viruses (6/31) developed broadly neutralization activity (Figure 7C), which is defined as having a geometric mean ID_{50} of greater than 100 and being able to neutralize 90% of the strains in the global panel with an ID_{50} greater than or equal to 100 [320, 321]. The frequency of patients with bNAbs in this patient cohort (about 20%) was comparable to previously report frequencies observed in another HIV-1 Virus Controller patient cohort (Boston area) [210] and also chronically-infected patients with very high viral loads [166, 295]. All the VC patients with bNAb activity were infected for at least 10 years (Figure 8).

Taken together, nAb analysis revealed the development of broadly neutralizing antibodies (bNAbs) in a subset of HIV-1 VCs (6/30 = 20%) that is partly influenced by viral load and infection duration.

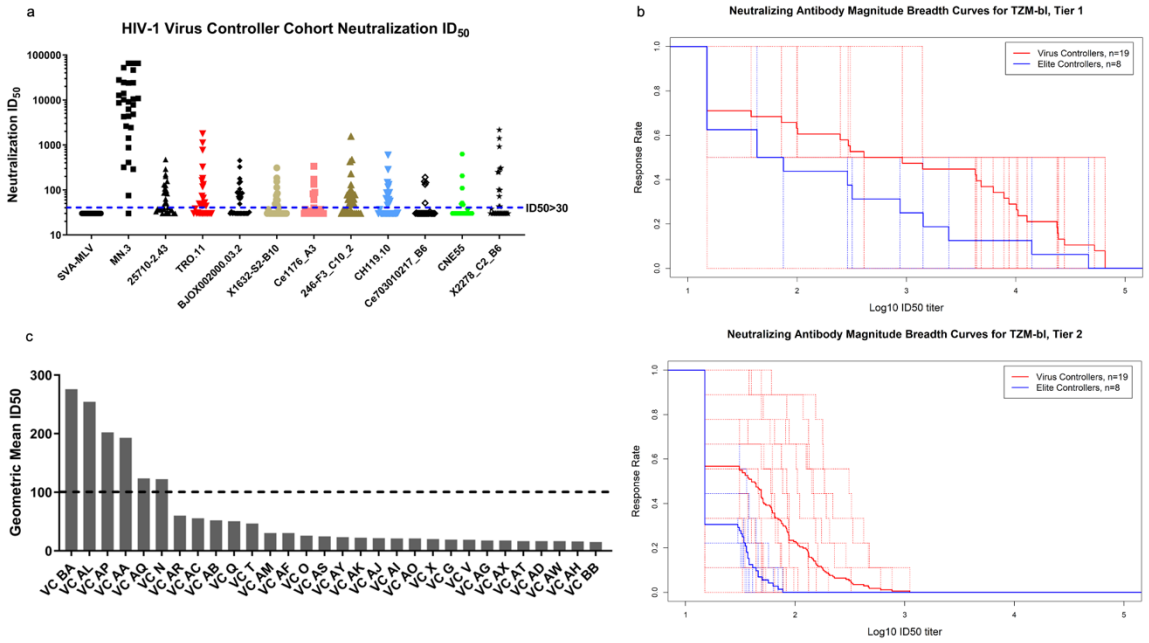

Figure 7: A subset of HIV-1 VCs develop bNAbs.

A. A 11 global virus panel was used to measure the magnitude and breadth of neutralizing antibodies (nAbs) in 30 HIV-1 Virus and Elite Controller plasma samples using a standardized TZMbl neutralization assay. Murine Leukemia Virus (MLV) was used as the negative control. The cut-off for a positive neutralization signal against the tested virus was ID_{50} > 30 based on the criterion of signal greater than or equal to three times that against the negative control MLV-pseudotyped virus. Each plasma sample was tested in triplicate against each virus in the panel. B. The nAb magnitude and breadth against Tier 1 and Tier 2 viruses for VCs and ECs were compared using the Magnitude-Breadth (M-B) Curve. (Tier 1 viruses Mean AUC: VCs = 2.840 and ECs = 2.216, Tier 2 viruses Mean AUC: VCs = 1.628 and ECs = 1.311). C. Identification of HIV-1 VC plasma samples with bNAb activity was done using the bNAb criteria of having a geometric mean ID_{50} >100 and also neutralizing 90% of the viruses in the neutralization virus panel with an ID_{50} of at least 100. All the patients above the black dotted line fit the bNAb criteria. D. Montefiori and C. LaBranche designed the TZMbl neutralization experiment, supervised the TZMbl neutralization experiment and analyzed the results. R. Spreng generated the neutralization M-B Curves under the direction of T. Nyanhete. T. Nyanhete designed the experiment, analyzed and interpreted the TZMbl neutralization and neutralization M-B Curves results.

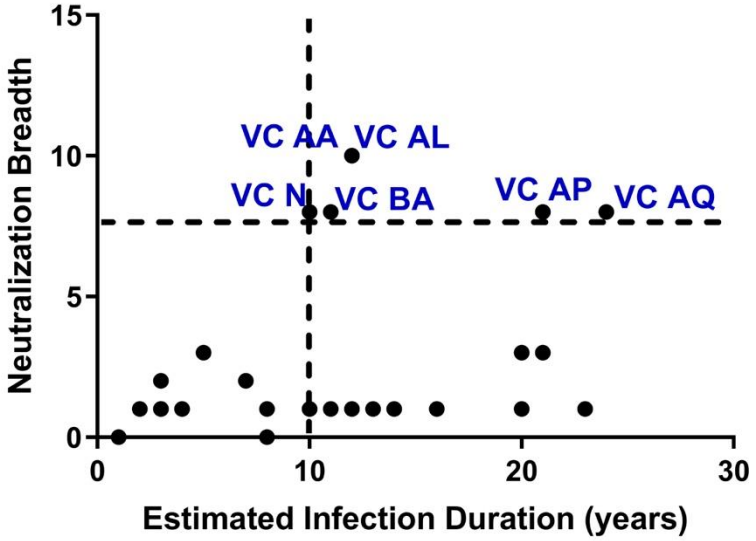

Figure 8: bNAb development in HIV-1 VCs is associated with infection duration.

Spearman correlation analysis of the neutralization breadth (the number of viruses neutralized with an ID_{50} of at least 100) and the estimated duration of infection based on the estimated date of diagnosis ($r = 0.465$, $p = 0.0084$). The HIV-1 VC patients in blue are the patients with bNAb activity and they have all been infected for at least 10 years. T. Nyanhete analyzed and interpreted the TZMbl neutralization and infection duration correlation results.

Heterogenous ADCP activity in HIV-1 VCs that correlates with nAb breadth.

To determine whether nAb breadth in HIV-1 VCs was associated with ADCP activity, I first tested whether that plasma IgG from the HIV-1 VCs can mediate ADCP of HIV-1 virions by THP-1 cells and whether this ADCP activity can target multiple clades of tier 2 HIV-1 Viruses (BaL -clade B, 1086C – clade C and CM235 - clade A/E) (Figure 11A). As observed with nAb activity, ADCP activity was also heterogenous in this patient group, with a combination of high and low ADCP scores reported for each virus (Figure 9A).

To determine the epitope exposure on the virus particles used for the ADCP experiments, the infectious virus capture assay [322] together with selected neutralizing and non-neutralizing mAbs were used to measure the bNAb and non-neutralizing epitope exposure on the viruses. All three viruses lacked exposure of the non-neutralizing CD4bs and V3 epitopes, and expressed the neutralizing CD4bs epitope, while only BaL and CM235 expressed the neutralizing V3 glycan epitope. The 1086C viruses expressed the non-neutralizing gp41 epitope targeted by the monoclonal antibody 7B2 (Figure 9B-D).

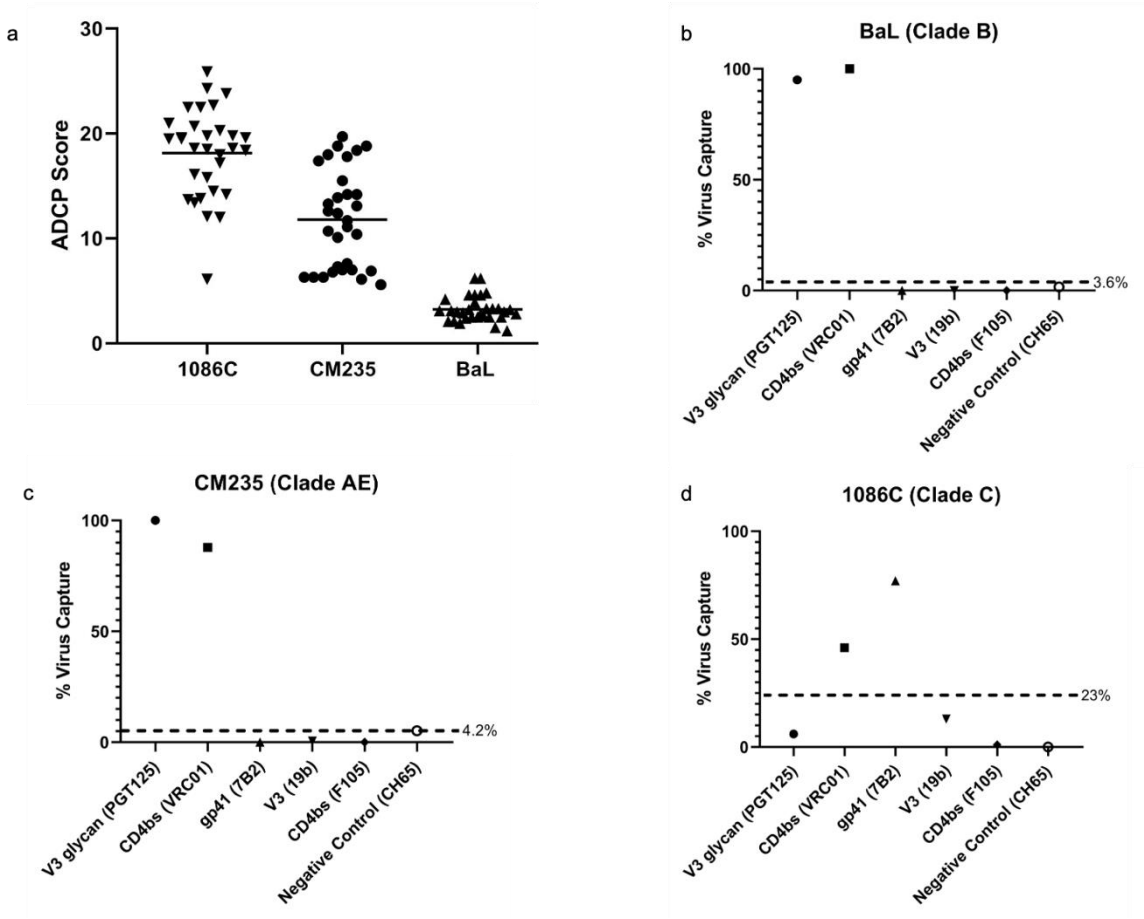

Figure 9: Heterogenous multi-clade virion ADCP in HIV-1 VCs and ECs.

A. The ability of purified IgG from HIV-1 VCs to internalize fluorescently labeled infectious Tier 2 viruses (1086C, CM235 and BaL) was measured in a THP-1 based ADCP assay. CH65 influenza mAb was used as the negative control in all assays, while CH31 mAb was the positive control for the BaL and CM235 viruses, and HIVIG for the 1086C virus. All assays were run in duplicate (%CV < 35%) and the ADCP score was calculated as described in the Materials and Methods section. Epitope exposure on the fluorescently labelled viruses BaL (B), CM235 (C) and 1086C (D) was represented as a % of virus particles captured by the representive mAb (bNAbs PGT125 and VRC01, non-neutralizing 19b, 7b2 and F105 mAbs) in an infectious virus capture assay. CH65 mAb and media only (RPMI) were used as negative controls. Positivity cut-off for virus capture was calculated as 3 times the media only % capture: BaL assay % capture cut-off = 3.6%, CM235 assay capture cut-off = 4.2%, and 1086C assay capture cut-off = 23.4%. The ability of each mAb to capture virus was measured in triplicate. T. Nyanhete designed the experiments, performed the experiments, analyzed and interpreted the results.

To investigate the possible coordination of neutralization breadth and virion ADCP activity in HIV-1 VCs and ECs, we calculated the Spearman correlation coefficient for the correlation between neutralization breadth and the ADCP score for both each virus and the ADCP breadth score.

Strong to moderate correlation of nAb breadth and ADCP activity was observed, with the patient cohort clade-mismatched virus, clade AE CM235 virus, having the highest correlation with neutralization breadth (Figure 10A). The viruses exposing neutralizing epitopes (BaL and CM235), mainly the CD4bs and V3 glycan epitopes, were also the ones that showed significant correlation with neutralization breadth ($r = 0.43$ and $p = 0.017$ for CM235) (Figure 10A), $r = 0.39$ and $p = 0.033$ for BaL) (Figure 10B), while ADCP scores for the 1086C virus that did not express the V3 glycan epitope had no significant correlation with nAb ($r = 0.26$ and $p = 0.166$)(Figure 10C). An ADCP breadth score was calculated by averaging the ADCP scores for the tier 2 Clade B (BaL), Clade C (1086C) and Clade AE (CM235)

viruses. Using the calculated ADCP breadth score, we observed a correlation between nAb breadth and ADCP breadth (r = 0.46 and p = 0.011) (Figure 10D). Of main interest was observation that the HIV-1 VC patients grouped into clusters of high ADCP/nAb breadth scores and low ADCP/nAb breadth scores (Figure 10D). This observed clustering was further confirmed using a hierarchical clustering approach (Figure 11). This approach showed the presence of 2 statistically significant distinct clusters which we referred to as high and low responder clusters, with the high responder cluster made up of HIV-1 VCs with both high nAb and ADCP breadth (Figure 11).

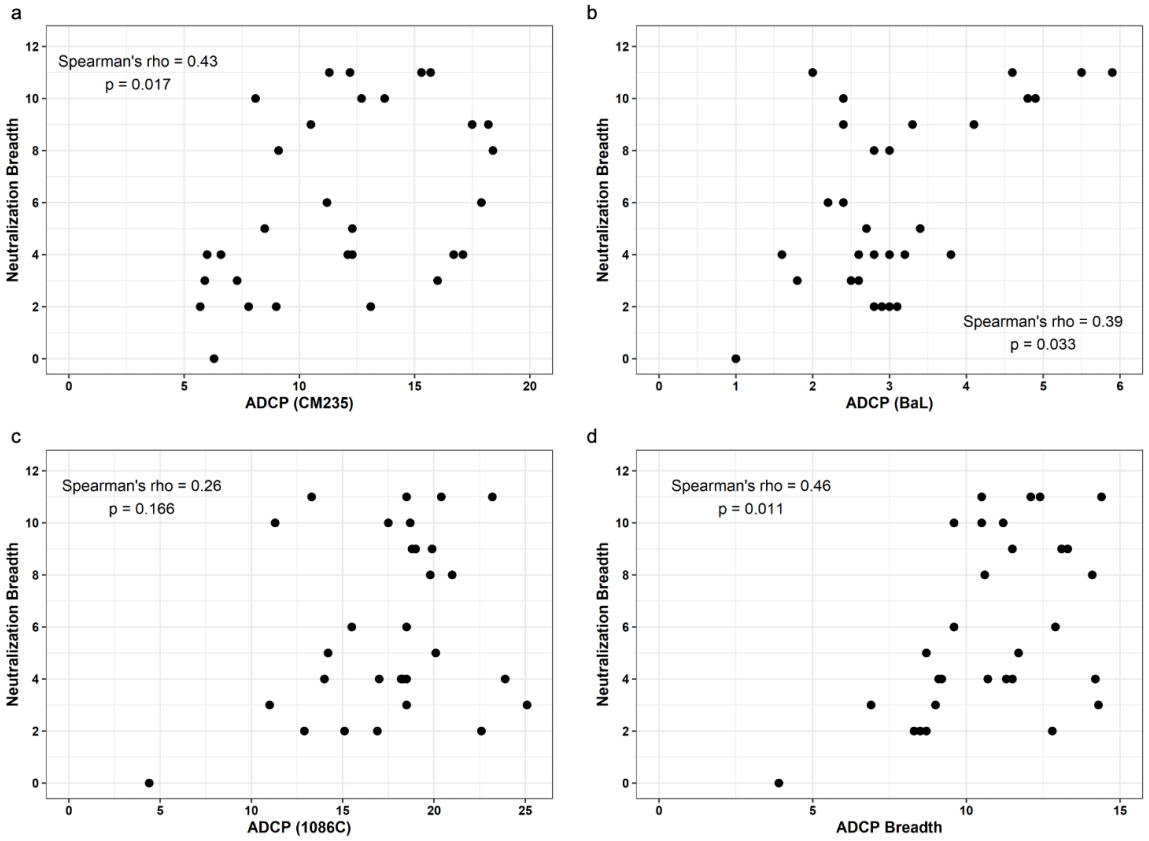

Figure 10: Heterogenous virion ADCP activity correlates with nAb breadth.

Spearman correlation coefficient was calculated for the correlation between neutralization breadth and BaL ADCP (A), CM235 ADCP (B) and 1086C ADCP (C). D. An ADCP Breadth score was calculated by averaging the ADCP scores for the BaL (Clade B), CM235 (Clade AE) and 1086C (Clade C) for each HIV-1 VC patient, and the resulting ADCP breadth score was correlated with the neutralization breadth for the same HIV-1 VC patient using the Spearman Correlation coefficient (statistical analysis by Dr. Rachel Spreng). T. Nyanhete designed the experiment, analyzed and interpreted the results.

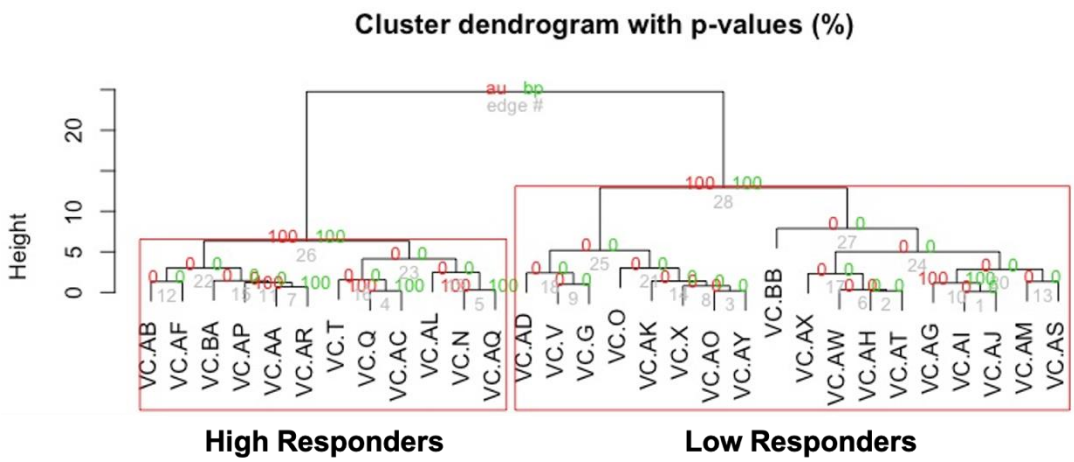

Figure 11: HIV-1 VCs and ECs cluster into distinct high and low responder groups.

Hierarchical clustering algorithm (pvclust) was used to group HIV-1 VC patients based on their virion ADCP and nAb breadth scores, with the algorithm separating out the HIV-1 VCs into two significantly distinct clusters: high responders (highest virion ADCP and nAb breadth scores) and low responders (have the lowest virion ADCP and nAb breadth scores). The Ward's minimum variance clustering method and Euclidean distance measures were used in the hierarchical clustering approach, with a p value of <0.05 denoting statistically distinct clusters. P value of a cluster indicates how strongly the cluster is supported by the data and it ranges from 0 to 1. Approximately Unbiased (AU) p-values are computed by multiscale bootstrap resampling and shown in red. Bootstrap Probability (BP) values are computed by normal bootstrap resampling and are shown in green. AU p-values represent the bias corrected BP values and are a better approximation to the unbiased p-value. T. Nyanhete designed the experiment, performed the clustering analysis, analyzed and interpreted the clustering analysis results.

The above findings demonstrated there is not only heterogenous ADCP activity, but also an association between nAb activity and ADCP activity. The HIV-1 VC and EC patients with high nAb breadth also exhibit high ADCP activity breadth.

ADCP and nAb breadth in HIV-1 VCs is influenced by IgG binding breadth, magnitude and avidity to HIV-1 *Env* monomeric and native-like trimeric HIV-1 *Env* glycoproteins

Given the heterogeneity of both the nAb and ADCP breadth and magnitude responses in the HIV-1 VCs, I hypothesized that IgG and IgG subclass binding magnitude and breadth stratified the high and low responder HIV-1 VCs.

IgG binding to target antigens is a prerequisite for antibody effector functions such as neutralization and ADCP, and specific subclasses such as IgG1 and IgG3 have been shown to be better suited for mediating neutralization and Fc effector functions [163, 225, 228]. Thus, to assess whether differential HIV-1 antigen binding breadth and magnitude define the ADCP and neutralization heterogeneity observed in the HIV-1 VC cohort, I measured the binding magnitude of IgG, IgG1, IgG2 and IgG3 from the patients with high nAb/ADCP breadth scores (high responder cluster) and patients with low nAb/ADCP breadth scores (low responder clusters) to global HIV-1 *Env* glycoprotein gp120 (Table 13), gp140 (Table 14) and V1V2 (Table 15) antigen breadth panels [309]. These HIV-1 *Env*

breadth panels broadly map antibody responses with minimal redundancy [309]. IgG, IgG1, IgG2 and IgG3 binding to the HIV-1 Env V1V2 antigens, together with IgG3 binding to gp140 and gp120 antigen breadth panels did not separate out high and low responders (Extended Data 7B, Extended Data 8B, Extended Data 9B and Extended Data 10B). HIV-1 VC patients with high nAb and ADCP (high responder cluster) exhibited higher IgG (Figure 12A) and IgG1 (Figure 12B) binding breadth and magnitude to gp120 and gp140 antigens, and also higher IgG2 (Figure 12C) binding breadth and magnitude to gp140 antigens.

I also measured the binding avidity of IgG, IgG1, IgG2 and IgG3 from the high, intermediate and low responder clusters to HIV-1 monomeric gp120, gp140 and V1V2 breadth panels [309]. IgG, IgG1, IgG2 and IgG3 binding avidity to the HIV-1 Env V1V2 antigens, together with IgG1 binding avidity to gp120, IgG2/IgG3 binding avidity to gp140 and gp120 antigen breadth panels did not separate out high and low responders (Extended Data 7A, Extended Data 8A, Extended Data 9A and Extended Data 10A). However, HIV-1 VC patients with high nAb and ADCP breadth (high responder cluster) had high avidity IgG (Figure 13A) and IgG1 (Figure 13B) responses that exhibit higher binding breadth and magnitude to gp120 and gp140 respectively (Figure 13).

Table 13: HIV-1 Env gp120 Breadth Panel.

HIV-1 Env gp120 Glycoproteins from Diverse HIV-1 Clades Selected Based on Genetic and Geographic Diversity to Cover the Global Epidemic [309]

ANTIGEN NAME	CLADE	COUNTRY OF ORIGIN
51802_D11gp120	A1	Kenya
BORI_D11gp120	B	USA
TT31P.2792_D11gp120	B	Trinidad/Tobago
B.6240_D11gp120	B	USA
A244_D11gp120	CRF01-AE	Thailand
254008_D11gp120	CRF01-AE	Thailand
CNE20_D11gp120	CRF07-BC	China (Xinjiang)
BJOX002_D11gp120	CRF07-BC	China (Bejing)

Table 14: HIV-1 Env gp140 Breadth Panel.

HIV-1 Env gp140 Glycoproteins from Diverse HIV-1 Clades Selected Based on Genetic and Geographic Diversity to Cover the Global Epidemic [309]

ANTIGEN NAME	CLADE	COUNTRY OF ORIGIN
9004S.gp140C	A1	Uganda
RHPA4259_C7.gp140C	B	USA
SC42261_gp140	B	Trinidad/Tobago
WITO4160.gp140C	B	USA
BF1266_gp140C	C	Malawi
1086C_gp140C	C	Malawi
C.CH505TF_gp140	C	Malawi
AE.01.con_env03 gp140CF	AE Consensus	

Table 15: HIV-1 Env V1V2 Breadth Panel.

HIV-1 Env V1V2 Glycoproteins from Diverse HIV-1 Clades Selected Based on Genetic and Geographic Diversity to Cover the Global Epidemic [309]

ANTIGEN NAME	CLADE	COUNTRY OF ORIGIN
gp70-191084_B7 V1V2	A	Uganda
gp70-B.CaseA_V1_V2	B	USA
gp70-RHPA4259.7 V1V2	B	USA
gp70-62357.14 V1V2	B	USA
gp70-700010058 V1V2	B	USA
gp70-TT31P.2F10.2792 V1V2	B	Trinidad/Tobago
gp70-BF1266_431a_V1V2	C	Malawi
gp70-7060101641 V1V2	C	South Africa
gp70-96ZM651.02 V1V2	C	Zambia
gp70-001428.2.42 V1V2	C	India
gp70-CAP210.2.00.E8 V1V2	C	South Africa
gp70-TV1-21 V1V2	C	South Africa
gp70-Ce1086_B2 V1V2	C	Malawi
gp70-CM244.ec1 V1V2	CRF01_AE	Thailand
gp70-C2101.c01_V1V2	CRF01_AE	Thailand
gp70-BJOX002000.03.2 V1V2	CRF07-BC	China

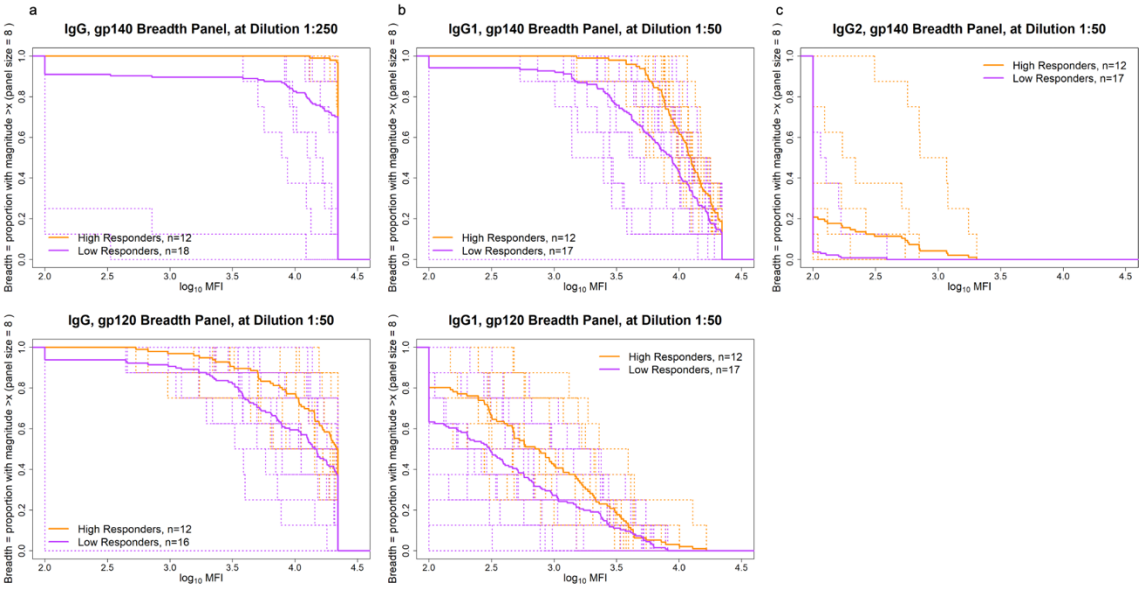

Figure 12: IgG, IgG1 and IgG2 binding magnitude and breadth against global HIV-1 Env gp120 and gp140 antigen breadth panels is higher in high responders compared to low responders.

BAMA was used to measure the IgG (A), IgG1 (B) and IgG2 (C) binding magnitude of HIV-1 VC patients in the high and low responder groups to the gp120 and gp140 breadth panels described in Tables 13 and 14, and the area under the curve (AUC) of the IgG (A), IgG1 (B) and IgG2 (C) binding to the gp120 and gp120 breadth panels was measured using the Magnitude-Breadth (M-B) Curve as described in the Materials and Methods section. M-B Curve AUC min – max scores: IgG (gp140) – High Responders (HR) = 4.3143 – 4.3424 and Low Responders (LR) = 2.0656 – 4.3424; IgG (gp120) – HR = 3.8263 – 4.3238 and LR = 2 - 4.299; IgG1 (gp140) – HR = 3.8709 - 4.2249 and LR = 2 – 4.1973; IgG1 (gp120) – HR = 2.4671 – 3.3905 and LR – 2 – 3.1727; IgG2 (gp140) – HR = 2 – 2.9555 and LR = 2 – 2.1472. All BAMA assays were performed in duplicate (%CV <15% between sample replicates). T. Nyanhete designed the experiments, performed the experiments, analyzed and interpreted the BAMA M-B Curve results. BAMA M-B Curves generated by L. Zhang under the direction of T. Nyanhete.

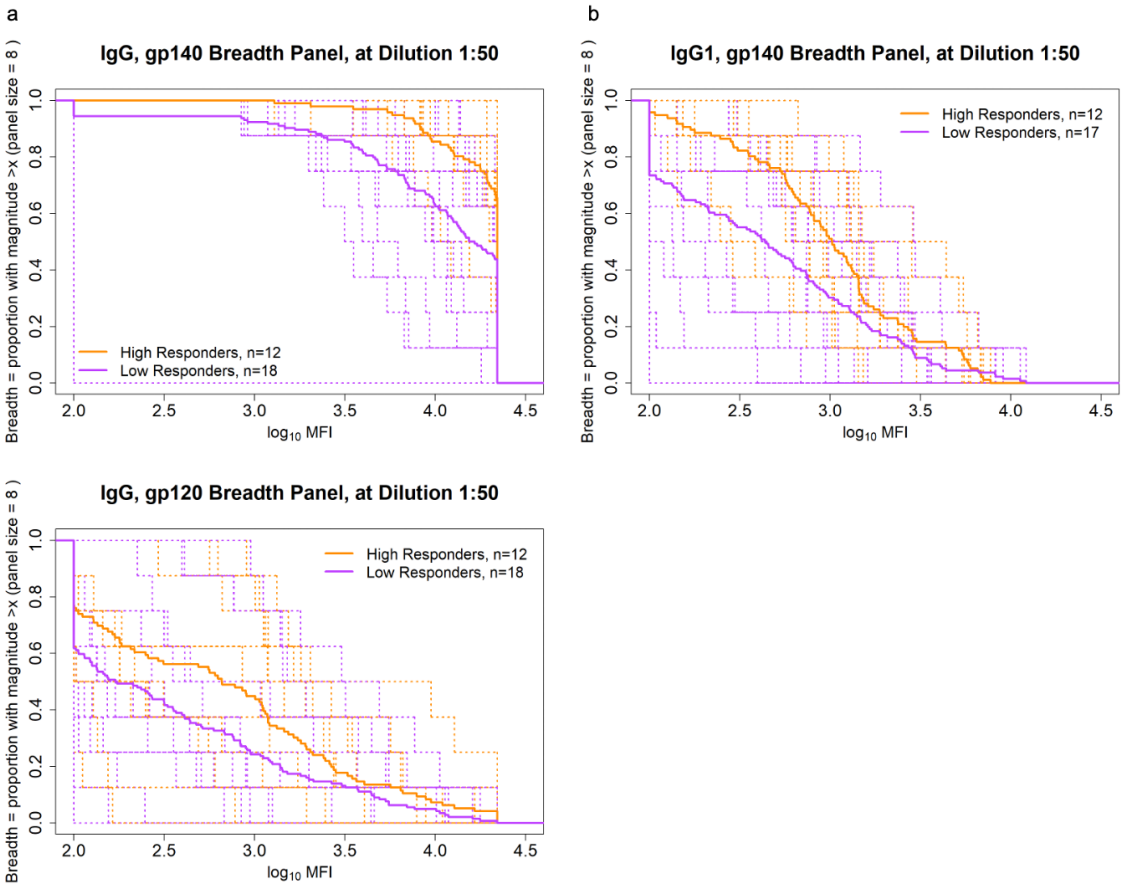

Figure 13: IgG and IgG1 binding avidity and breadth against HIV-1 Env gp120 and gp140 antigen breadth panels separates out high from low responders.

BAMA was used to measure the IgG (A) and IgG1 (B) binding avidity to the gp120 and gp140 breadth panels after treatment with citrate buffer, and the area under the curve (AUC) of the IgG binding avidity to the gp120 breadth panel was measured using the M-B Curve as described in the Materials and Methods section. M-B Curve AUC min – max scores: IgG (gp140) – High Responders (HR) = 4.0137 – 4.3424 and Low Responders (LR) = 2 – 4.3159; IgG (gp120) – HR = 2.0821 – 3.6676 and LR = 2 – 3.4685; IgG1 (gp140) – HR = 2.4911 – 3.3638 and LR = 2 – 3.4167. All BAMA assays were performed in duplicate (%CV <15% between sample replicates). T. Nyanhete designed the experiments, performed the experiments, analyzed and interpreted the BAMA M-B Curve results. BAMA M-B Curves generated by L. Zhang under the direction of T. Nyanhete.

Previous studies have shown that antibody binding to the trimeric HIV-1 envelope rather than binding to monomeric HIV-1 gp120 is a better predictor of

functional IgG responses (nAb response) since trimeric envelope glycoproteins are the targets for nAbs [148, 323]. Neutralization-guided down-selection of the ideal recombinant trimeric HIV-1 Envelope glycoprotein (SOSIP) (Extended Data 11) to use was done based on the sensitivity of HIV-1 sequences from the 3 commonly used SOSIP candidates to neutralization by the HIV-1 VC patients with bNAb activity. I choose to use BG505gp140 T332N SOSIP.664 because it was sensitive to neutralization by all six HIV-1 VC plasma samples (Extended Data 11). BG505gp140 T332N SOSIP.664 also happens to be the most widely used recombinant HIV-1 Envelope trimer that has also been used in rabbit immunization studies that generated autologous nAbs [147, 149].

Biolayer interferometry (BLI) was used for the biophysical characterization of the polyclonal IgG Fab interactions with the recombinant trimeric HIV-1 envelope (BG505gp140 T332N SOSIP.664) in real time. Prior to measuring SOSIP interactions with HIV-1 specific IgG from high and low responders, I first confirmed that immobilization of the biotinylated BG505gp140 T332N SOSIP.664 on streptavidin BLI biosensors does not result in conformational changes of the SOSIP and exposure of non-neutralizing epitopes as indicated by lack of binding of non-neutralizing mAbs (19b CL2 and F105) to the immobilized BG505gp140 T332N SOSIP.664 (Figure 14A). Using a subset of high responders (VC AL, VC AA, VC AP, VC AQ, VC N and VC BA) and low responders (VC AI, VC AW, VC AX, and VC BB), I show that only high responders exhibit IgG Fab binding to the BG505gp140 T332N SOSIP.664, while no binding to the SOSIP is observed with

the low responder HIV-1 VC patients (Figure 14B). This remarkable finding further highlighted that the BG505gp140 T332N SOSIP.664 trimer, a good mimic of a functional HIV-1 *Env,* could accurately differentiate HIV-1 VC patients with polyfunctional polyclonal plasma responses (ADCP and nAb breadth) from those with no to limited nAb/ADCP breadth activity.

To investigate the presence of any downstream effector function after binding to the native-like trimeric HIV-1 *Env* glycoproteins (SOSIPs), I tested the ability of IgG from both low and high responder HIV-1 VCs to mediate phagocytosis of the clade-mismatched native-like trimeric HIV-1 *Env* glycoprotein BG505gp140 T332N SOSIP.664 conjugated onto carboxylated beads. Unlike all of the low responders, only a subset of high responders (VC AP, VC AL, VC AB) were able to mediate internalization of both trimeric HIV-1 *Env* glycoproteins (Figure 14C) thus further demonstrating that only patients with high nAb and ADCP breadth response can not only bind to the HIV-1 *Env* but also mediate phagocytosis of the HIV-1 *Env*. Thus, confirming that binding to the HIV-1 *Env* can lead to downstream effector functions such as ADCP.

Taken together, the IgG and IgG Fab binding data shows that HIV-1 antigen binding breadth, magnitude, avidity and binding kinetics with the native-like trimeric HIV-1 *Env* glycoproteins can distinguish high responders from low responders (defined by clustering HIV-1 VC patients using their ADCP and nAb breadth scores).

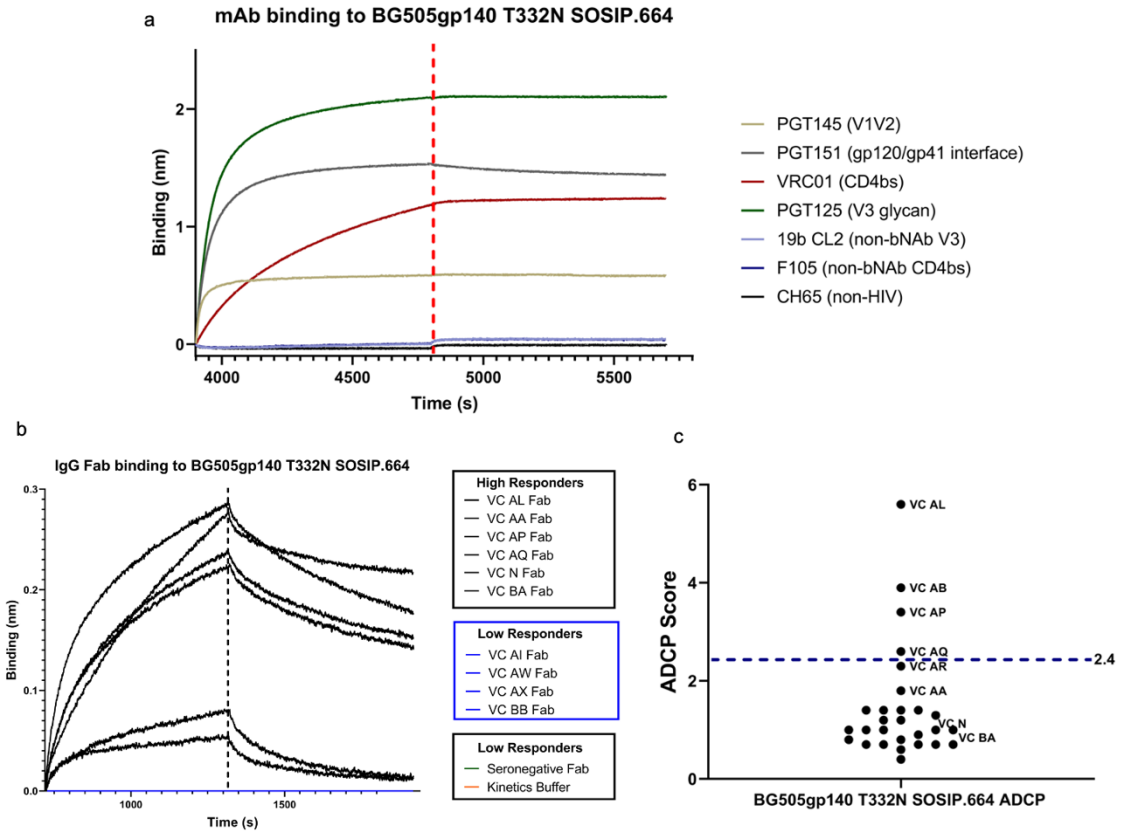

Figure 14: HIV-1 IgG and Fab binding to the trimeric native-like recombinant HIV-1 Env is only observed in the high responder group.

A. Epitope exposure on the BG505/T332N SOSIP.664 was measured by testing the binding of a panel mAbs (with and without bNAb activity) (20ug/ml) to the BG505 SOSIP.664 immobilized to streptavidin biosensors in a BLI assay. The influenza CH65 mAb was used as the negative control, and BSA immobilized to the streptavidin biosensor was used for reference (background) subtractions. This assay was done in duplicate. B. A subset of high and low responder IgG Fab fragments (200ug/ml) were tested for their ability to bind to BG505/T332N SOSIP.664 immobilized to streptavidin biosensors in a BLI assay. IgG Fab from a healthy donor (seronegative Fab) and a kinetics buffer solution were used as negative controls. BSA immobilized to the streptavidin biosensor was used for reference (background) subtractions. This assay was done in duplicate. C. The ability of purified IgG from HIV-1 VCs to form immune complexes with and mediate ADCP of BG505/T332N SOSIP.664 conjugated to 1um fluorescent beads was measured in a THP-1 ADCP assay. The bNAbs PGT125, PGT145, PGT151 and VRC01 were used as positive controls, while the non-neutralizing mAb F105 and CH65 were used as negative controls. Positive ADCP signal (above the blue dotted line) was calculated as 3X the ADCP score for the negative control CH65 mAb which was a score of 0.8. The assay was run in duplicate (%CV < 35% between replicates). T. Nyanhete designed the experiments, performed the experiments, analyzed and the interpreted the results.

High responder HIV-1 VCs with bNAb activity bind to conserved vulnerable sites on the HIV-1 Envelope

Given that 6 high responder VC patients with bNAb activity (Figure 7C) displayed binding to the recombinant trimeric HIV-1 *Env*, BG505gp140 T332N SOSIP.664, I hypothesized that this binding indicated the presence of bNAbs targeting both known and potentially novel previously unidentified vulnerable regions on the HIV-1 *Env*. To determine whether the polyclonal antibody response from HIV-1 VCs with bNAb activity targeted previously characterized vulnerable bNAb epitopes, I performed epitope mapping of the polyclonal plasma and purified IgG from these patients.

Mapping of the polyclonal HIV-1 antibody response was first done using the neutralization fingerprinting assay [146] that predicts epitope specificities of polyclonal antibody responses to HIV-1 infection. Epitope specificities of the nAbs in the plasma from the 6 VC patients was elucidated from the plasma pattern of neutralization against a panel of optimized 30 HIV-1 isolates (Table 12). The neutralization profile (fingerprint) of the 6 VC plasma samples were compared with a reference set of 10 epitope-specific neutralization profiles representing distinct epitope specific antibody clusters [146]. This computational approach predicted the prevalence of PGT128-like (V3 Glycan), 10E8-like (MPER) and VRC01-like (CD4bs) bNAb responses in the tested VC patients, with the polyclonal antibody response characterized by targeting of multiple bNAb specificities – VC N (V3 glycan and MPER), VC AA (V3 glycan, MPER and gp120-gp41 interface), VC AL

(V3 glycan and MPER), VC AP (CD4bs and V3 glycan), VC AQ (CD4bs and V3 glycan), and VC BA (V3 glycan only) (Figure 15A). The presence of VRC01-like bNAb activity in some of the VC patients (VC AP and VC AQ), a broad and potent class of bNAbs targeting a functionally conserved epitope less masked by the glycan shield [135], was confirmed by measuring the IgG differential binding to RSC3 and RSC3Δ371I/P363N in a binding antibody multiplexed assay (BAMA) (Table 16) and also in a BLI assay (Fig 15B). Both BAMA (Table 16) and BLI (Fig 15B) showed the presence of CD4bs-specific IgG in VC AP and VC AQ.

a

	CD4bs			V2	V3	MPER		gp120-gp41 interface			
serum	VRC01-like	b12-like	HJ16-like	PG9-like	PGT128-like	2F5-like	10E8-like	35O22-like	PGT151-like	8ANC195-like	Neut breadth (%)
VC N		0.17			0.37		0.37			0.09	73%
VC AA				0.05	0.31		0.24	0.07	0.25	0.08	33%
VC AL			0.11		0.33	0.01	0.48			0.07	83%
VC AP	0.50				0.36	0.04	0.00	0.10			90%
VC AQ	0.40		0.04		0.37		0.19	0.01			77%
VC BA	0.06	0.02			0.39	0.22	0.22			0.08	63%

b

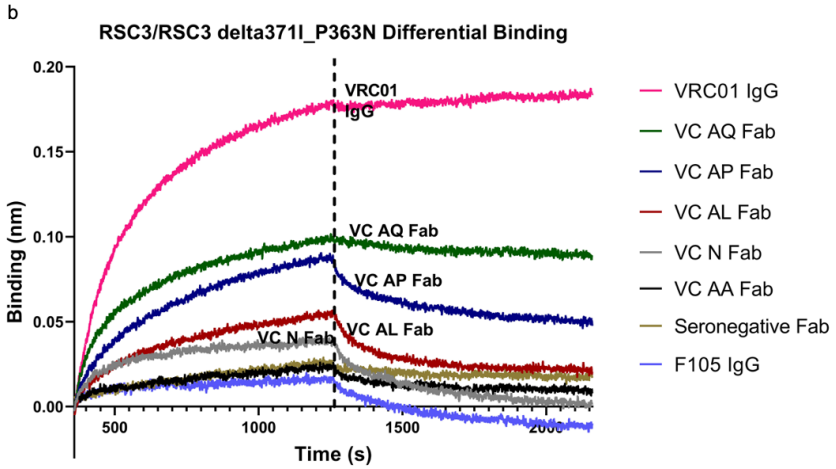

Figure 15: HIV-1 VC patients with bNAb activity bind to previously characterized vulnerable epitopes on the HIV-1 Envelope.

A. Neutralization Fingerprinting (NFP) algorithm was used to predict the plasma neutralization pattern of the HIV-1 VCs with bNAb activity against a panel of diverse HIV-1 isolates shown in Table. For each HIV-1 VC plasma sample, the predicted prevalence of each of the reference bNAb cluster is shown as a score ranging from 0 – 1, where scores greater than or equal to 0.25 signals the presence of a neutralization pattern by the bNAb cluster and scores closer to 1 represents stronger neutralization signal by the bNAb cluster. Breadth represents the percentage of viruses neutralized with an $ID_{50} > 40$. The neutralization assay was performed in triplicate. B. Resurfaced Core Protein (RSC3) and its mutant RSC3 delta 371I/P363N are protein probes that can be used to pick out binding to the CD4bs that is VRC01-like. IgG Fab binding to the RSC3 immobilized to streptavidin biosensors was measured using BLI, and binding to the mutant RSC3 delta 371I/P363N was used for reference subtraction. IgG Fab from a healthy donor (seronegative Fab) was used as a negative control together with the non-neutralizing mAb F105, while VRC01 was used as the positive control. IgG Fab binding to RSC3 and RSC3 delta 371I/P363N was done in duplicate. I. Georgiev designed and performed the NFP computational modeling (17A). T. Nyanhete designed the experiments, performed the BLI experiment (17B), analyzed and interpreted the NFP and BLI results.

Table 16: HIV-1 VC High Responders Possess VRC01-like CD4bs Antibodies.

Differential binding of HIV-1 VC IgG from a subset of high responders (HR) and low responders (LR) to wild type (WT) RSC3 and the RSC3Δ371I/P363N mutant with mutations that diminish binding to VRC01 and b12. A differential binding ratio >2.5 (in black bold) represents the presence of VRC01 or b12-like CD4bs antibodies. T. Nyanhete designed the experiment, performed the experiment, analyzed and interpreted the results.

Patient	Cluster	WT RSC3	RSC3 Mutant	WT/Mutant Ratio
VC N	HR	630	100	**6.3**
VC AA	HR	216	377	0.6
VC AL	HR	2597	581	**4.5**
VC AP	HR	1236	142	**8.7**
VC AQ	HR	10741	100	**107.4**
VC BA	HR	625	100	**6.3**
VC AI	LR	100	100	1
VC AW	LR	304	316	1
VC AX	LR	100	100	1
VC BB	LR	100	100	1
VRC01	CD4bs bNAb	27247	114	**239**

To investigate the functional relevance of targeting of the vulnerable epitopes of interest highlighted by the neutralization fingerprinting assay (Figure 16A), we mapped the nAb specificities in plasma samples that neutralized the parent virus with a titer ID_{50} >100. Based on this criteria, the parent viruses TRO.11 (Tier 2), COT6 (Tier 2), JR-FL (Tier 1) and CH505TF (Tier 2) were down-selected for use in the epitope mapping TZM-bl neutralization assay, and these viruses had

variants with mutations in the CD4bs (Figure 16A), MPER (Figure 16B), V3 glycan (Figure 17A), and gp120-gp41 interface (Figure 17B) epitopes of interest plus the vulnerable V2 glycan epitope (Figure 17B) that is also known to be targeted by bNAbs [144, 145]. A three-fold decrease in the neutralization titer (ID_{50}) in the mutant compared to the wild-type parent virus indicates dependency on that mutation for neutralization sensitivity. For all the wild-type parent/mutant variants pairings, only the mutation in the V3 glycan epitope (N332A) in the TRO.11 virus resulted in at least a 3-fold decrease in neutralization titer for VC BA (Figure 17A). None of the other tested epitope mutations in the down-selected parent viruses of choice resulted in loss of neutralization sensitivity to VC N, VC AA, VC AL, VC AP and VC AQ plasma (Figures 16 and 17) despite the predicted presence of IgG responses against the tested epitopes (Figure 15 and Table 16). In some instances, mutations in vulnerable epitopes resulted in a significant increase (>3 fold) in neutralization titer compared to the parent wild-type (represented in italics) –CD4bs G458Y mutation increased sensitivity of TRO.11 to neutralization by VC AA plasma (Figure 16A), while the MPER W672A mutation increased sensitivity of TRO.11 and COT6,15 viruses to neutralization by VC AL plasma (Figure 16B), and the V3 glycan ADIR.4 mutation increased sensitivity of JR-FL to neutralization by VC N, VC AA, VC AL, VC AP and VC AQ plasma (Figure 17A).

Taken together, the above results emphasize the polyclonal nature of the nAb response in the patients with bNAb activity where multiple known vulnerable bNAb epitopes are targeted by the polyclonal nAb response in these patients (as

shown in the NFP results) (except for VCBA where there is only one dominant targeted epitope, V3 glycan) and hence providing a synergistic effect contributing to the neutralization of HIV-1 viruses tested in this study.

a

		ID_{50} Titer in TZMbl Cells						IC_{50} Titer
Virus Name	Target	VC N	VC AA	VC AL	VC AP	VC AQ	VC BA	VRC01
TRO.11	WT	436	171	990	794	189	1454	0.45
TRO.11.N280D	CD4bs	419	475	582	1172	95	1521	**>16.7**
TRO.11.S365P.3	CD4bs	503	343	2535	1973	428	1046	
TRO.11.G458Y	CD4bs	834	*1120*	1532	*2355*	329	2179	>16.7
TRO.11.N279A	CD4bs	739	*839*	1447	1650	245	2329	**>16.7**
CH505TF	WT				738	99		**0.12**
CH505TF.N280D	CD4bs				894	<30		**>16.7**
CH505TF.S365P.5	CD4bs				1400	122		
CH505TF.G458Y.4	CD4bs				2034	198		**>16.7**

b

		ID_{50} Titer in TZMbl Cells						IC_{50} Titer
Virus Name	Target	VC N	VC AA	VC AL	VC AP	VC AQ	VC BA	10E8
TRO.11	WT	436	171	990	794	189	1454	0.08
TRO.11.W672A	MPER	587	408	*6253*	1577	524	1582	**>16.7**
COT6.15	WT	74	88	276	72			0.08
COT6.15_W672A	MPER	108	189	*1020*	3404	324	36	>3.3

Figure 16: No dominant CD4bs or MPER epitopes that mediate neutralization by HIV-1 VC plasma.

The ability of HIV-1 VC plasma to neutralize TRO.11, CH505TF and COT6.15 wild type viruses, together with their mutant counterparts was assayed in a TZMbl neutralization assay. The mAbs VRC01 (A) and 10E8 (B) were used as positive controls for targeting of the CD4bs and MPER epitopes, respectively. The IC_{50} values are reported for the mAbs, while ID_{50} values are reported for the HIV-1 VC plasma samples. Lower IC_{50} represents better neutralization, while higher ID_{50} represents better neutralization. ID_{50} values >30 are considered positive for neutralizing antibody activity based on the criterion

of signal >= 3 times that against the negative control murine leukemia virus (MLV)-pseudotyped virus. A three-fold decrease in the neutralization titer (ID_{50}) (only ID_{50} values above 100 for the WT virus are considered) in the mutant compared to the wild-type parent virus (denoted by black, bold type) indicates a loss in neutralization sensitivity as a result of the corresponding mutation. Black italics values denote HIV-1 VC plasma samples whereby the ID_{50} had a three-fold increase as a result of the corresponding mutation and hence indicating improved neutralization sensitivity. C. LaBranche and A. Eaton designed and supervised the TZMbl neutralization epitope mapping assay. T. Nyanhete designed, analyzed and interpreted the TZMbl neutralization epitope mapping assay results.

a

		ID_{50} Titer in TZMbl Cells						IC_{50} Titer	
Virus Name	Target	VC N	VC AA	VC AL	VC AP	VC AQ	VC BA	PGT128	PGT121
TRO.11	WT	436	171	990	794	189	1454	0.05	0.02
TRO.11.N332A	V3-glycan	189	61	926	782	137	**169**	**>3.3**	
JR-FL	WT	253	255	2625	3367	315	87	0.05	0.04
JR-FL.N332A.67A.6	V3-glycan	190	197	3836	3404	324	36	**>3.3**	**>3.3**
JR-FL.ADIR.4	V3-glycan	*1786*	*4815*	*25555*	4927	*1044*	1810	**>3.3**	**0.43**
JR-FL.GAIR.4	V3-glycan	231	429	3782	3523	516	130	**0.66**	**0.66**
JR-FL.GDAR.2	V3-glycan	269	469	2247	2634	294	149	0.06	**0.09**
JR-FL.GDIA.3	V3-glycan	213	572	2146	2773	265	158	**0.62**	**0.08**
JR-FL.GAIA.4	V3-glycan	265	722	2339	4156	375	127	**>3.3**	**>3.3**
JR-FL.V1_3Q	V3-glycan	316	281	5696	3841	360	70	0.01	0.01

b

		ID_{50} Titer in TZMbl Cells						IC_{50} Titer	
Virus Name	Target	VC N	VC AA	VC AL	VC AP	VC AQ	VC BA	PG16	2G12
TRO.11	WT	436	171	990	794	189	1454	2.2	0.52
TRO.11.N160K	V2-glycan	320	84	1020	917	171	1450	**>6.7**	
TRO.11.N295V	2G12	209	74	731	575	123	489		**>16.7**
TRO.11.N88A	gp120-gp41	350	283	1639	974	160	1390		
TRO.11.N611A	gp120-gp41	329	135	895	792	212	938		

Figure 17: The N332A V3 glycan mutation desensitizes the TRO.11 virus to neutralization by HIV-1 VC BA plasma.

The ability of HIV-1 VC plasma to neutralize TRO.11 and JR-FL wild type viruses, together with their mutant counterparts (V3 glycan mutants for TRO.11 and JR-FL (A), gp120-gp41 interface mutants for TRO.11 (B), V2 glycan mutant for TRO.11 (B), and

2G12 epitope mutant for TRO.11 (B)) was assayed in a TZMbl neutralization assay. The mAbs PGT121 and PGT129 for the V3 glycan (A), PG16 for the V2 glycan (B), 2G12 for the 2G12 epitope (B), and CH01-31 for the gp120-gp41 interface (B) were used as positive controls. The IC_{50} values are reported for the mAbs, while ID_{50} values are reported for the HIV-1 VC plasma samples. Lower IC_{50} represents better neutralization, while higher ID_{50} represents better neutralization. ID_{50} values >30 are considered positive for neutralizing antibody activity based on the criterion of signal >= 3 times that against the negative control murine leukemia virus (MLV)-pseudotyped virus. A three-fold decrease in the neutralization titer (ID_{50}) (only ID_{50} values above 100 for the WT virus are considered) in the mutant compared to the wild-type parent virus (denoted by black, bold type) indicates a loss in neutralization sensitivity as a result of the corresponding mutation and hence a dependency on that mutation for neutralization sensitivity. Black italics values denote HIV-1 VC plasma samples whereby the ID_{50} had a three-fold increase as a result of the corresponding mutation and hence indicating improved neutralization sensitivity. C. LaBranche and A. Eaton designed and supervised the TZMbl neutralization epitope mapping assay. T. Nyanhete designed, analyzed and interpreted the TZMbl neutralization epitope mapping assay results.

nsEM analysis of polyclonal HIV-1 VC Fab-Env complexes reveal dominant CD4bs antibody class in HIV-1 VCs

The lack of loss of neutralization sensitivity after mutating single known bNAb epitopes led me to hypothesize that HIV-1 VC nAbs target multiple known and novel unidentified epitopes that act in concert to mediate neutralization of target viruses. I also hypothesized that dominant antibody responses in polyclonal HIV-1 VC plasma could be mapped by direct electron microscopy of polyclonal antibody complexed with recombinant HIV-1 *Env.* It is possible that the nAb activity in HIV-1 VCs might be directed to novel, previously unidentified epitopes on the trimeric HIV-1 envelope which might also be involved in the controller status unique to this patient cohort.

To avoid the limitation of only focusing on already known targeted epitopes from non-controller (chronic progressor) studies and potentially identify novel

classes of antibodies targeting previously unidentified epitopes or with different *Env* binding profiles (angle of approach and binding stoichiometry), we employed a novel recently described method [147] that involves directly imaging immune complexes formed between the BG505gp140 T332N SOSIP.664 and polyclonal plasma antibodies by negative stain electron microscopy (nsEM). Protein A purified polyclonal IgG antibodies from one of the six patients with bNAb activity (VC AQ) were processed into Fabs with immobilized papain and then subjected to quality control using SDS-PAGE (purity and correct size) prior to incubation with the BG505gp140 T332N SOSIP.66 to form Fab-SOSIP immune complexes (ICs). The ICs were then deposited onto nsEM grids and imaged using nsEM. 25,720 image particles consisting of bare (unliganded) and Fab-bound SOSIPs were selected for 3D classification and 3D refinement which showed the presence of a predominant CD4bs antibody class in VC AQ (Figure 18).

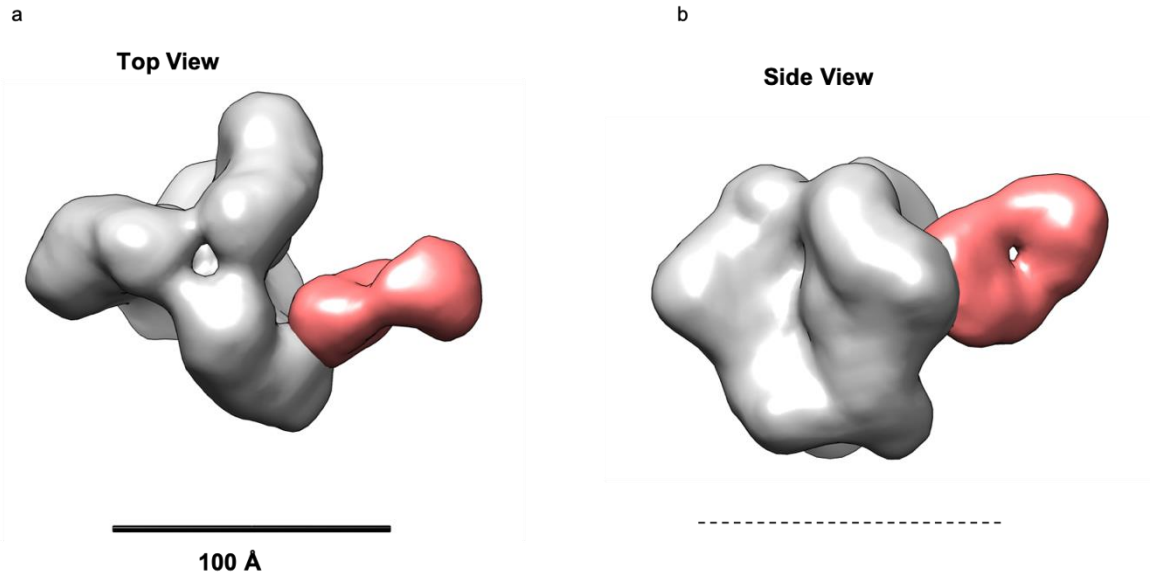

Figure 18: CD4bs antibodies in HIV-1 VC AQ.

Top view (A) and side view (B) of the VC AQ Fab (red) bound to the CD4bs region on the HIV-1 BG505gp140 T332N SOSIP.664 (grey). Two Fab-bound classes that were identical within limits of nsEM resolution (~20 angstroms) were combined and used for final 3D refinement. The final reconstruction has a resolution 21 angstroms. Top view looks down towards the viral membrane (A) and the dashed line indicates the viral membrane (B). T. Nyanhete, P. Acharya and RJ. Edwards designed the nsEM imaging experiment. T. Nyanhete prepared the IgG Fabs, evaluated binding of Fabs to BG505gp140 T332N SOSIP.664, made and purified Fab-SOSIP immune complexes by FPLC. P. Acharya, K. Mansouri and RJ. Edwards performed and analyzed nsEM experiments. T. Nyanhete designed, analyzed and interpreted the nsEM experiment results.

To determine whether the CD4bs antibody class in VC AQ was similar to or different from other known CD4bs antibodies, the VC AQ Fab-bound BG505gp140 T332N SOSIP.664 was superimposed to BG505gp140 T332N SOSIP.664 bound to known CD4bs monoclonal antibodies (bNAbs and non-bNAbs) as a rigid body using the UCSF Chimera's fitmap function (Figure 19A). The automated fitmap function determines how similar the VC AQ Fab is to other known CD4bs

antibodies by counting the number of mismatched residues between the VC AQ Fab and the reference CD4bs antibody Fab. The number is reported as 'Fit', and hence the smaller the Fit number the more similar the VC AQ Fab is to the reference antibody. Using the available 18 structures in the Protein Data Bank (PDB) of CD4bs antibodies bound to the BG505gp140 T332N SOSIP.664, the CD4bs bNAbs 45-46m2, 3BNC117 and CH235 had the lowest Fit scores (Figure 19B). The other CD4bs antibodies had Fit scores that were at least 2-fold higher, thus indicating that the above 3 CD4bs bNAbs were more similar to the VCAQ Fab (Figure 19B).

a

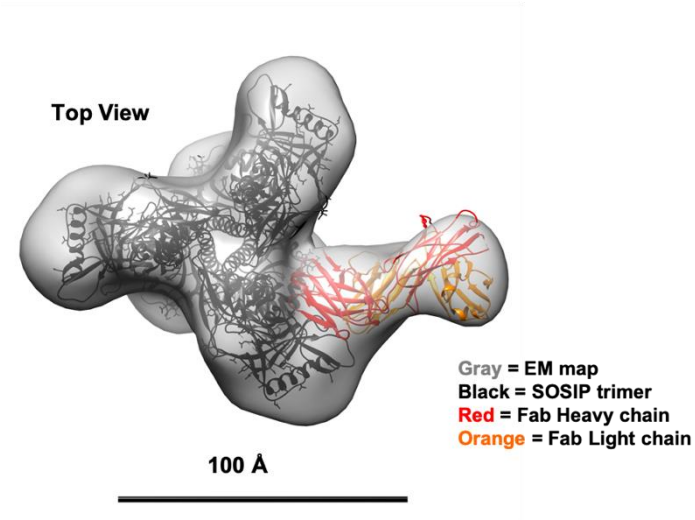

b

CD4bs Antibody	PDB Code	Fit
VRC01	4lst	948
VRC01	3ngb	1147
DH427	5f6j	2447
CH235	**5f9w**	**560**
F105	3hi1	2017
B12	2ny7	2338
CH103	4jan	2249
3BNC117	**4jpv**	**451**
8ANC131	4rwy	1404
VRC13	4ydj	2476
VRC16	4ydk	2520
HJ16	4ye4	1702
IOMA	5t3z	1273
b13	3idx	2463
1B2530	4yfl	1162
VRC07	4olu	1065
8ANC134	4rx4	1306
45-46m2	**4jkp**	**433**

Figure 19: 45-46m2, 3BNC117 and CH235-like CD4bs potent bNAbs in HIV-1 VC AQ.

A. Top view of a known SOSIP (black)-Fab (red and orange) ribbon structure superimposed onto the VC AQ Fab-bound SOSIP electron microscopy (EM) map (gray).

B. 18 mAb-SOSIP structures representing all known classes of CD4bs mAbs were fit into the EM map using UCSF Chimera's fitmap function. Chimera fitmap reports number of atoms outside of the EM map as the 'Fit' with a smaller Fit representing a better alignment of the two structures. T. Nyanhete, P. Acharya and RJ. Edwards designed the nsEM imaging experiment. T. Nyanhete prepared the IgG Fabs, evaluated binding of Fabs to BG505gp140 T332N SOSIP.664, made and purified Fab-SOSIP immune complexes by FPLC. P. Acharya, K. Mansouri and RJ. Edwards performed and analyzed nsEM experiments. T. Nyanhete designed, analyzed and interpreted the nsEM experiment results.

With the proof-of-concept showing that the nsEM epitope mapping approach can detect antibody classes in HIV-1 VC polyclonal plasma samples, I then interrogated the specificity of the polyclonal antibody response in other HIV-1 VCs with bNAbs.

Protein A purified polyclonal IgG antibodies from three of the six patients with bNAb activity (VC AL, VC AP and VC AQ) were processed into Fabs with immobilized papain and then subjected to quality control using SDS-PAGE (purity and correct size) and size-exclusion chromatography (SEC). Fab-SOSIP immune complexes were generated by incubating Fabs from each patient with the BG505gp140 T332N SOSIP.664 overnight at room temperature. Glutaraldehyde cross-linked HIV-1 VC polyclonal Fab-Env complexes were then purified by SEC (Extended Data 12), the purified SEC peak 1 complex (Extended Data 12) deposited onto nsEM grids and imaged using nsEM. Individual particle images ranging from 9,924 – 14,353 (minimal datasets for each sample that are sufficient to generate structures) were collected for each sample (VC AL – 14,353 particles, VC AP – 12,733, VC AQ – 9,924) and submitted to reference-free 2D classification.

3D refinement yielded 3D classes representing the most predominant immune complexes for all the VC patients that yielded immune complexes.

Remarkably, we detected the CD4bs antibody class in all of the three HIV-1 VC patients (Figure 20). Not only were the CD4bs antibodies similar in all the 3 patients (based on the Fab angle of approach and binding to the CD4bs), they were also similar to the potent 45-46m2, 3BNC117 and CH235 CD4bs bNAbs (Figure 20). We also identified another antibody class in VC AL that was binding to the gp120-gp41 interface region (Figure 21A). Of all the available gp120-gp41 interface binding antibodies (PGT151, 8ANC195 and 35O22), 35O22 looked similar to the VC AL Fab-bound BG505gp140 T332N SOSIP.664. Thus, the BG505gp140 T332N SOSIP.664 bound by the 35O22 gp120-gp41 interface binding bNAb was superimposed onto the VC AL Fab-bound BG505gp140 T332N SOSIP.664. Even though the Fab variable regions were aligned, the angle of approach of the VC AL Fab was different from that of 35O22 (Figure 21B). The 35O22 Fab constant region was also sticking out of the VC AL Fab-bound SOSIP 3D model (Figure 21B). This meant that the VC AL gp120-gp41 interface binding antibody class was 35O22-like, but not exactly like it.

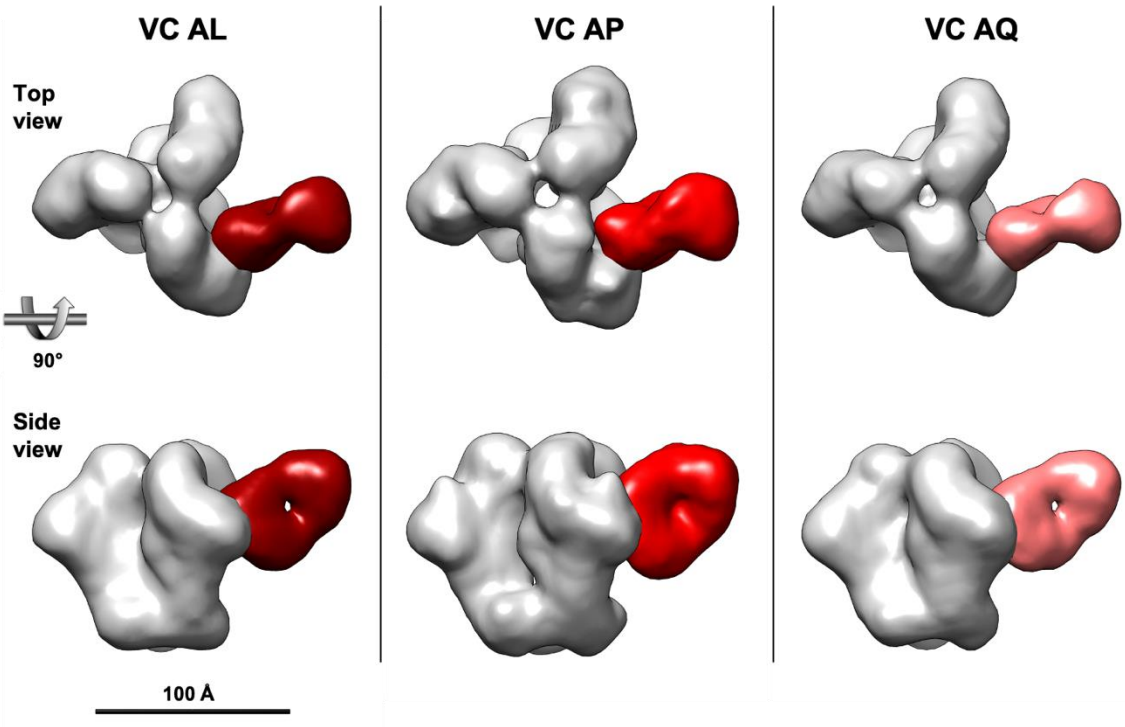

Figure 20: Predominant CD4bs antibodies in HIV-1 VCs with bNAbs.

Top view and side view of the VC AL, VC AP and VC AQ Fabs (red) bound to the CD4bs region on the HIV-1 BG505gp140 T332N SOSIP.664 (grey). T.Nyanhete, P. Acharya and RJ. Edwards designed the nsEM imaging experiment. T. Nyanhete prepared the IgG Fabs, evaluated binding of Fabs to BG505gp140 T332N SOSIP.664, made and purified Fab-SOSIP immune complexes by FPLC. P. Acharya, K. Mansouri and RJ. Edwards performed and analyzed nsEM experiments. T. Nyanhete designed, analyzed and interpreted the nsEM experiment results.

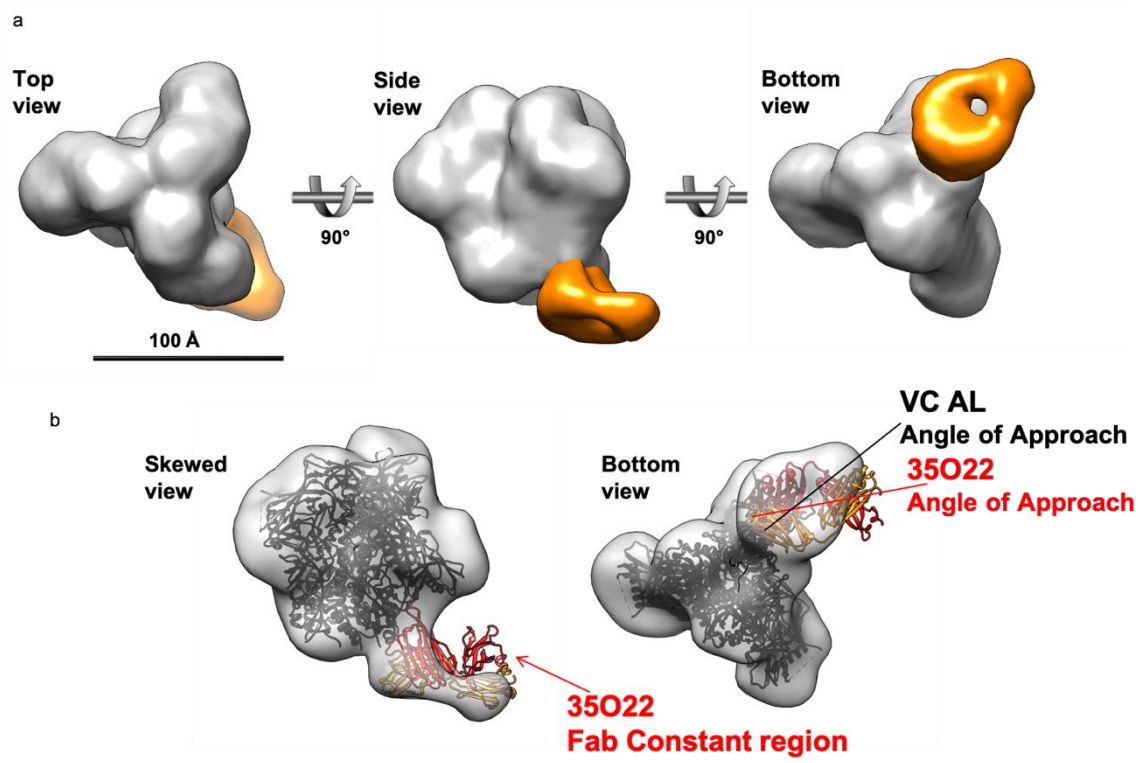

Figure 21: A novel gp120-gp41 interface antibody in HIV-1 VC AL.

A. Top, side and bottom views of the HIV-1 BG505gp140 T332N SOSIP.664 (grey) bound by a VC AL Fab (orange) targeting the gp120-gp41 interface region. B. 35O22 Fab-bound SOSIP superimposed onto the VC AL Fab-bound EM map (skewed view showing the protruding 35O22 Fab constant region, and bottom view showing the angle of approach of the VC AL and 35O22 Fabs). PGT151 and 8ANC195 did not fit at all to the VC AL Fab-bound EM map. T. Nyanhete, P. Acharya and RJ. Edwards designed the nsEM imaging experiment. T. Nyanhete prepared the IgG Fabs, evaluated binding of Fabs to BG505gp140 T332N SOSIP.664, made and purified Fab-SOSIP immune complexes by FPLC. P. Acharya, K. Mansouri and RJ. Edwards performed and analyzed nsEM experiments. T. Nyanhete designed, analyzed and interpreted the nsEM experiment results.

These findings confirm the predominant targeting of the vulnerable CD4bs on the HIV-1 *Env* by the polyclonal antibody response from HIV-1 VCs with bNAb activity, and also the presence of a previously unidentified and novel gp120-gp41 interface binding antibody in HIV-1 VC AL.

3.4 Discussion

I utilized a novel state of the art polyclonal nsEM imaging approach to visualize and map the specificity of the polyclonal antibody response to natural HIV-1 infection in HIV-1 VCs with coordinated high nAb and virion ADCP breadth. Using this approach, I showed that CD4bs antibodies were predominant in HIV-1 VCs that possessed bNAbs and also mediated ADCP of multi-clade viruses.

In an effort to bridge the Fab and Fc-mediated effector functions in patients naturally controlling HIV-1 infection, I discovered a correlation between nAb breadth and ADCP of viruses representative of the primary circulating strains (tier 2 viruses). The nAb breadth and virion ADCP correlation was more pronounced for viruses expressing at least two major bNAb epitopes (CDbs and V3 glycan). Thus, suggesting a potential antigen-specific relationship between the antibodies mediating neutralization and those mediating phagocytosis in the same patient. These results are consistent with the recent Lofano et al finding that showed enriched ADCP of monomeric gp120 in HIV-1 VCs with bNAbs compared to HIV-1 VCs without bNAbs [165]. In this study ADCP assays were performed using viruses (BaL, CM235 and 1086C) expressing some of the known nAb target epitopes (CD4bs and V3 glycan) instead of the antigen-coated beads which typically have limited epitope exposure and are not representative of what the ADCP-mediating Abs encounter *in vivo.*

The relationship between ADCP and nAb breadth is in line with some previous studies that have shown the importance of the Fc region in enhancing the

in-vivo protective efficacy of HIV-1 bNAbs [224, 324, 325], and also recent findings showing that specific Fc effector function profiles (ADCD and ADCT) can either predict bNAb development in an acute HIV-1 patient cohort [166] or identify HIV-1 VCs with bNAbs [165]. The antibody Fc region has been shown to be involved in shaping the maturation of the humoral immune response by mediating efficient delivery of antigens to the germinal center (GC) in the form of immune complexes (ICs). Antibodies with sialylated glycans in their Fc region have been shown to promote rapid and effective deposition of ICs within GCs, with complement being involved in the immune complex-mediated antigen deposition on follicular dendritic cells [165]. Thus, certain Fc region profiles that mediate binding to the correct complement or Fc receptors to ensure efficient delivery of antigens to GCs might also be same ones mediating ADCP and hence explain why ADCP activity is enriched in HIV-1 VCs with high nAb breadth. There is a need to characterize the Fc regions of the antibodies in HIV-1 VC patients with bNAb activity to confirm whether they have sialylated glycans or if they have a unique profile that could be associated with bNAb development in this patient cohort. It is also possible that ADCP activity might be acting as a surrogate for other Fc effector functions such as ADCD and ADCT that have been associated with bNAb development [166] since ADCP has been shown to be part of an enriched network of Fc effector functions in HIV-1 ECs [163]. Thus, it will important to investigate the potential relationship of other Fc effector functions with nAb breadth in this patient, and also

isolate the bNAbs from this patient cohort to directly probe their neutralization and Fc effector function profile.

The emergence of nAb and virion ADCP breadth was not linked to the presence or absence of protective HLA alleles. A previous study using HIV-1 VCs had shown that the Fc-effector function, ADCC, was enriched in HIV-1 VCs lacking protective HLA alleles (HLA*B57), thus probably compensating for the absence of a strong cellular response [222]. We show that in our HIV-1 VC cohort, the presence of nAb and ADCP breadth is not correlated with the presence or absence of protective HLA alleles, potentially indicating that the presence or absence of a strong CD8+ T cell response does not preclude the emergence of a strong humoral response.

My findings show that bNAbs can develop in HIV-1 patients with low viral loads (<5000 copies/mL), that the emergence of bNAbs is influenced by infection duration since only patients infected for at least 10 years had bNAbs. This finding is in line with the recent growing body of data showing that bNAbs can develop in patients with very low viral loads, thus suggesting that a high viral load is not required for the development of neutralization breadth. Further stratification of our controller patient group based on plasma viral load into HIV-1 VCs (viral load: >50 and <5000 copies/ml) and HIV-1 ECs (viral load <50 copies/ml) seems to indicate that there might be a very low viral load threshold required for bNAb development. This could explain the antigenic persistence and also the inflammatory environment due to low level viral replication reported to be critical for the

development of bNAbs in a low viral load setting [210]. The antigenic persistence and inflammation could also be involved in promoting higher levels of immune activation of monocytes, myeloid dendritic cells, and the well preserved CD4+ T and B cell compartments linked with bNAb development in HIV-1 VCs [205]. It will also be crucial to investigate the mechanistic link between certain Fc effector function profiles (ADCP, ADCD and ADCD) and bNAb development since this might represent another potential mechanism for bNAb development in HIV-1 VCs and other low viremia settings.

With the aid of the novel computational modeling of the polyclonal plasma neutralization fingerprint (NFP), I went on to show the predominant targeting of the V3 glycan, CD4bs, MPER and gp120-gp41 interface bNAb epitopes by the plasma from HIV-1 VCs with bNAbs and ADCP activity. Previous studies analyzing the bNAb response in HIV-1 VCs have shown predominant targeting of the V3 glycan epitope [203, 208], with Freund et al showing these V3 glycan targeting bNAbs isolated from an HIV-1 VC patient to be potent and also capable of controlling autologous viral replication in mice when co-administered with the less potent CD4bs and V1V2 targeting bNAbs from the same patient [203]. Thus, my findings not only further emphasize the predominant targeting of the V3 glycan in HIV-1 VCs, but also show the polyclonal nature of the bNAb response in VCs.

The polyclonality of the bNAb response if further emphasized by the TZMbl neutralization assay using mutant viruses highlighting that single bNAb epitopes on viruses do not confer neutralization sensitivity. The only exception is VC BA

whose neutralization fingerprint only shows targeting of the V3 glcyan and hence it is not surprising that a single V3 N332A glycan mutation results in loss of neutralization sensitivity. It is more likely that the observed nAb breadth in this patient cohort is mediated by polyclonal antibodies targeting distinct bNAb epitopes and hence resulting in a synergistic effect that gives rise to the broad nAb response (except for VC BA) as was also evident in an HIV-1 VC patient and HIV-1 EC cohort from the Freund et al [203] and Scheid et al [204] studies, respectively. Future work isolating mAbs of different specificities from these patients will help determine their neutralization potency and their potential involvement in mediating virus neutralization either alone in combination with other mAb specificities.

It is also plausible that targeting of novel, previously uncharacterized vulnerable epitopes on the HIV-1 Envelope (indicative of a unique humoral response only present in HIV-1 VCs) might also contribute to the broad nAb response present in these patients. This theory could be indicative of a different class of antibodies present in HIV-1 VCs targeting a unique set of epitopes that could be more potent than the responses observed by bNAbs isolated from chronic viremics. It is also possible that because of the coordinated Fab and Fc-effector functions in these patients, binding of non-neutralizing Abs to the HIV-1 Env might result in allosteric effects that result in better targeting of known and novel bNAb epitopes by neutralizing antibodies. Thus, mapping epitopes targeted by the polyclonal antibody response (both neutralizing and non-neutralizing) provides a more complete picture of the antibody response to HIV-1.

Using polyclonal IgG Fab fragments isolated from HIV-1 VC plasma samples, I first showed that these polyclonal Fabs can bind to a recombinant HIV-1 *Env* glycoprotein to form immune complexes. The ability to use the novel nsEM imaging of stable immune complexes approach [147] allowed me to identify the CD4bs class of antibodies as one of the predominant antibody classes elicited by natural HIV-1 infection in HIV-1 VCs. The presence of the CD4bs antibody class in all of the three tested HIV-1 VCs with bNAbs raises the hypothesis that this antibody class might be commonly elicited in HIV-1 VCs. The CD4bs antibodies have been reported to be commonly elicited in HIV-1 infection, with VRC01-like CD4bs antibodies having been detected in 79% of a chronic viremic patient cohort from Amsterdam, 30% of a subset of CHAVI chronic viremic patients and 31% of a subset of the CAPRISSA chronic viremics [316]. The common occurrence of this antibody class might mean that this could be an easy antibody class to target given its prevalence in not only chronic viremics but also a subset of the HIV-1 VCs in this study.

The similarity of the CD4bs antibody class in all the three HIV-1 VCs with bNAbs suggests the possibility of the viruses in these patients having the same antibody-imprinting capacity that results in a similar predominant antibody response in the infected individuals. The idea of virus-mediated bNAb-imprinting was described by Kuoyos et al as being one of the determinants of bNAb evolution that could be leveraged for the development of bNAb-based HIV vaccines using immunogens based on viruses with strong bNAb-imprinting capacities [326].

Analysis of the transmitter/founder viruses in the HIV-1 VCs with similar antibody responses will be required to confirm whether these patients have the same viruses that could be driving the observed similar predominant CD4bs antibody response.

The observed similarity of the detected HIV-1 VC CD4bs Abs to highly potent CD4bs bNAbs 45-46m2 (neutralizes 96% of circulating viruses [140]), CH235 (neutralizes 90% of circulating viruses [139]) and 3BNC117 (suppresses viremia after passive infusion [327]) highlighted the presence of potent class of CD4bs in these patients. Future isolation and characterization of the ontogeny and lineages of mAbs from these CD4bs Ab classes will help shed more light on their biologic activity including ability to neutralize contemporaneous autologous viruses. These studies will also help shed more light on the previously unidentified gp120-gp41 interface antibody in VC AL since it appears to be distinct from the 35O22, PGT151 and 8ANC195 gp120-gp41 interface bNAbs. Functional characterization of the CDbs and gp120-gp41 interface antibodies will also help highlight the biologic activity of these antibody classes in HIV-1 VCs and whether they might be involved in virus control.

Investigating different classes of antibodies present in the HIV-1 VC polyclonal plasma using nsEM imaging of polyclonal Fabs in complex with trimeric HIV-1 *Env* has some limitations which could partially explain why we only picked out 2 dominant antibody classes (CD4bs and gp120-gp41 interface antibodies) in our initial analysis. The nsEM approach is known to have difficulties in picking out

less frequent antibody classes [147] and also difficulties in detecting V3 supersite or apex-specific antibodies when using fully glycosylated trimers which is thought to be a result of low affinity and fast off rates [147]. Thus, one approach to overcome this limitation would involve the use of partially deglycosylated SOSIPs [328, 329]. We avoided this approach since partially deglycosylated SOSIPs are not a true representation of what the antibodies encounter *in-vivo*. Optimizing the nsEM approach so as to image more SOSIP-Fab complex particles might help increase the ns-EM imaging resolution that will result in the detection of more less frequent or hard to detect antibody classes.

In summary, I discovered a coordinated bNAb and virion ADCP humoral response in a subset of Southern U.S HIV-1 VCs characterized by the targeting of the CD4bs, V3 glycan, gp120-gp41 interface and MPER vulnerable sites on the HIV-1 envelope that potentially act in synergy to mediate the broad nAb and ADCP responses observed in the patient cohort. The HIV-1 VCs with bNAb activity contain a potent class of CD4bs bNAbs and a novel gp120-gp41 interface antibodies that have not previously been reported for HIV-1 VCs without evidence of autoimmunity. These findings not only suggest the presence of potent humoral responses in HIV-1 VCs, but also suggest a possible role of ADCP in modulating the bNAb response in a low viremia setting.

4. Discussion and Implications

4.1 Unconventional HLA class II-restricted CD8+ T cells in HIV-1 VCs

Chapter 2 expands our understanding of the CD8+ T cell response in HIV-1 infection and also challenges the conventional definition of what makes an anti-viral CD8+ T cell response in an HIV-1 infection setting. Traditionally, anti-CD8+ T cell responses in HIV-1 infection and also in other viral infections have long been thought to be strictly restricted by HLA class I molecules. This work, together with that of Hansen et al [73, 74] and Ranasinghe et al [75], highlights that the CD8+ T cell response to HIV-1/SIV can violate the CD8+ T cell epitope recognition paradigm and see antigen in the context of HLA (MHC) class II molecules in addition to HLA (MHC) class I molecules.

Unconventional HLA class II-restricted CD8+ T cells have the potential to offer a unique and very attractive vaccine target compared to the conventional HLA class I-restricted CD8+ T cells because of a number of reasons. Analysis of the class II-restricted CD8+ T cell response in the RhCMV-vaccinated macaques protected from SIV infection showed that class II-restricted CD8+ T cells had a broader coverage of viral proteins characterized by targeting more and distinct SIV epitopes. The class II-restricted CD8+ T response targeted three times more the number of SIV epitopes targeted by class I-restricted CD8+ T cells, while the distinct SIV epitope targeting pattern means that this unconventional response has the capability to complement the class I response in an infection setting. Class I-

restricted CD8+ T cells tend to usually recognize an epitope presented by a single class I molecule, while in a class II-restricted antigen presentation setting the CD8+ T cell response can recognize a particular epitope in the context of several different MHC (HLA) molecules (epitope promiscuity) [233]. Unlike the class I-restricted CD8+ T cell response where strong responses are usually seen in patients with protective HLA alleles, the class II-restricted CD8+ T cell response was not associated with protective HLA alleles and hence this response seems to have utility in individuals expressing a variety of HLA alleles. The presence of class II-restricted CD8+ T cells also means that it might be possible to directly target and kill infected cells expressing class II molecules [233, 330].

Given the unique features and the association between the presence of MHC class II-restricted CD8+ T cells and protection from SIV infection there was interest in investigating whether these macaque findings could be translated to humans. The unconventional class II-restricted CD8+ T cells in the macaque study were induced by a reprogrammable CMV vector and hence it was not clear whether such a CMV-vectored vaccine approach would also be needed in humans or whether these cells could be induced by natural HIV-1 infection. This works addresses this uncertainty by showing not only the presence of HIV-1 specific HLA class II-restricted CD8+ T cells in humans (also reported in another study [75]), but also suggesting that these unconventional CD8+ T cells can be detected in a natural HIV-1 infection setting and hence do not need induction by a CMV vector. A key finding from this work is the observation that these cells are undetectable in

uninfected individuals thus suggesting that HIV-1 infection might be involved in eliciting or enhancing this unconventional CD8+ T cell response since these cells were undetectable in uninfected individuals. In HIV-1 patients we show that the distribution of these unconventional class II-restricted CD8+ T cells is different in patients controlling HIV-1 infection (HIV-1 VCs) compared to non-controlling patients (chronic viremics), with the HIV-1 VCs having a higher frequency of these cells compared to chronic viremic patients. The observed higher frequency in HIV-1 VCs is interesting given the functionally superior anti-viral CD8+ T cell response often reported in this patient group and also the reported association between induction of class II-restricted CD8+ T cells and protection from SIV infection. Thus, it is possible that part of the potent HIV-1 VC anti-CD8+ T cell response might include the unconventional HLA class II-restricted CD8+ T cell response which could be one of the distinguishing factors between controllers and non-controllers whereby controllers either have a superior ability to elicit more HLA class II-restricted CD8+ T cells to complement the HLA class I-restricted CD8+ T cell response or that the HLA class II-restricted CD8+ T cells are well maintained (superior survival phenotype) during the course of HIV-1 infection in controllers compared to non-controllers.

Future work is already planned to address the timing of the induction of these cells in response to HIV-1 infection and also track their fate during the course of infection as patients transition from the acute phase to the chronic phase of HIV-1 infection. Using a cohort of longitudinal patient samples that either up controlling

(HIV-1 VCs) or not controlling HIV-1 infection (chronic viremics), analysis of the frequency of these cells over time will help highlight whether it's an induction timing or maintenance/survival phenomenon that partly explains the differences in the frequency of HLA class-II restricted CD8+ T cells in different patient cohorts. Understanding the mechanisms behind the induction of these unconventional cells in humans will be key in further enhancing our understanding of these unconventional cells and also how they can be induced either naturally or with the aid of vaccine approaches. One of the hypotheses for the induction of these cells in an HIV-1 infection setting is that the cytokine storm that takes place in the early acute phase of HIV-1 infection [59] might be responsible for the induction and/or expansion of these cells by creating a pro-inflammatory and immunogenic environment that has been previously associated with the induction of these cells [81]. The use of longitudinal HIV-1 patient samples will help test this hypothesis since we have patient samples from the early acute phase of infection and also from the chronic phase of infection.

Given the observed low frequency of these unconventional HLA class II-restricted CD8+ T cells, future plans include utilizing more sensitive techniques of accurately detecting these rare cells in circulation. One such approach involves the use of more sensitive multimers such as dodecamers which are currently undergoing testing in our lab and have previously been shown to be better suited for the detection, isolation, and phenotypic analysis of both rare and low-affinity antigen specific T cells [331].

With mounting evidence of the presence of HLA class II-restricted CD8+ T cells in an HIV-1 infection setting there is now interest in understanding the ontogeny of these unconventional CD8+ T cells. It is not quite clear whether these cells represent a unique CD8+ T cell subset derived from the CD8 lineage or whether they might be from the CD4 lineage and undergo reprogramming to adopt CD8+ T cell like features given the now widely appreciated plastic nature of CD4+ T cells [103, 104] and the observed presence of cytotoxic CD4+ T cells in HIV-1 infection [105, 332]. Ranasinghe et al [75] showed that HLA class II-restricted CD8+ T cells express two distinct TCRα chains and they speculated that one of the TCRα chain (TRAV26) is responsible for mediating positive selection during the CD8+ T cell lineage specification, while the other TCRα chain (TRAV6) is part of the TCR that is class II-restricted. These findings seem to point towards the hypothesis that HLA class II-restricted CD8+ T cells are a distinct CD8+ T cell subset that undergoes the CD8 lineage specification developmental pathway [75]. This work, on the other hand, suggests that the HLA class II-restricted CD8+ T cells are 'ex-CD4+ T cells' that undergo reprogramming to adopt CD8+ T cell like features. The findings in this work are in line with the observation of cytotoxic CD4+ T cells that have been detected in an HIV-1 infection setting further justifying the plastic nature of CD4+ T cells. However, due to sample size limitations in both this work [226] (n = 2) and in Ranasinghe et al findings [75] (n =1) there is need to study more patients so as to gain a better understanding of the ontogeny of these cells and how HIV-1 infection influences this process since our hypothesis

implicates the inflammatory environment during acute HIV-1 infection as being one of the triggers for the reprogramming of CD4+ T cells and/or expansion of the class II-restricted CD8+ T cell pool. TCR analysis together with the analysis of lineage specific markers/genes in a larger patient cohort will help address the ontogeny issue in an HIV-1 infection, while lineage tracing using humanized mouse models will provide a more elegant way of identifying the precursors of these cells and also provide useful markers that can be used to study the growth, differentiation and the genes necessary for the development of these cells.

One of the key outstanding questions is understanding the functional properties/capacity of HLA class II-restricted CD8+ T cells and their possible role in directly mediating virus control since the ultimate goal is to harness these cells to provide protection from and control of HIV-1 infection. The SIV NHP findings did not directly prove the anti-viral activity of the class II- and also the class E-restricted CD8+ T cells that were both associated with protection. This work shows that HIV-1 specific CD8+ T cells from several HIV-1 VCs have an anti-viral gene signature and that they can suppress HIV-1 replication in infected autologous CD4+ T cells in an HLA class II dependent manner. Thus, this work together with the findings from Ranasinghe et al [75] represent the first bodies of work directly showing the anti-viral properties of HLA class II-restricted CD8+ T cells. Despite these findings, it is still not clear whether this unconventional CD8+ T cell subset is directly involved in mediating virus control together with the conventional class I-restricted CD8+ T cell subset. Thus, the next steps to address this question will involve

protection studies using humanized mouse models and adoptive transfer of class II-restricted CD8+ T cells to test their ability to control infection and suppress viremia *in vivo* in the absence of class I-restricted CD8+ T cells. There is also a question on whether HLA class II-restricted CD8+ T cells are functionally superior compared to HLA class I-restricted CD8+ T cells. Thus, it will be necessary to directly compare the ability of these two CD8+ T cell subsets to mediate lysis of infected target cells and also suppress viral replication in infected target cells. Probing the HLA class II-restricted CD8+ TCR signaling and antigen binding mechanism using recombinant TCRs and MHC molecules will also help improve understanding of this unconventional TCR signaling mechanism and how that differs from the conventional TCR signaling.

Biology/Basic Science Implications:

This work questions our classical understanding of antigen presentation and CD8+ T cell biology as it provides a potential new paradigm for antigen presentation, especially in the setting of viral infections such as HIV and SIV. It also raises questions on the possible plastic nature of CD8+ T cells and CD8+ T cell subsets, especially in the setting of infection. More work still needs to be done to fully appreciate the ontogeny and CD8+ TCR mediated signaling in the context of HLA class II molecules of HLA class II-restricted CD8+ T cells, as well as identifying unique markers that define this unique CD8+ T cell subset. CD4+ T cells have already been shown to be plastic in nature as they have the ability to acquire

RUNX3 expression by downregulating *ThPOK* expression, thus it will be interesting to see whether these cells arise from plastic CD4+ T cells or CD8+ T cell precursors that can also reprogram themselves to acquire CD4-like properties.

Translational/Therapeutic Implications:

This body of work has further reinforced the presence of anti-viral HIV-1 specific HLA class II-restricted CD8+ T cells in an HIV-1 infection setting. These findings together with those of Ranasinghe et al and Hansen et al highlight the need to further characterize this unique CD8+ T cell subset as it might provide a unique vaccine target that could be utilized to boost and complement the conventional CD8+ T cell response and hence provide a more effective T cell based HIV-1 vaccine. The current interest in the use of T cell therapies in HIV-1 patients [333-336] also represents a potentially utility of HLA class II-restricted CD8+ T cells and their TCR mediated signaling if they prove to be functionally superior or target distinct epitopes compared to HLA class I-restricted CD8+ T cells. The potential induction of class II-restricted CD8+ T cells from CD4+ T cell precursors could also be seen as a host defense mechanism from HIV-1 infection since it reduces the number of available potential targets and transforms them into effector anti-viral CD8+ T cells.

4.2 Coordinated Fab and Fc-effector Functions in HIV-1 VCs

This work shows that high viral loads and viral diversity usually observed in chronic viremics are not required for bNAbs development in patients with very low viral loads such as HIV-1 VCs that we have shown to develop bNAbs at a similar frequency as that observed in chronic viremics. There is now mounting evidence showing that factors such as low but persistent viral load, low antigenic diversity, unique inflammatory environment, highly functional myeloid dendritic cells, preservation of Tfh cells and B cell function can drive germinal center (GC) reactions and affinity maturation, thus leading to bNAb development in HIV-1 VCs [205, 210, 337].Thus, this work is consistent with other findings that show bNAb development in a low viral load setting, and suggesting a potential role of these antibodies in mediating virus control. bNAbs from chronic viremics are not capable of controlling autologous viruses [338] and hence the high viral loads observed in these bNAb donors. However, some of the bNAbs isolated from HIV-1 VCs and ECs can neutralize autologous viruses [203], thus this could be an indication that the bNAbs from HIV-1 VCs are unique and more potent since they are capable of controlling autologous virus replication. It is still not clear whether the bNAb response in HIV-1 VCs is one of the factors mediating virus control, thus there is a need to isolate autologous viruses from our HIV-1 VC patients at longitudinal time points so as to determine whether the bNAbs can neutralize autologous viruses isolated at the earlier, the same(contemporaneous) and later time points so as to gain a broader understanding of the nature of virus-Ab relationship in

these patients. The expectation will be that the bNAb response should be able to neutralize autologous viruses from earlier time points since the antibody response would have evolved so as to better target the earlier viruses, but neutralization of contemporaneous and later time point viruses will be interesting since this will suggest that the autologous viruses cannot evolve to escape the antibody response in these patients. HIV-1 *Env* longitudinal sequence analysis will also be crucial to study so as to gain an appreciation of how the virus is responding to the immune pressure exerted by the autologous antibody response since the *Env* region is the primary target of bNAbs.

One of the key findings in this project was the association of neutralization breadth and virion ADCP breadth, one of the Fc-effector associated with decreased risk of infection in human vaccine recipients [162] and also enriched in HIV-1 VCs [158]. HIV-1 VC patients with nAb breadth and bNAbs were also recently shown to be enriched for monomeric HIV-1 gp120 ADCP activity [165], thus showing a link between the two arms of the anti-HIV-1 humoral immune response. There is growing evidence showing the link and interplay between the Fab and Fc arms of the humoral response to HIV-1. ADCD and ADCT are two key Fc effector functions that were recently shown to predict the development of bNAbs in cohort of HIV-1 infected individuals [166], while antibodies with sialylated glycans in their Fc region were shown to be enriched in HIV-1 VCs that developed bNAbs compared to HIV-1 VCs without bNAbs [165]. The antibody Fc domain has been shown to directly influence the neutralizing potency of bNAbs [223, 224], and

now there are suggestions that the Fc domain might also be involved in driving and promoting bNAb development. One proposed mechanism involves the role of the Fc domain in preserving immune complexes and enhancing their delivery to the GC where they are involved in antigen presentation and B-cell activation driving GC reactions and affinity maturation [165]. In this scenario, it is plausible that antibodies with an Fc domain that binds to the ADCP receptor, FcyRIIa, are better at promoting bNAb development, and hence explaining the enrichment of IgG antibodies capable of mediating multi-clade ADCP in patients with bNAbs. Isolation of antibodies from HIV-1 VCs with and without bNAbs and profiling their Fc domains and ADCP activity will help highlight whether antibodies from HIV-1 VCs with bNAb have a unique Fc domain glycosylation pattern that could potentially be used to identify patients that will naturally develop bNAbs.

In an effort to gain a much more representative understanding of ADCP activity *in vivo*, the ADCP assays will need to performed using autologous ADCP effector primary cells such as monocytes and neutrophils since *in vivo* ADCP activity is also affected by the expression levels and allelic variants of Fc receptors on effector cells as well as the balance between activating and inhibitory Fc receptors as reviewed in Tay et al [155]. The autologous neutralization and ADCP assays will clearly highlight whether these associated effector functions can directly mediate virus control *in vivo*.

In this study we employed a novel electron microscopy structure-based polyclonal antibody response epitope mapping technique that was recently

described for analyzing the polyclonal antibody response in rabbits [147] and newly established at Duke University in collaboration with Dr. Acharya to study the polyclonal antibody response in HIV-1 VCs. This polyclonal epitope mapping approach allows for the detection of epitopes targeted by both neutralizing and non-neutralizing antibodies, and thus providing a much more broader understanding of the antibody response given the importance of non-neutralizing antibodies that have been associated with protection. For studies analyzing the antibody response in novel patient cohorts such as HIV-1 VCs that might not mount a traditional/conventional response targeting known vulnerable sites on the HIV-1 envelope, this approach is ideal as it is not restricted by focusing on already known vulnerable sites defined by studying responses in chronic viremics. Thus, this has the potential to uncover immune targeting of potentially new vulnerable sites that might only be targeted by the antibody response in patients naturally controlling infection. This unbiased epitope mapping approach might help resolve whether the patients with the ability to naturally control HIV-1 infection have a distinct humoral response to HIV-1 infection that might partly explain the ability to control infection.

Biological/Basic Science Implications:

This work further highlights the potential role of the antibody Fc domain in mediating antigen presentation, GC reactions, antibody affinity maturation and bNAb development in an HIV-1 infection setting. This also provides evidence for the coordination of different immune compartments and links between the innate

and adaptive immune responses likely to be crucial in mounting an effective immune response. This work also adds to the growing literature highlighting the complex nature of bNAb development and how these rare antibodies can be induced in the absence of high viral loads and viral diversity. There are also interesting potential implications in the arms race between the virus and the host immune response given that there is evidence of the host antibody response in HIV-1 VCs capable of controlling virus replication. Thus, isolating bNAbs and examining the B cell repertoire from this HIV-1 VC patient cohort might provide more insights into the nature of bNAbs that can control autologous virus replication.

Translational/Therapeutic Implications:

This work further emphasizes the immunologic heterogeneity in HIV-1 VCs since all patients regardless of nAb and virion ADCP breadth still had low to undetectable viral load and normal CD4+ T cell counts. This work highlights the multi-faceted immune response in HIV-1 VCs and how targeting of the Fc region could be leveraged to drive bNAb development in response to HIV-1 infection. This work also lays the groundwork for the potential identification of new class of antibodies that might prove to have potent antiviral effects and hence be of use in vaccine efforts that might involve passive infusion approaches or targeting of specific antibody lineages.

5. Conclusions

This body of work has highlighted the presence of unconventional anti-viral HLA class II-restricted CD8+ T cells that represent a distinct CD8+ T cell subset whose role in mediating HIV-1 virus control is still an open question. I have also identified a distinct humoral immune response network in HIV-1 VCs characterized by the coordination of the Fc and Fab humoral compartments. This humoral response is dominated by a dominant class of CD4bs antibodies that are similar in epitope specificity to a potent class of CD4bs bNAbs (45-46m2, 3BNC117 and CH235). Deciphering the biologic activity of these antibodies will help shed more light about their potency and potential involvement in mediating virus control in the HIV-1 VC patients.

Given the reported potential role of the Fc domain in bNAb development, this work supports the potential targeting and modulation of the antibody Fc domain in effort to drive bNAb development in patients. There is a need for the further elucidation of the mechanistic link between the Fab and Fc arms of the antibody response to HIV-1 infection, and how this is modulated in HIV-1 VCs.

Understanding mechanisms of natural immune response to HIV-1 infection in patients naturally controlling HIV-1 infection (HIV-1 VCs and ECs) will help the immunology research community to uncover potentially novel and potent immune response mechanisms that might help guide the design of effective vaccines capable of providing protection from viral infections.

Appendix A (Extended Data)

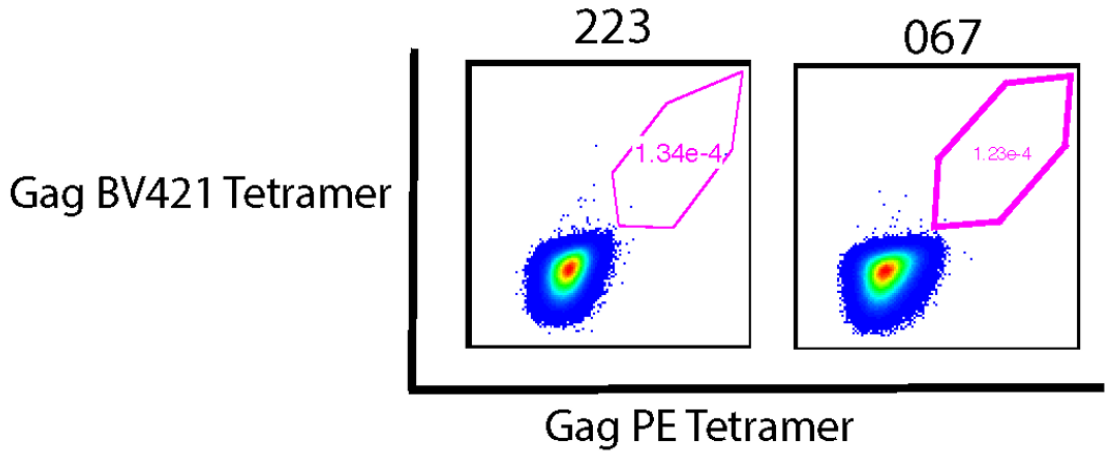

Extended Data 1 (related to Figures 1 and 2). HLA DRB1*0701 Gag Tetramer does not bind to HLA mismatched CD8+ T cells.

CD8+ T cells from HLA mismatched chronic donors (223 and 067) were stained with the $Gag_{293-312}$ HLA DRB1*0701 tetramers conjugated to either BV421 or PE fluorochromes using the dual tetramer approach. Tetramer positive CD8+ T cells expressed both the BV421 and PE. T. Nyanhete designed the experiments, performed the experiments, analyzed and interpreted the results.

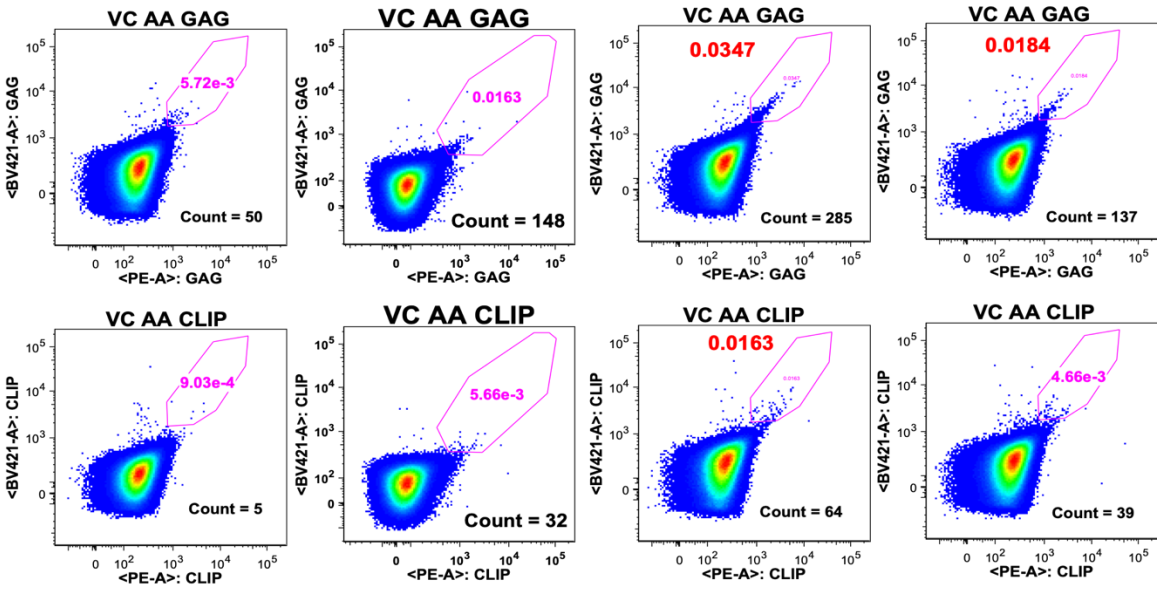

Extended Data 2 (related to Figures 1 and 2). Gag-specific HLA DRB1*0701-restricted CD8+ T cells are present in VC AA at different draw dates.

CD8+ T cells from VC AA from multiple draw dates (time points) were stained with the $Gag_{293\text{-}312}$ HLA DRB1*0701 tetramers conjugated to either BV421 or PE fluorochromes using the dual tetramer approach. Gag or CLIP tetramer positive CD8+ T cells expressed both BV421 and PE. The human $CLIP_{87\text{-}101}$ –DRB1 tetramer served as the negative control. T. Nyanhete designed the experiments, performed the experiments, analyzed and interpreted the results.

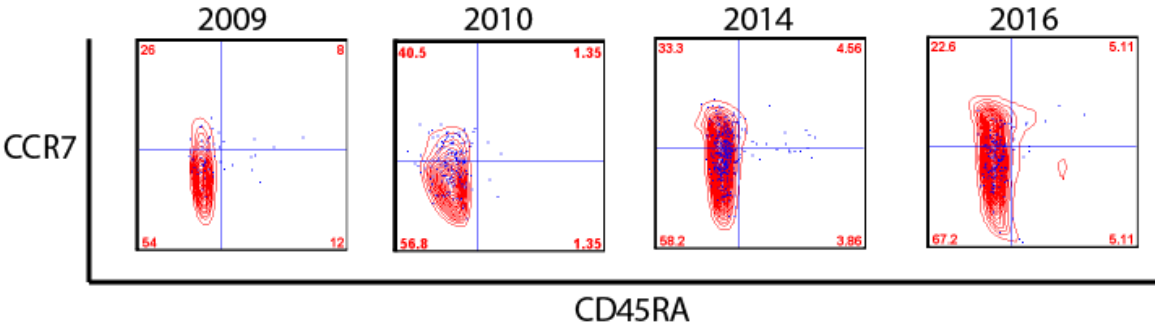

Extended Data 3 (related to Figures 1 and 2). Gag-specific HLA DRB1*0701-restricted CD8+ T cells in VC AA have predominant effector and central memory phenotypes.

The memory phenotypes of the VC AA Gag tetramer positive events were defined by the surface expression of CCR7 and CD45RA. Naïve tetramer positive events were double positive for CCR7 and CD45RA. Central Memory tetramer positive events were CCR7+ and CD45RA-. Effector Memory tetramer positive events were CCR7- and CD45RA-. Terminally differentiated effector memory (TEMRA) tetramer positive events were CCR7- and CD45RA+ [256]. T. Nyanhete designed the experiments, performed the experiments, analyzed and interpreted the results.

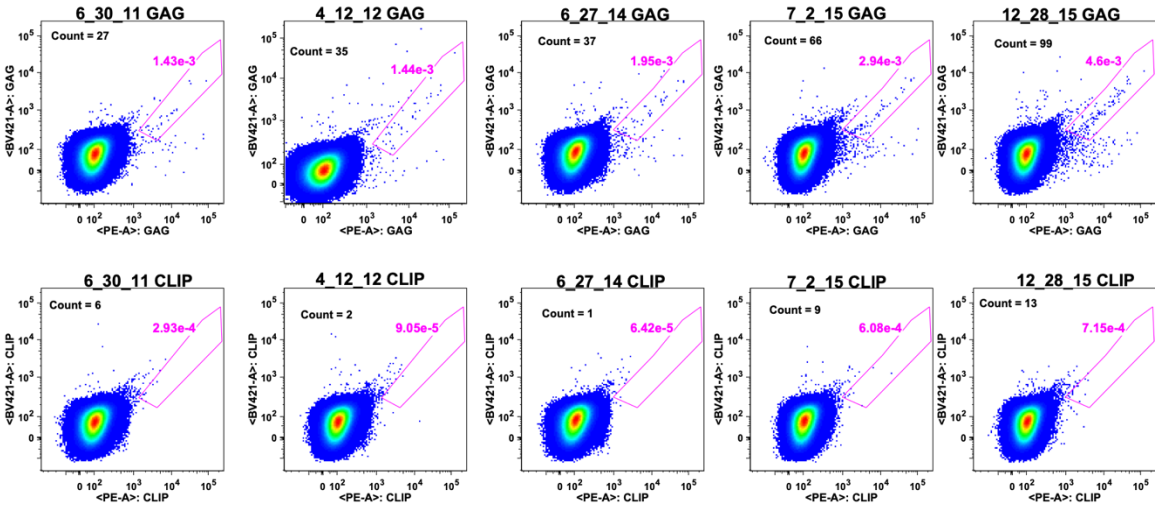

Extended Data 4 (related to Figures 1 and 2). Gag-specific HLA DRB1*0701-restricted CD8+ T cells are present in VC AD at different draw dates.

CD8+ T cells from VC AD from multiple draw dates (time points) were stained with the $Gag_{293\text{-}312}$ HLA DRB1*0701 tetramers conjugated to either BV421 or PE fluorochromes using the dual tetramer approach. Gag or CLIP tetramer positive CD8+ T cells expressed both BV421 and PE. The human $CLIP_{87\text{-}101}$ –DRB1 tetramer served as the negative control. T. Nyanhete designed the experiments, performed the experiments, analyzed and interpreted the results.

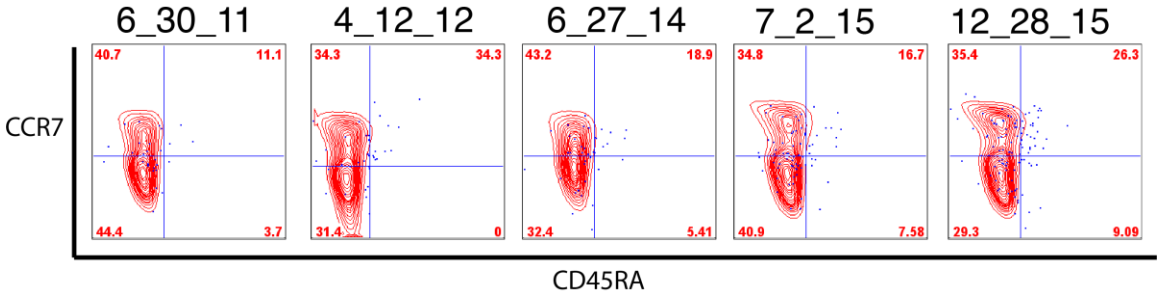

Extended Data 5 (related to Figures 1 and 2). Gag-specific HLA DRB1*0701-restricted CD8+ T cells in VC AD have predominant effector and central memory phenotypes.

The memory phenotypes of the VC AD Gag tetramer positive events were defined by the surface expression of CCR7 and CD45RA. Naïve tetramer positive events were double positive for CCR7 and CD45RA. Central Memory tetramer positive events were CCR7+ and CD45RA-. Effector Memory tetramer positive events were CCR7- and CD45RA-. Terminally differentiated effector memory (TEMRA) tetramer positive events were CCR7- and CD45RA+ [256]. T. Nyanhete designed the experiments, performed the experiments, analyzed and interpreted the results.

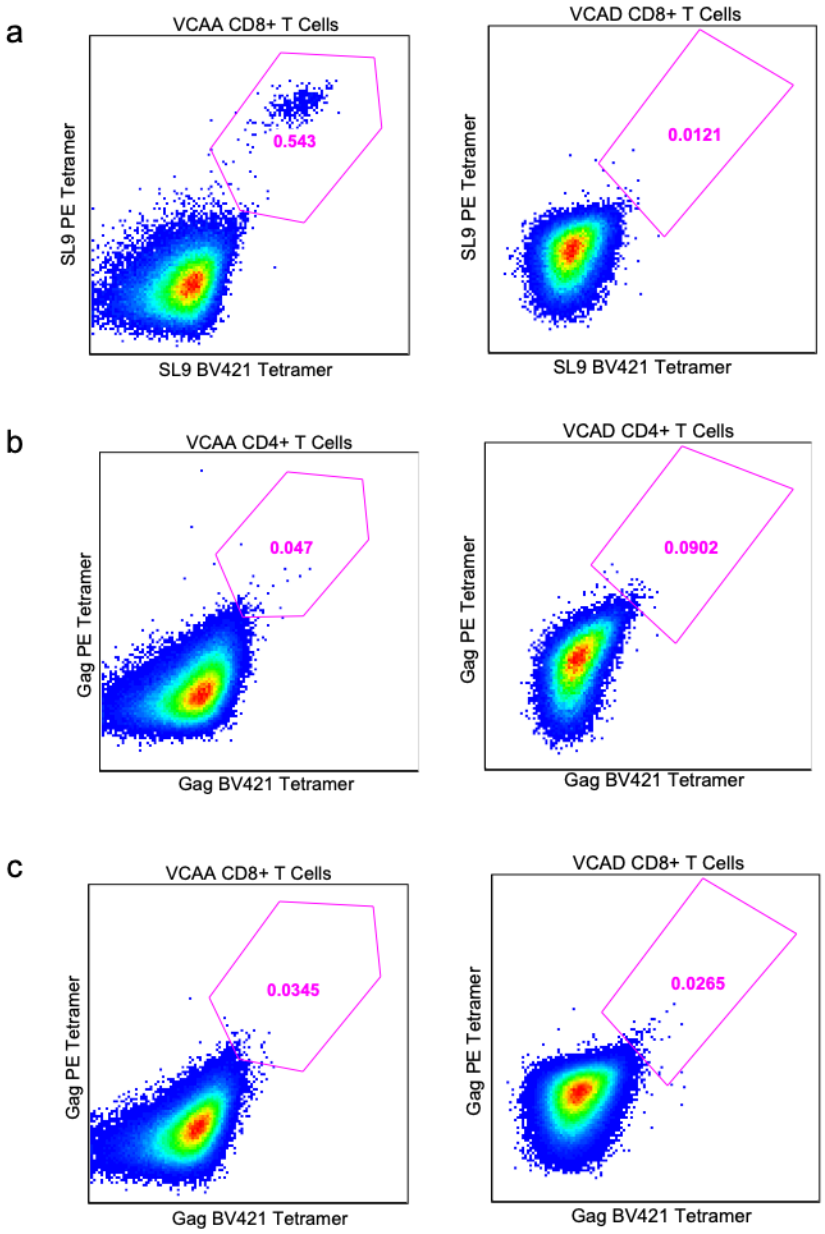

Extended Data 6 (related to Figures 3, 4, 5 and 6). Flow Cytometry bulk cell sorting gates for cells from VC AA and VC AD patients.

Sorting gates for Gag-specific class I-restricted CD8+ (A), class II-restricted CD4+ (B) and class II-restricted CD8+ T cells (C) from VC AA and AD patients. T. Nyanhete designed

the experiments and performed the experiments with the help of P. McDermott and D. Marshall. T. Nyanhete analyzed and interpreted the results.

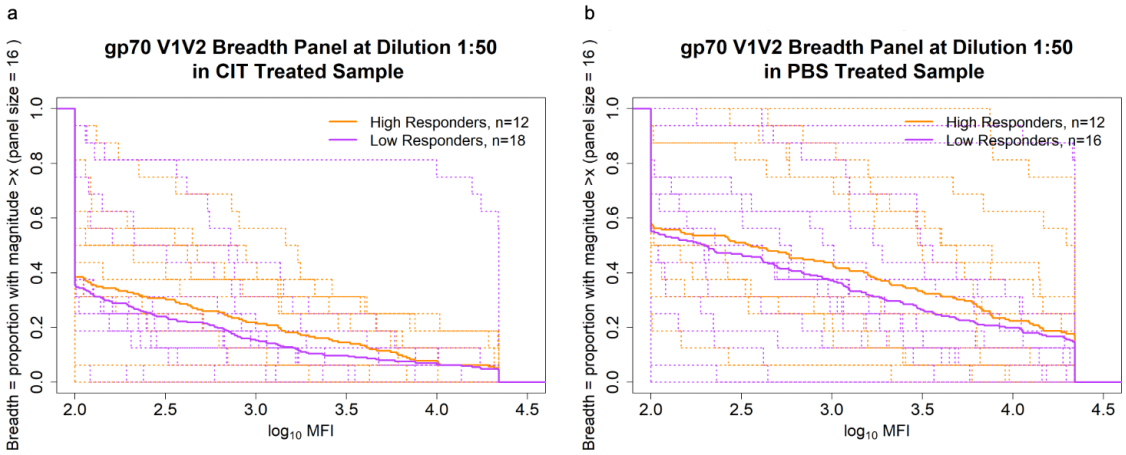

Extended Data 7 (related to Figures 11, 12 and 13). Comparable IgG binding magnitude, binding avidity and breadth against the global HIV-1 V1V2 *Env* breadth panel.

BAMA was used to measure the IgG binding avidity (A) and IgG binding magnitude (B) to the V1V2 *Env* breadth panels. The area under the curve (AUC) was measured using the M-B Curve as described in the Materials and Methods section. M-B Curve AUC min – max scores: IgG in CIT (V1V2) – High Responders (HR) = 2 – 3.1073 and Low Responders (LR) = 2 – 3.8798; IgG in PBS (V1V2) – HR = 2 – 4.2396 and LR = 2 - 4.1779. All BAMA assays were performed in duplicate (%CV <15% between sample replicates). T. Nyanhete designed the experiments, performed the experiments, analyzed and interpreted the BAMA M-B Curve results. BAMA M-B Curves generated by L. Zhang under the direction of T. Nyanhete.

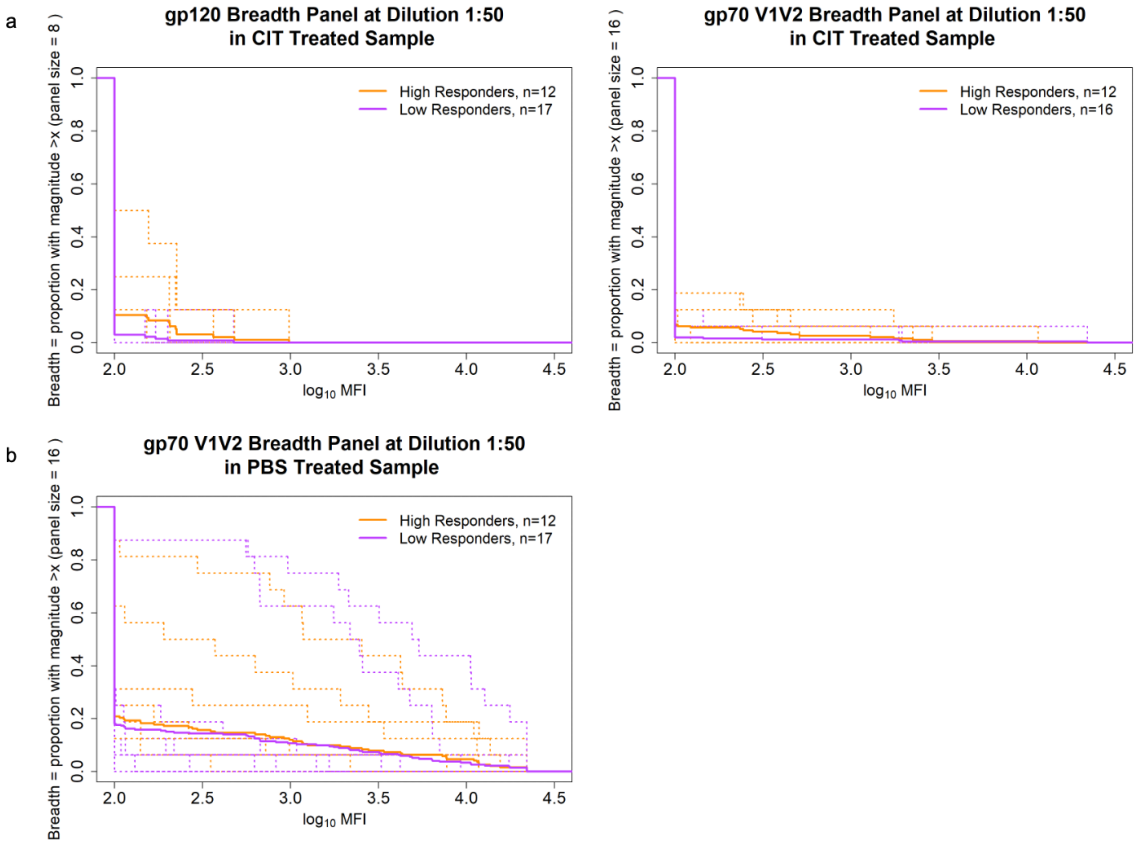

Extended Data 8 (related to Figures 11, 12 and 13). Comparable IgG1 binding magnitude, binding avidity and breadth against the global HIV-1 gp120 and V1V2 *Env* breadth panels.

BAMA was used to measure the IgG1 binding avidity to gp120 and V1V2 *Env* breadth panels (A), and IgG1 binding magnitude to the V1V2 *Env* breadth panels (B). The area under the curve (AUC) was measured using the M-B Curve as described in the Materials and Methods section. M-B Curve AUC min – max scores: IgG1 in CIT (gp120) – High Responders (HR) = 2 – 2.2365 and Low Responders (LR) = 2 – 2.0847; IgG1 in CIT (V1V2) – HR = 2 – 2.2312 and LR = 2 – 2.1464; IgG1 in PBS (V1V2) – HR = 2 – 3.2087 and LR = 2 – 3.5438. All BAMA assays were performed in duplicate (%CV <15% between sample replicates). T. Nyanhete designed the experiments, performed the experiments,

analyzed and interpreted the BAMA M-B Curve results. BAMA M-B Curves generated by L. Zhang under the direction of T. Nyanhete.

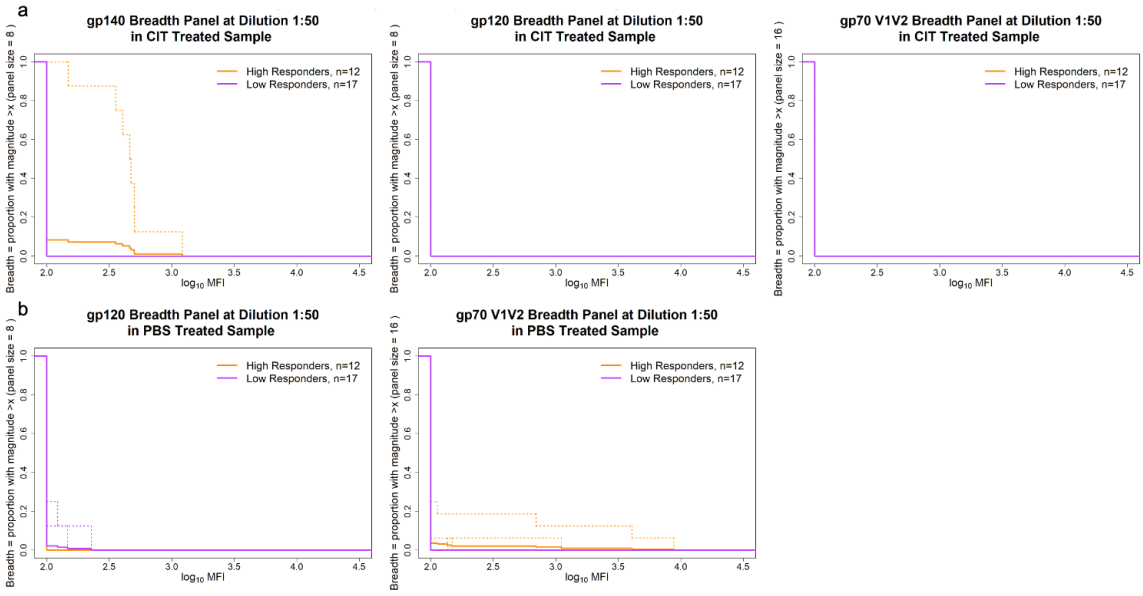

Extended Data 9 (related to Figures 11, 12 and 13). Comparable to no IgG2 binding magnitude and breadth against the global HIV-1 gp140, gp120 and V1V2 Env breadth panels.

BAMA was used to measure the IgG2 binding avidity to gp140, gp120 and V1V2 *Env* breadth panels (A), and IgG2 binding magnitude to the gp120 and V1V2 *Env* breadth panels (B). The area under the curve (AUC) was measured using the M-B Curve as described in the Materials and Methods section. M-B Curve AUC min – max scores: IgG2 in CIT (gp140) – High Responders (HR) = 2 – 2.6437 and Low Responders (LR) = 2 – 2; IgG2 in CIT (gp120) – HR = 2 – 2 and LR = 2 - 2; IgG2 in CIT (V1V2) – HR = 2 – 2 and LR = 2 – 2; IgG2 in PBS (gp120) – HR = 2 – 2 and LR = 2 – 2.0555; IgG2 in PBS (V1V2) – HR = 2 – 2.2782 and LR = 2 – 2. All BAMA assays were performed in duplicate (%CV <15% between sample replicates). T. Nyanhete designed the experiments, performed the

experiments, analyzed and interpreted the BAMA M-B Curve results. BAMA M-B Curves generated by L. Zhang under the direction of T. Nyanhete.

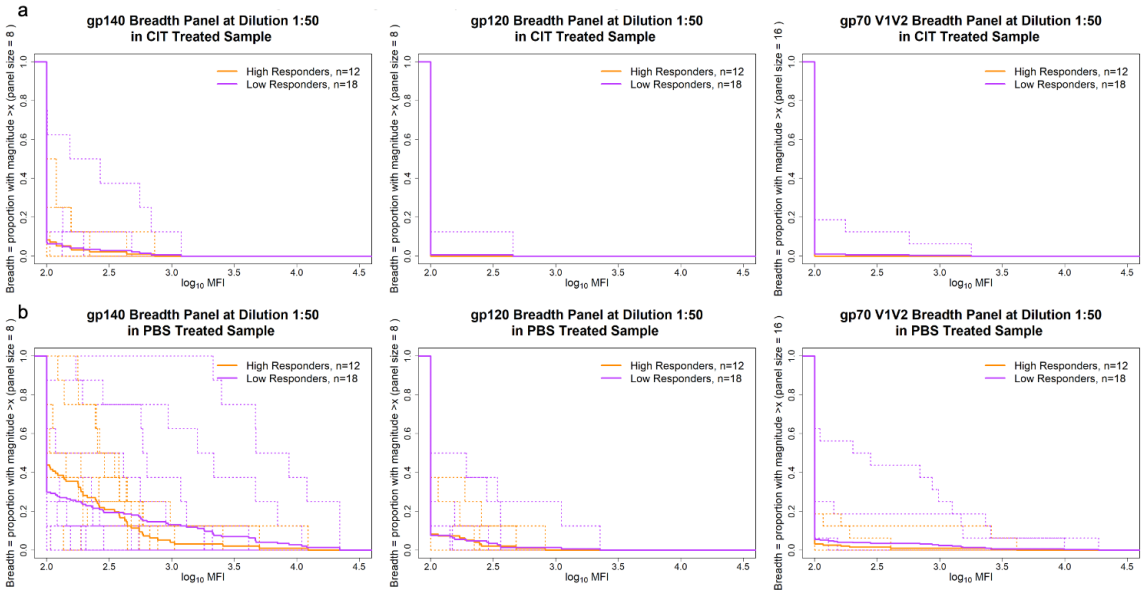

Extended Data 10 (related to Figures 11, 12 and 13). Comparable to no IgG3 binding magnitude and breadth against the global HIV-1 gp140, gp120 and V1V2 Env breadth panel in Citrate buffer treated samples for binding avidity measures (A) and PBS treated samples (B).

BAMA was used to measure the IgG3 binding avidity to gp140, gp120 and V1V2 *Env* breadth panels (A), and IgG3 binding magnitude to the gp140, gp120 and V1V2 *Env* breadth panels (B). The area under the curve (AUC) was measured using the M-B Curve as described in the Materials and Methods section. M-B Curve AUC min – max scores: IgG3 in CIT (gp140) – High Responders (HR) = 2 – 2.1232 and Low Responders (LR) = 2 – 2.4088; IgG3 in CIT (gp120) – HR = 2 – 2 and LR = 2 – 2.0824; IgG3 in CIT (V1V2) – HR = 2 – 2 and LR = 2 – 2.1408; IgG3 in PBS (gp140) – HR = 2 – 2.6309 and LR = 2 – 3.8465; IgG3 in PBS (gp120) – HR = 2 – 2.1725 and LR = 2 – 2.3918; IgG3 in PBS (V1V2)

– HR = 2 – 2.1936 and LR = 2 – 2.6067. All BAMA assays were performed in duplicate (%CV <15% between sample replicates). T. Nyanhete designed the experiments, performed the experiments, analyzed and interpreted the BAMA M-B Curve results. BAMA M-B Curves generated by L. Zhang under the direction of T. Nyanhete.

	ID_{50} in TZMbl Cells			
Patient	MLV	CH505TF	BG505 T332N	JR-FL
VC N	<20	**44**	**158**	**268**
VC AA	<20	**68**	**64**	**255**
VC AL	<20	**51**	**175**	**2551**
VC AP	<20	**738**	**418**	**3191**
VC AQ	<20	**99**	**202**	**337**
VC BA	<20	<20	**118**	**85**

Extended Data 11 (related to Figure 14). Neutralization-guided down-selection of BG505gp140 T332N SOSIP.664 for use in structure-based studies.

Neutralization-guided down-selection of recombinant HIV-1 Env SOSIP to use for structure-based studies. The neutralization sensitivities of the CH505TF, BG505/T332N and JR-FL HIV-1 pseudotyped viruses to HIV-1 VC plasma samples with bNAb activity were measured in a TZMbl neutralization assay, with MLV being used as the negative control. Values in black bold type are considered positive for neutralizing antibody activity in the sample based on the criterion of signal greater than or equal to three times that against the negative control MLV-pseudotyped virus. The CH01-31 mAb was used as the positive control (IC_{50} for CH505TF = 0.08, BG505 T332 = 0.06 and JR-FL = 0.04). Values

are plasma dilution at which relative luminescence units (RLUs) were reduced 50% compared to virus control wells (no test sample). Each HIV-1 VC plasma sample was tested in triplicate. D. Montefiori and C. LaBranche designed, supervised and analyzed the TZMbl neutralization experiment. T. Nyanhete designed and analyzed and interpreted the TZMbl neutralization experiment results.

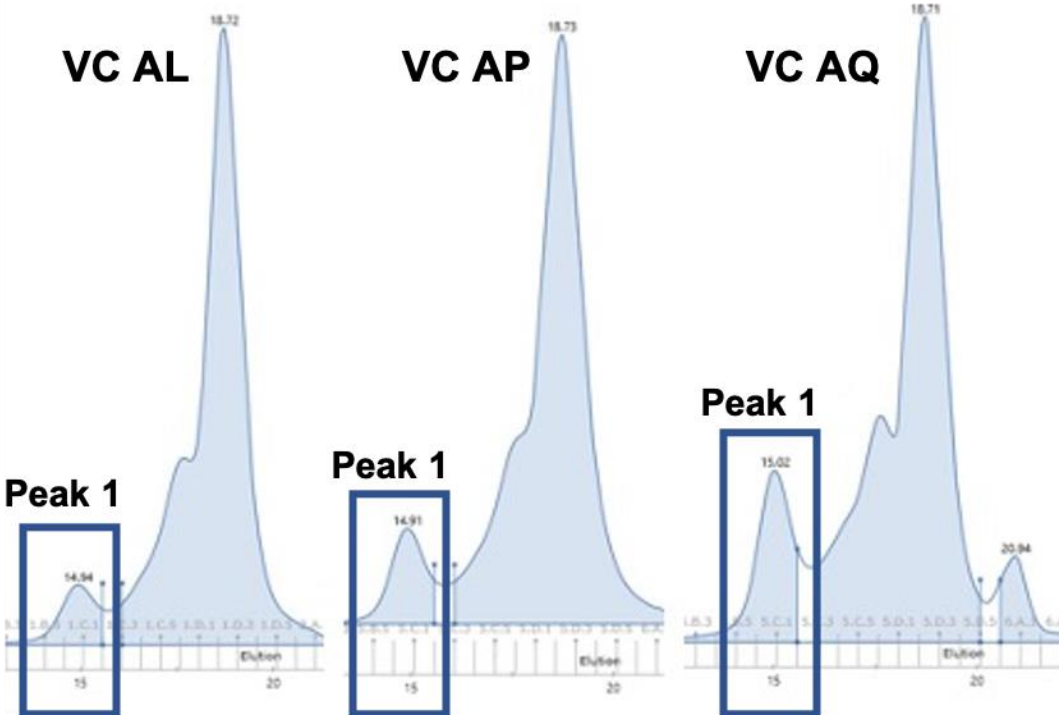

Extended Data 12 (related to Figures 20 and 21). SEC purified VC AL, VC AP and VC AQ Fab-bound HIV-1 BG505gp140 T332N SOSIP.664

HIV-1 VC IgG Fab complexed with BG505gp140 T332N SOSIP.664 was purified from unbound HIV-1 VC IgG Fab and BG505gp140 T32N SOSIP.664 fractions using size exclusion chromatography (SEC). The first peak represented the fraction containing the HIV-1 VC IgG Fab complexed with BG505gp140 T332N SOSIP.664, whereas the second

and third peaks represent the unbound BG505gp140 T332N SOSIP.664 and HIV-1 VC IgG Fab, respectively. VC AQ SEC profile has an extra peak due to the presence of Fc fragments. T. Nyanhete prepared the IgG Fabs, evaluated binding of Fabs to BG505gp140 T332N SOSIP.664, made and purified Fab-SOSIP immune complexes by FPLC.

References

1. Sharp, P.M. and B.H. Hahn, *Origins of HIV and the AIDS pandemic.* Cold Spring Harb Perspect Med, 2011. **1**(1): p. a006841.

2. Faria, N.R., et al., *HIV epidemiology. The early spread and epidemic ignition of HIV-1 in human populations.* Science, 2014. **346**(6205): p. 56-61.

3. Chen, Z., et al., *Human immunodeficiency virus type 2 (HIV-2) seroprevalence and characterization of a distinct HIV-2 genetic subtype from the natural range of simian immunodeficiency virus-infected sooty mangabeys.* J Virol, 1997. **71**(5): p. 3953-60.

4. Greene, W.C., *A history of AIDS: looking back to see ahead.* Eur J Immunol, 2007. **37 Suppl 1**: p. S94-102.

5. Barre-Sinoussi, F., et al., *Isolation of a T-lymphotropic retrovirus from a patient at risk for acquired immune deficiency syndrome (AIDS).* Science, 1983. **220**(4599): p. 868-71.

6. Gallo, R.C., et al., *Frequent detection and isolation of cytopathic retroviruses (HTLV-III) from patients with AIDS and at risk for AIDS.* Science, 1984. **224**(4648): p. 500-3.

7. De Leys, R., et al., *Isolation and partial characterization of an unusual human immunodeficiency retrovirus from two persons of west-central African origin.* J Virol, 1990. **64**(3): p. 1207-16.

8. Peeters, M., et al., *Geographical distribution of HIV-1 group O viruses in Africa.* Aids, 1997. **11**(4): p. 493-8.

9. Plantier, J.C., et al., *A new human immunodeficiency virus derived from gorillas.* Nat Med, 2009. **15**(8): p. 871-2.

10. van der Loeff, M.F., et al., *Sixteen years of HIV surveillance in a West African research clinic reveals divergent epidemic trends of HIV-1 and HIV-2.* Int J Epidemiol, 2006. **35**(5): p. 1322-8.

11. Berry, N., et al., *Low level viremia and high CD4% predict normal survival in a cohort of HIV type-2-infected villagers.* AIDS Res Hum Retroviruses, 2002. **18**(16): p. 1167-73.

12. Rowland-Jones, S.L. and H.C. Whittle, *Out of Africa: what can we learn from HIV-2 about protective immunity to HIV-1?* Nat Immunol, 2007. **8**(4): p. 329-31.

13. Korber, B., et al., *Timing the ancestor of the HIV-1 pandemic strains.* Science, 2000. **288**(5472): p. 1789-96.

14. Sharp, P.M. and B.H. Hahn, *AIDS: prehistory of HIV-1.* Nature, 2008. **455**(7213): p. 605-6.

15. Taylor, B.S., et al., *The challenge of HIV-1 subtype diversity.* N Engl J Med, 2008. **358**(15): p. 1590-602.

16. Gilbert, M.T., et al., *The emergence of HIV/AIDS in the Americas and beyond.* Proc Natl Acad Sci U S A, 2007. **104**(47): p. 18566-70.

17. Gallo, R., et al., *HIV/HTLV gene nomenclature.* Nature, 1988. **333**(6173): p. 504.

18. Sauter, D., et al., *Human tetherin exerts strong selection pressure on the HIV-1 group N Vpu protein.* PLoS Pathog, 2012. **8**(12): p. e1003093.

19. Gelderblom, H.R., *Assembly and morphology of HIV: potential effect of structure on viral function.* Aids, 1991. **5**(6): p. 617-37.

20. Overbaugh, J. and L. Morris, *The Antibody Response against HIV-1.* Cold Spring Harb Perspect Med, 2012. **2**(1): p. a007039.

21. UNAIDS, *Number of people living with hiv.* 2019, June 30.

22. HIV.gov, *U.S. Statistics.* 2020, January 16.

23. Shaw, G.M. and E. Hunter, *HIV transmission.* Cold Spring Harb Perspect Med, 2012. **2**(11).

24. Galvin, S.R. and M.S. Cohen, *The role of sexually transmitted diseases in HIV transmission.* Nat Rev Microbiol, 2004. **2**(1): p. 33-42.

25. Gray, R.H., et al., *Increased risk of incident HIV during pregnancy in Rakai, Uganda: a prospective study.* Lancet, 2005. **366**(9492): p. 1182-8.

26. Quinn, T.C., *Circumcision and HIV transmission.* Curr Opin Infect Dis, 2007. **20**(1): p. 33-8.

27. Miller, W.C., et al., *Role of acute and early HIV infection in the sexual transmission of HIV.* Curr Opin HIV AIDS, 2010. **5**(4): p. 277-82.

28. Fideli, U.S., et al., *Virologic and immunologic determinants of heterosexual transmission of human immunodeficiency virus type 1 in Africa.* AIDS Res Hum Retroviruses, 2001. **17**(10): p. 901-10.

29. Boily, M.C., et al., *Heterosexual risk of HIV-1 infection per sexual act: systematic review and meta-analysis of observational studies.* Lancet Infect Dis, 2009. **9**(2): p. 118-29.

30. Tindall, B. and D.A. Cooper, *Primary HIV infection: host responses and intervention strategies.* Aids, 1991. **5**(1): p. 1-14.

31. Fauci, A.S., et al., *Immunopathogenic mechanisms of HIV infection.* Ann Intern Med, 1996. **124**(7): p. 654-63.

32. Pantaleo, G., C. Graziosi, and A.S. Fauci, *The immunopathogenesis of human immunodeficiency virus infection.* N Engl J Med, 1993. **328**(5): p. 327-35.

33. Altfeld, M. and M. Gale, Jr., *Innate immunity against HIV-1 infection.* Nat Immunol, 2015. **16**(6): p. 554-62.

34. Lapenta, C., et al., *Type I interferon is a powerful inhibitor of in vivo HIV-1 infection and preserves human CD4(+) T cells from virus-induced depletion in SCID mice transplanted with human cells.* Virology, 1999. **263**(1): p. 78-88.

35. Li, Q., et al., *Glycerol monolaurate prevents mucosal SIV transmission.* Nature, 2009. **458**(7241): p. 1034-8.

36. Brenchley, J.M., et al., *Microbial translocation is a cause of systemic immune activation in chronic HIV infection.* Nat Med, 2006. **12**(12): p. 1365-71.

37. Lore, K., et al., *Accumulation of DC-SIGN+CD40+ dendritic cells with reduced CD80 and CD86 expression in lymphoid tissue during acute HIV-1 infection.* Aids, 2002. **16**(5): p. 683-92.

38. Stacey, A.R., et al., *Induction of a striking systemic cytokine cascade prior to peak viremia in acute human immunodeficiency virus type 1 infection, in*

contrast to more modest and delayed responses in acute hepatitis B and C virus infections. J Virol, 2009. **83**(8): p. 3719-33.

39. Manches, O., et al., *HIV-activated human plasmacytoid DCs induce Tregs through an indoleamine 2,3-dioxygenase-dependent mechanism.* J Clin Invest, 2008. **118**(10): p. 3431-9.

40. Lubong Sabado, R., et al., *In vitro priming recapitulates in vivo HIV-1 specific T cell responses, revealing rapid loss of virus reactive CD4 T cells in acute HIV-1 infection.* PLoS One, 2009. **4**(1): p. e4256.

41. Alter, G., et al., *Evolution of innate and adaptive effector cell functions during acute HIV-1 infection.* J Infect Dis, 2007. **195**(10): p. 1452-60.

42. Alter, G., et al., *HLA class I subtype-dependent expansion of KIR3DS1+ and KIR3DL1+ NK cells during acute human immunodeficiency virus type 1 infection.* J Virol, 2009. **83**(13): p. 6798-805.

43. Martin, M.P., et al., *Epistatic interaction between KIR3DS1 and HLA-B delays the progression to AIDS.* Nat Genet, 2002. **31**(4): p. 429-34.

44. O'Connor, G.M., et al., *Peptide-Dependent Recognition of HLA-B*57:01 by KIR3DS1.* J Virol, 2015. **89**(10): p. 5213-21.

45. Pulendran, B., *Learning immunology from the yellow fever vaccine: innate immunity to systems vaccinology.* Nat Rev Immunol, 2009. **9**(10): p. 741-7.

46. Sandler, N.G., et al., *Type I interferon responses in rhesus macaques prevent SIV infection and slow disease progression.* Nature, 2014. **511**(7511): p. 601-5.

47. Burrows, S.R., J. Rossjohn, and J. McCluskey, *Have we cut ourselves too short in mapping CTL epitopes?* Trends Immunol, 2006. **27**(1): p. 11-6.

48. McMichael, A.J. and L.J. Picker, *Unusual antigen presentation offers new insight into HIV vaccine design.* Curr Opin Immunol, 2017. **46**: p. 75-81.

49. Lefranc, M.P., *IMGT, the international ImMunoGeneTics database.* Nucleic Acids Res, 2001. **29**(1): p. 207-9.

50. Bianconi, E., et al., *An estimation of the number of cells in the human body.* Ann Hum Biol, 2013. **40**(6): p. 463-71.

51. Davis, M.M. and P.J. Bjorkman, *T-cell antigen receptor genes and T-cell recognition.* Nature, 1988. **334**(6181): p. 395-402.

52. Chen, H., et al., *TCR clonotypes modulate the protective effect of HLA class I molecules in HIV-1 infection.* Nat Immunol, 2012. **13**(7): p. 691-700.

53. Messaoudi, I., et al., *Direct link between mhc polymorphism, T cell avidity, and diversity in immune defense.* Science, 2002. **298**(5599): p. 1797-800.

54. Chaara, W., et al., *RepSeq Data Representativeness and Robustness Assessment by Shannon Entropy.* Front Immunol, 2018. **9**: p. 1038.

55. Cheroutre, H. and M.M. Husain, *CD4 CTL: living up to the challenge.* Semin Immunol, 2013. **25**(4): p. 273-81.

56. Koup, R.A. and D.C. Douek, *Vaccine design for CD8 T lymphocyte responses.* Cold Spring Harb Perspect Med, 2011. **1**(1): p. a007252.

57. Migueles, S.A. and M. Connors, *The Role of CD4(+) and CD8(+) T Cells in Controlling HIV Infection.* Curr Infect Dis Rep, 2002. **4**(5): p. 461-467.

58. Borrow, P., et al., *Virus-specific CD8+ cytotoxic T-lymphocyte activity associated with control of viremia in primary human immunodeficiency virus type 1 infection.* J Virol, 1994. **68**(9): p. 6103-10.

59. McMichael, A.J., et al., *The immune response during acute HIV-1 infection: clues for vaccine development.* Nat Rev Immunol, 2010. **10**(1): p. 11-23.

60. Freel, S.A., et al., *Initial HIV-1 antigen-specific CD8+ T cells in acute HIV-1 infection inhibit transmitted/founder virus replication.* J Virol, 2012. **86**(12): p. 6835-46.

61. Hersperger, A.R., et al., *Qualitative features of the HIV-specific CD8+ T-cell response associated with immunologic control.* Curr Opin HIV AIDS, 2011. **6**(3): p. 169-73.

62. Saez-Cirion, A., et al., *HIV controllers exhibit potent CD8 T cell capacity to suppress HIV infection ex vivo and peculiar cytotoxic T lymphocyte activation phenotype.* Proc Natl Acad Sci U S A, 2007. **104**(16): p. 6776-81.

63. Mudd, P.A., et al., *Vaccine-induced CD8+ T cells control AIDS virus replication.* Nature, 2012. **491**(7422): p. 129-33.

64. Shasha, D., et al., *Elite controller CD8+ T cells exhibit comparable viral inhibition capacity, but better sustained effector properties compared to chronic progressors.* J Leukoc Biol, 2016. **100**(6): p. 1425-1433.

65. Yan, J., et al., *HIV-specific CD8+ T cells from elite controllers are primed for survival.* J Virol, 2013. **87**(9): p. 5170-81.

66. Jin, X., et al., *Dramatic rise in plasma viremia after CD8(+) T cell depletion in simian immunodeficiency virus-infected macaques.* J Exp Med, 1999. **189**(6): p. 991-8.

67. Schmitz, J.E., et al., *Control of viremia in simian immunodeficiency virus infection by CD8+ lymphocytes.* Science, 1999. **283**(5403): p. 857-60.

68. Liu, J., et al., *Immune control of an SIV challenge by a T-cell-based vaccine in rhesus monkeys.* Nature, 2009. **457**(7225): p. 87-91.

69. Shiver, J.W., et al., *Replication-incompetent adenoviral vaccine vector elicits effective anti-immunodeficiency-virus immunity.* Nature, 2002. **415**(6869): p. 331-5.

70. Tomaras, G.D. and B.F. Haynes, *Advancing Toward HIV-1 Vaccine Efficacy through the Intersections of Immune Correlates.* Vaccines (Basel), 2014. **2**(1): p. 15-35.

71. Mutua, G., et al., *Broad HIV-1 inhibition in vitro by vaccine-elicited CD8(+) T cells in African adults.* Mol Ther Methods Clin Dev, 2016. **3**: p. 16061.

72. Ahmed, T., et al., *Control of HIV-1 replication in vitro by vaccine-induced human CD8(+) T cells through conserved subdominant Pol epitopes.* Vaccine, 2016. **34**(9): p. 1215-24.

73. Hansen, S.G., et al., *Profound early control of highly pathogenic SIV by an effector memory T-cell vaccine.* Nature, 2011. **473**(7348): p. 523-7.

74. Hansen, S.G., et al., *Cytomegalovirus vectors violate CD8+ T cell epitope recognition paradigms.* Science, 2013. **340**(6135): p. 1237874.

75. Ranasinghe, S., et al., *Antiviral CD8+ T Cells Restricted by Human Leukocyte Antigen Class II Exist during Natural HIV Infection and Exhibit Clonal Expansion.* Immunity, 2016. **45**(4): p. 917-930.

76. Kirberg, J., et al., *Thymic selection of CD8+ single positive cells with a class II major histocompatibility complex-restricted receptor.* J Exp Med, 1994. **180**(1): p. 25-34.

77. Lopez, D., et al., *Cross-reactive T cell clones from unrelated individuals reveal similarities in peptide presentation between HLA-B27 and HLA-DR2.* J Immunol, 1993. **150**(7): p. 2675-86.

78. Matechak, E.O., et al., *MHC class II-specific T cells can develop in the CD8 lineage when CD4 is absent.* Immunity, 1996. **4**(4): p. 337-347.

79. Shimizu, T. and S. Takeda, *CD8 T cells from major histocompatibility complex class II-deficient mice respond vigorously to class II molecules in a primary mixed lymphocyte reaction.* Eur J Immunol, 1997. **27**(2): p. 500-8.

80. Tyznik, A.J., J.C. Sun, and M.J. Bevan, *The CD8 population in CD4-deficient mice is heavily contaminated with MHC class II-restricted T cells.* J Exp Med, 2004. **199**(4): p. 559-65.

81. Hirosawa, T., et al., *Mismatched human leukocyte antigen class II-restricted CD8(+) cytotoxic T cells may mediate selective graft-versus-leukemia effects following allogeneic hematopoietic cell transplantation.* Cancer Sci, 2011. **102**(7): p. 1281-6.

82. Rist, M., et al., *Cross-recognition of HLA DR4 alloantigen by virus-specific CD8+ T cells: a new paradigm for self-/nonself-recognition.* Blood, 2009. **114**(11): p. 2244-53.

83. Heemskerk, M.H., et al., *Dual HLA class I and class II restricted recognition of alloreactive T lymphocytes mediated by a single T cell receptor complex.* Proc Natl Acad Sci U S A, 2001. **98**(12): p. 6806-11.

84. Pietra, G., et al., *HLA-E-restricted recognition of cytomegalovirus-derived peptides by human CD8+ cytolytic T lymphocytes.* Proc Natl Acad Sci U S A, 2003. **100**(19): p. 10896-901.

85. Heinzel, A.S., et al., *HLA-E-dependent presentation of Mtb-derived antigen to human CD8+ T cells.* J Exp Med, 2002. **196**(11): p. 1473-81.

86. Hansen, S.G., et al., *Broadly targeted CD8(+) T cell responses restricted by major histocompatibility complex E.* Science, 2016. **351**(6274): p. 714-20.

87. Ramduth, D., et al., *Differential immunogenicity of HIV-1 clade C proteins in eliciting CD8+ and CD4+ cell responses.* J Infect Dis, 2005. **192**(9): p. 1588-96.

88. Janssen, E.M., et al., *CD4+ T cells are required for secondary expansion and memory in CD8+ T lymphocytes.* Nature, 2003. **421**(6925): p. 852-6.

89. Sun, J.C. and M.J. Bevan, *Defective CD8 T cell memory following acute infection without CD4 T cell help.* Science, 2003. **300**(5617): p. 339-42.

90. Streeck, H., et al., *Harnessing CD4(+) T cell responses in HIV vaccine development.* Nat Med, 2013. **19**(2): p. 143-9.

91. Moir, S., et al., *Perturbations in B cell responsiveness to CD4+ T cell help in HIV-infected individuals.* Proc Natl Acad Sci U S A, 2003. **100**(10): p. 6057-62.

92. Soghoian, D.Z., et al., *HIV-specific cytolytic CD4 T cell responses during acute HIV infection predict disease outcome.* Science translational medicine, 2012. **4**(123): p. 123ra25-123ra25.

93. Walker, B. and A. McMichael, *The T-Cell Response to HIV.* Cold Spring Harbor Perspectives in Medicine, 2012. **2**(11): p. a007054.

94. Rosenberg, E.S., et al., *Vigorous HIV-1-specific CD4+ T cell responses associated with control of viremia.* Science, 1997. **278**(5342): p. 1447-50.

95. Duvall, M.G., et al., *Maintenance of HIV-specific CD4+ T cell help distinguishes HIV-2 from HIV-1 infection.* J Immunol, 2006. **176**(11): p. 6973-81.

96. Chevalier, M.F., et al., *HIV-1-specific interleukin-21+ CD4+ T cell responses contribute to durable viral control through the modulation of HIV-specific CD8+ T cell function.* J Virol, 2011. **85**(2): p. 733-41.

97. Williams, L.D., et al., *Interleukin-21-producing HIV-1-specific CD8 T cells are preferentially seen in elite controllers.* J Virol, 2011. **85**(5): p. 2316-24.

98. Kalams, S.A., et al., *Association between virus-specific cytotoxic T-lymphocyte and helper responses in human immunodeficiency virus type 1 infection.* J Virol, 1999. **73**(8): p. 6715-20.

99. Kaufmann, D.E., et al., *Comprehensive analysis of human immunodeficiency virus type 1-specific CD4 responses reveals marked immunodominance of gag and nef and the presence of broadly recognized peptides.* J Virol, 2004. **78**(9): p. 4463-77.

100. Rychert, J., et al., *Sequence variation occurs in CD4 epitopes during early HIV infection.* J Acquir Immune Defic Syndr, 2007. **46**(3): p. 261-7.

101. Lacap, P.A., et al., *Associations of human leukocyte antigen DRB with resistance or susceptibility to HIV-1 infection in the Pumwani Sex Worker Cohort.* Aids, 2008. **22**(9): p. 1029-38.

102. Julg, B., et al., *Possession of HLA class II DRB1*1303 associates with reduced viral loads in chronic HIV-1 clade C and B infection.* J Infect Dis, 2011. **203**(6): p. 803-9.

103. Mucida, D., et al., *Transcriptional reprogramming of mature CD4(+) helper T cells generates distinct MHC class II-restricted cytotoxic T lymphocytes.* Nat Immunol, 2013. **14**(3): p. 281-9.

104. Reis, B.S., et al., *Mutual expression of the transcription factors Runx3 and ThPOK regulates intestinal CD4(+) T cell immunity.* Nat Immunol, 2013. **14**(3): p. 271-80.

105. Johnson, S., et al., *Cooperativity of HIV-Specific Cytolytic CD4 T Cells and CD8 T Cells in Control of HIV Viremia.* J Virol, 2015. **89**(15): p. 7494-505.

106. Sun, Y., et al., *Virus-specific cellular immune correlates of survival in vaccinated monkeys after simian immunodeficiency virus challenge.* J Virol, 2006. **80**(22): p. 10950-6.

107. Lin, L., et al., *COMPASS identifies T-cell subsets correlated with clinical outcomes.* Nat Biotechnol, 2015. **33**(6): p. 610-6.

108. Staprans, S.I., et al., *Enhanced SIV replication and accelerated progression to AIDS in macaques primed to mount a CD4 T cell response to the SIV envelope protein.* Proc Natl Acad Sci U S A, 2004. **101**(35): p. 13026-31.

109. Hoffman, W., F.G. Lakkis, and G. Chalasani, *B Cells, Antibodies, and More.* Clin J Am Soc Nephrol, 2016. **11**(1): p. 137-54.

110. Beerli, R.R. and C. Rader, *Mining human antibody repertoires.* MAbs, 2010. **2**(4): p. 365-78.

111. Matsuda, F., et al., *The complete nucleotide sequence of the human immunoglobulin heavy chain variable region locus.* J Exp Med, 1998. **188**(11): p. 2151-62.

112. Chu, T.H., et al., *Hinge length contributes to the phagocytic activity of HIV-specific IgG1 and IgG3 antibodies.* PLoS Pathog, 2020. **16**(2): p. e1008083.

113. Stavnezer, J. and C.E. Schrader, *IgH chain class switch recombination: mechanism and regulation.* J Immunol, 2014. **193**(11): p. 5370-8.

114. Tomaras, G.D., et al., *Initial B-cell responses to transmitted human immunodeficiency virus type 1: virion-binding immunoglobulin M (IgM) and IgG antibodies followed by plasma anti-gp41 antibodies with ineffective control of initial viremia.* J Virol, 2008. **82**(24): p. 12449-63.

115. Tomaras, G.D. and B.F. Haynes, *HIV-1-specific antibody responses during acute and chronic HIV-1 infection.* Curr Opin HIV AIDS, 2009. **4**(5): p. 373-9.

116. Liu, P., et al., *Dynamic Antibody Specificities and Virion Concentrations in Circulating Immune Complexes in Acute to Chronic HIV-1 Infection.* J Virol, 2011. **85**(21): p. 11196-207.

117. Davis, K.L., et al., *High titer HIV-1 V3-specific antibodies with broad reactivity but low neutralizing potency in acute infection and following vaccination.* Virology, 2009. **387**(2): p. 414-26.

118. Burton, D.R. and L. Hangartner, *Broadly Neutralizing Antibodies to HIV and Their Role in Vaccine Design.* Annu Rev Immunol, 2016. **34**: p. 635-59.

119. Haynes, B.F., et al., *B-cell-lineage immunogen design in vaccine development with HIV-1 as a case study.* Nat Biotechnol, 2012. **30**(5): p. 423-33.

120. Kwong, P.D. and J.R. Mascola, *Human antibodies that neutralize HIV-1: identification, structures, and B cell ontogenies.* Immunity, 2012. **37**(3): p. 412-25.

121. Klein, F., et al., *Somatic mutations of the immunoglobulin framework are generally required for broad and potent HIV-1 neutralization.* Cell, 2013. **153**(1): p. 126-38.

122. Subbaraman, H., M. Schanz, and A. Trkola, *Broadly neutralizing antibodies: What is needed to move from a rare event in HIV-1 infection to vaccine efficacy?* Retrovirology, 2018. **15**(1): p. 52.

123. Walker, L.M., et al., *Broad and potent neutralizing antibodies from an African donor reveal a new HIV-1 vaccine target.* Science, 2009. **326**(5950): p. 285-9.

124. Mouquet, H., et al., *Complex-type N-glycan recognition by potent broadly neutralizing HIV antibodies.* Proc Natl Acad Sci U S A, 2012. **109**(47): p. E3268-77.

125. Huang, J., et al., *Broad and potent neutralization of HIV-1 by a gp41-specific human antibody.* Nature, 2012. **491**(7424): p. 406-12.

126. Williams, L.D., et al., *Potent and broad HIV-neutralizing antibodies in memory B cells and plasma.* Sci Immunol, 2017. **2**(7).

127. Burton, D.R., et al., *Efficient neutralization of primary isolates of HIV-1 by a recombinant human monoclonal antibody.* Science, 1994. **266**(5187): p. 1024-7.

128. Wu, X., et al., *Rational design of envelope identifies broadly neutralizing human monoclonal antibodies to HIV-1.* Science, 2010. **329**(5993): p. 856-61.

129. Huang, J., et al., *Broad and potent HIV-1 neutralization by a human antibody that binds the gp41-gp120 interface.* Nature, 2014. **515**(7525): p. 138-42.

130. van Gils, M.J., et al., *An HIV-1 antibody from an elite neutralizer implicates the fusion peptide as a site of vulnerability.* Nat Microbiol, 2016. **2**: p. 16199.

131. Kong, R., et al., *Fusion peptide of HIV-1 as a site of vulnerability to neutralizing antibody.* Science, 2016. **352**(6287): p. 828-33.

132. Zhou, T., et al., *A Neutralizing Antibody Recognizing Primarily N-Linked Glycan Targets the Silent Face of the HIV Envelope.* Immunity, 2018. **48**(3): p. 500-513.e6.

133. Garces, F., et al., *Affinity Maturation of a Potent Family of HIV Antibodies Is Primarily Focused on Accommodating or Avoiding Glycans.* Immunity, 2015. **43**(6): p. 1053-63.

134. Bonsignori, M., et al., *Antibody-virus co-evolution in HIV infection: paths for HIV vaccine development.* Immunol Rev, 2017. **275**(1): p. 145-160.

135. Cheng, H.D., et al., *Fine epitope signature of antibody neutralization breadth at the HIV-1 envelope CD4-binding site.* JCI Insight, 2018. **3**(5).

136. Scheid, J.F., et al., *Sequence and structural convergence of broad and potent HIV antibodies that mimic CD4 binding.* Science, 2011. **333**(6049): p. 1633-7.

137. Grobben, M., R.A. Stuart, and M.J. van Gils, *The potential of engineered antibodies for HIV-1 therapy and cure.* Curr Opin Virol, 2019. **38**: p. 70-80.

138. Gao, F., et al., *Cooperation of B cell lineages in induction of HIV-1-broadly neutralizing antibodies.* Cell, 2014. **158**(3): p. 481-91.

139. Bonsignori, M., et al., *Maturation Pathway from Germline to Broad HIV-1 Neutralizer of a CD4-Mimic Antibody.* Cell, 2016. **165**(2): p. 449-63.

140. Diskin, R., et al., *Restricting HIV-1 pathways for escape using rationally designed anti-HIV-1 antibodies.* J Exp Med, 2013. **210**(6): p. 1235-49.

141. Pantophlet, R., et al., *Fine mapping of the interaction of neutralizing and nonneutralizing monoclonal antibodies with the CD4 binding site of human immunodeficiency virus type 1 gp120.* J Virol, 2003. **77**(1): p. 642-58.

142. Ozorowski, G., et al., *Open and closed structures reveal allostery and pliability in the HIV-1 envelope spike.* Nature, 2017. **547**(7663): p. 360-363.

143. Stiegler, G., et al., *A potent cross-clade neutralizing human monoclonal antibody against a novel epitope on gp41 of human immunodeficiency virus type 1.* AIDS Res Hum Retroviruses, 2001. **17**(18): p. 1757-65.

144. McCoy, L.E., *The expanding array of HIV broadly neutralizing antibodies.* Retrovirology, 2018. **15**(1): p. 70.

145. Landais, E. and P.L. Moore, *Development of broadly neutralizing antibodies in HIV-1 infected elite neutralizers.* Retrovirology, 2018. **15**(1): p. 61.

146. Doria-Rose, N.A., et al., *Mapping Polyclonal HIV-1 Antibody Responses via Next-Generation Neutralization Fingerprinting.* PLoS Pathog, 2017. **13**(1): p. e1006148.

147. Bianchi, M., et al., *Electron-Microscopy-Based Epitope Mapping Defines Specificities of Polyclonal Antibodies Elicited during HIV-1 BG505 Envelope Trimer Immunization.* Immunity, 2018. **49**(2): p. 288-300.e8.

148. Sanders, R.W., et al., *A next-generation cleaved, soluble HIV-1 Env trimer, BG505 SOSIP.664 gp140, expresses multiple epitopes for broadly neutralizing but not non-neutralizing antibodies.* PLoS Pathog, 2013. **9**(9): p. e1003618.

149. McCoy, L.E., et al., *Holes in the Glycan Shield of the Native HIV Envelope Are a Target of Trimer-Elicited Neutralizing Antibodies.* Cell Rep, 2016. **16**(9): p. 2327-38.

150. Schroeder, H.W., Jr. and L. Cavacini, *Structure and function of immunoglobulins.* J Allergy Clin Immunol, 2010. **125**(2 Suppl 2): p. S41-52.

151. Gunn, B., et al., *Enhanced binding of antibodies generated during chronic HIV infection to mucus component MUC16.* Mucosal immunology, 2016. **9**(6): p. 1549-1558.

152. Arnold, J.N., et al., *The impact of glycosylation on the biological function and structure of human immunoglobulins.* Annu Rev Immunol, 2007. **25**: p. 21-50.

153. Anand, S.P. and A. Finzi, *Understudied Factors Influencing Fc-Mediated Immune Responses against Viral Infections.* Vaccines (Basel), 2019. **7**(3).

154. Levin, R., S. Grinstein, and J. Canton, *The life cycle of phagosomes: formation, maturation, and resolution.* Immunol Rev, 2016. **273**(1): p. 156-79.

155. Tay, M.Z., K. Wiehe, and J. Pollara, *Antibody-Dependent Cellular Phagocytosis in Antiviral Immune Responses.* Front Immunol, 2019. **10**: p. 332.

156. Chung, A.W., et al., *Polyfunctional Fc-effector profiles mediated by IgG subclass selection distinguish RV144 and VAX003 vaccines.* Sci Transl Med, 2014. **6**(228): p. 228ra38.

157. Dugast, A.S., et al., *Decreased Fc receptor expression on innate immune cells is associated with impaired antibody-mediated cellular phagocytic*

activity in chronically HIV-1 infected individuals. Virology, 2011. **415**(2): p. 160-7.

158. Ackerman, M.E., et al., *Enhanced phagocytic activity of HIV-specific antibodies correlates with natural production of immunoglobulins with skewed affinity for FcgammaR2a and FcgammaR2b.* J Virol, 2013. **87**(10): p. 5468-76.

159. Brouwer, K.C., et al., *Polymorphism of Fc receptor IIa for IgG in infants is associated with susceptibility to perinatal HIV-1 infection.* Aids, 2004. **18**(8): p. 1187-94.

160. Biggs, B.A., et al., *HIV-1 infection of human macrophages impairs phagocytosis and killing of Toxoplasma gondii.* J Immunol, 1995. **154**(11): p. 6132-9.

161. Kedzierska, K., et al., *HIV-1 down-modulates gamma signaling chain of Fc gamma R in human macrophages: a possible mechanism for inhibition of phagocytosis.* J Immunol, 2002. **168**(6): p. 2895-903.

162. Neidich, S.D., et al., *Antibody Fc effector functions and IgG3 associate with decreased HIV-1 risk.* J Clin Invest, 2019. **129**(11): p. 4838-4849.

163. Ackerman, M.E., *Polyfunctional HIV-Specific Antibody Responses Are Associated with Spontaneous HIV Control.* 2016. **12**(1).

164. Alvarez, R.A., et al., *Enhanced FCGR2A and FCGR3A signaling by HIV viremic controller IgG.* JCI Insight, 2017. **2**(4): p. e88226.

165. Lofano, G., et al., *Antigen-specific antibody Fc glycosylation enhances humoral immunity via the recruitment of complement.* Sci Immunol, 2018. **3**(26).

166. Richardson, S.I., et al., *HIV-specific Fc effector function early in infection predicts the development of broadly neutralizing antibodies.* PLoS Pathog, 2018. **14**(4): p. e1006987.

167. Veazey, R.S. and A.A. Lackner, *Nonhuman Primate Models and Understanding the Pathogenesis of HIV Infection and AIDS.* Ilar j, 2017. **58**(2): p. 160-171.

168. Evans, D.T. and G. Silvestri, *Nonhuman primate models in AIDS research.* Curr Opin HIV AIDS, 2013. **8**(4): p. 255-61.

169. Lackner, A.A. and R.S. Veazey, *Current concepts in AIDS pathogenesis: insights from the SIV/macaque model.* Annu Rev Med, 2007. **58**: p. 461-76.

170. Del Prete, G.Q., J.D. Lifson, and B.F. Keele, *Nonhuman primate models for the evaluation of HIV-1 preventive vaccine strategies: model parameter considerations and consequences.* Curr Opin HIV AIDS, 2016. **11**(6): p. 546-554.

171. Vidarsson, G., G. Dekkers, and T. Rispens, *IgG subclasses and allotypes: from structure to effector functions.* Front Immunol, 2014. **5**: p. 520.

172. Trist, H.M., et al., *Polymorphisms and interspecies differences of the activating and inhibitory FcgammaRII of Macaca nemestrina influence the binding of human IgG subclasses.* J Immunol, 2014. **192**(2): p. 792-803.

173. van der Neut Kolfschoten, M., et al., *Anti-inflammatory activity of human IgG4 antibodies by dynamic Fab arm exchange.* Science, 2007. **317**(5844): p. 1554-7.

174. Warncke, M., et al., *Different adaptations of IgG effector function in human and nonhuman primates and implications for therapeutic antibody treatment.* J Immunol, 2012. **188**(9): p. 4405-11.

175. Crowley, A.R. and M.E. Ackerman, *Mind the Gap: How Interspecies Variability in IgG and Its Receptors May Complicate Comparisons of Human and Non-human Primate Effector Function.* Front Immunol, 2019. **10**: p. 697.

176. Barre-Sinoussi, F., A.L. Ross, and J.F. Delfraissy, *Past, present and future: 30 years of HIV research.* Nat Rev Microbiol, 2013. **11**(12): p. 877-83.

177. Goulder, P. and S.G. Deeks, *HIV control: Is getting there the same as staying there?* PLoS Pathog, 2018. **14**(11): p. e1007222.

178. Namazi, G., et al., *The Control of HIV After Antiretroviral Medication Pause (CHAMP) Study: Posttreatment Controllers Identified From 14 Clinical Studies.* J Infect Dis, 2018. **218**(12): p. 1954-1963.

179. Etemad, B., E. Esmaeilzadeh, and J.Z. Li, *Learning From the Exceptions: HIV Remission in Post-treatment Controllers.* Front Immunol, 2019. **10**: p. 1749.

180. Descours, B., et al., *Immune responses driven by protective human leukocyte antigen alleles from long-term nonprogressors are associated with low HIV reservoir in central memory CD4 T cells.* Clin Infect Dis, 2012. **54**(10): p. 1495-503.

181. Veenhuis, R.T., et al., *Long-term remission despite clonal expansion of replication-competent HIV-1 isolates.* JCI Insight, 2018. **3**(18).

182. Deeks, S.G. and B.D. Walker, *Human immunodeficiency virus controllers: mechanisms of durable virus control in the absence of antiretroviral therapy.* Immunity, 2007. **27**(3): p. 406-16.

183. Hunt, P.W., *Natural control of HIV-1 replication and long-term nonprogression: overlapping but distinct phenotypes.* J Infect Dis, 2009. **200**(11): p. 1636-8.

184. Alexander, L., et al., *Unusual polymorphisms in human immunodeficiency virus type 1 associated with nonprogressive infection.* J Virol, 2000. **74**(9): p. 4361-76.

185. Yamada, T. and A. Iwamoto, *Comparison of proviral accessory genes between long-term nonprogressors and progressors of human immunodeficiency virus type 1 infection.* Arch Virol, 2000. **145**(5): p. 1021-7.

186. Blankson, J.N., et al., *Isolation and characterization of replication-competent human immunodeficiency virus type 1 from a subset of elite suppressors.* J Virol, 2007. **81**(5): p. 2508-18.

187. Kiepiela, P., et al., *Dominant influence of HLA-B in mediating the potential co-evolution of HIV and HLA.* Nature, 2004. **432**(7018): p. 769-75.

188. Bailey, J.R., et al., *Maintenance of viral suppression in HIV-1-infected HLA-B*57+ elite suppressors despite CTL escape mutations.* J Exp Med, 2006. **203**(5): p. 1357-69.

189. Migueles, S.A., et al., *HLA B*5701 is highly associated with restriction of virus replication in a subgroup of HIV-infected long term nonprogressors.* Proc Natl Acad Sci U S A, 2000. **97**(6): p. 2709-14.

190. Kiepiela, P., et al., *CD8+ T-cell responses to different HIV proteins have discordant associations with viral load.* Nat Med, 2007. **13**(1): p. 46-53.

191. Migueles, S.A., et al., *The differential ability of HLA B*5701+ long-term nonprogressors and progressors to restrict human immunodeficiency virus replication is not caused by loss of recognition of autologous viral gag sequences.* J Virol, 2003. **77**(12): p. 6889-98.

192. Martin, M.P., et al., *Innate partnership of HLA-B and KIR3DL1 subtypes against HIV-1.* Nat Genet, 2007. **39**(6): p. 733-40.

193. Fellay, J., et al., *A whole-genome association study of major determinants for host control of HIV-1.* Science, 2007. **317**(5840): p. 944-7.

194. Pereyra, F., et al., *Genetic and immunologic heterogeneity among persons who control HIV infection in the absence of therapy.* J Infect Dis, 2008. **197**(4): p. 563-71.

195. Brener, J., et al., *Disease progression despite protective HLA expression in an HIV-infected transmission pair.* Retrovirology, 2015. **12**: p. 55.

196. Huang, J., et al., *Leukocyte immunoglobulin-like receptors maintain unique antigen-presenting properties of circulating myeloid dendritic cells in HIV-1-infected elite controllers.* J Virol, 2010. **84**(18): p. 9463-71.

197. Barblu, L., et al., *Plasmacytoid dendritic cells (pDCs) from HIV controllers produce interferon-alpha and differentiate into functional killer pDCs under HIV activation.* J Infect Dis, 2012. **206**(5): p. 790-801.

198. Riedel, D.J., et al., *Natural viral suppressors of HIV-1 have a unique capacity to maintain gammadelta T cells.* Aids, 2009. **23**(15): p. 1955-64.

199. Altfeld, M., et al., *Influence of HLA-B57 on clinical presentation and viral control during acute HIV-1 infection.* Aids, 2003. **17**(18): p. 2581-91.

200. Migueles, S.A., et al., *HIV-specific CD8+ T cell proliferation is coupled to perforin expression and is maintained in nonprogressors.* Nat Immunol, 2002. **3**(11): p. 1061-8.

201. Betts, M.R., et al., *HIV nonprogressors preferentially maintain highly functional HIV-specific CD8+ T cells.* Blood, 2006. **107**(12): p. 4781-9.

202. Bailey, J.R., et al., *Neutralizing antibodies do not mediate suppression of human immunodeficiency virus type 1 in elite suppressors or selection of plasma virus variants in patients on highly active antiretroviral therapy.* J Virol, 2006. **80**(10): p. 4758-70.

203. Freund, N.T., et al., *Coexistence of potent HIV-1 broadly neutralizing antibodies and antibody-sensitive viruses in a viremic controller.* Sci Transl Med, 2017. **9**(373).

204. Scheid, J.F., et al., *Broad diversity of neutralizing antibodies isolated from memory B cells in HIV-infected individuals.* Nature, 2009. **458**(7238): p. 636-40.

205. Martin-Gayo, E., et al., *Immunological Fingerprints of Controllers Developing Neutralizing HIV-1 Antibodies.* Cell Rep, 2020. **30**(4): p. 984-996.e4.

206. Silver, Z.A., et al., *A Highly Unusual V1 Region of Env in an Elite Controller of HIV Infection.* J Virol, 2019. **93**(10).

207. Hutchinson, J.M., et al., *Unusual Cysteine Content in V1 Region of gp120 From an Elite Suppressor That Produces Broadly Neutralizing Antibodies.* Front Immunol, 2019. **10**: p. 1021.

208. Gonzalez, N., et al., *Characterization of broadly neutralizing antibody responses to HIV-1 in a cohort of long term non-progressors.* PLoS One, 2018. **13**(3): p. e0193773.

209. Martin-Gayo, E., et al., *Circulating CXCR5(+)CXCR3(+)PD-1(lo) Tfh-like cells in HIV-1 controllers with neutralizing antibody breadth.* JCI Insight, 2017. **2**(2): p. e89574.

210. Dugast, A.S., et al., *Virus-driven Inflammation Is Associated With the Development of bNAbs in Spontaneous Controllers of HIV.* Clin Infect Dis, 2017. **64**(8): p. 1098-1104.

211. Lucar, O., et al., *Neutralizing Antibodies Against a Specific Human Immunodeficiency Virus gp41 Epitope are Associated With Long-term Non-progressor Status.* EBioMedicine, 2017. **22**: p. 122-132.

212. Bonsignori, M., et al., *An autoreactive antibody from an SLE/HIV-1 individual broadly neutralizes HIV-1.* J Clin Invest, 2014. **124**(4): p. 1835-43.

213. Lambotte, O., et al., *Heterogeneous neutralizing antibody and antibody-dependent cell cytotoxicity responses in HIV-1 elite controllers.* Aids, 2009. **23**(8): p. 897-906.

214. Martinez, V., et al., *Anticardiolipin antibodies in HIV infection are independently associated with antibodies to the membrane proximal external region of gp41 and with cell-associated HIV DNA and immune activation.* Clin Infect Dis, 2009. **48**(1): p. 123-32.

215. Braibant, M., et al., *Antibodies to conserved epitopes of the HIV-1 envelope in sera from long-term non-progressors: prevalence and association with neutralizing activity.* Aids, 2006. **20**(15): p. 1923-30.

216. Madhavi, V., et al., *HIV-1 Env- and Vpu-Specific Antibody-Dependent Cellular Cytotoxicity Responses Associated with Elite Control of HIV.* J Virol, 2017. **91**(18).

217. Alsahafi, N., et al., *Impaired Downregulation of NKG2D Ligands by Nef Proteins from Elite Controllers Sensitizes HIV-1-Infected Cells to Antibody-Dependent Cellular Cytotoxicity.* J Virol, 2017. **91**(16).

218. Alsahafi, N., et al., *Nef Proteins from HIV-1 Elite Controllers Are Inefficient at Preventing Antibody-Dependent Cellular Cytotoxicity.* J Virol, 2015. **90**(6): p. 2993-3002.

219. Lai, J.I., et al., *Divergent antibody subclass and specificity profiles but not protective HLA-B alleles are associated with variable antibody effector function among HIV-1 controllers.* J Virol, 2014. **88**(5): p. 2799-809.

220. Madhavi, V., et al., *Breadth of HIV-1 Env-specific antibody-dependent cellular cytotoxicity: relevance to global HIV vaccine design.* Aids, 2014. **28**(13): p. 1859-70.

221. Wren, L.H., et al., *Specific antibody-dependent cellular cytotoxicity responses associated with slow progression of HIV infection.* Immunology, 2013. **138**(2): p. 116-23.

222. Lambotte, O., et al., *High antibody-dependent cellular cytotoxicity responses are correlated with strong CD8 T cell viral suppressive activity but not with B57 status in HIV-1 elite controllers.* PLoS One, 2013. **8**(9): p. e74855.

223. Parsons, M.S., A.W. Chung, and S.J. Kent, *Importance of Fc-mediated functions of anti-HIV-1 broadly neutralizing antibodies.* Retrovirology, 2018. **15**(1): p. 58.

224. Bournazos, S., et al., *Broadly neutralizing anti-HIV-1 antibodies require Fc effector functions for in vivo activity.* Cell, 2014. **158**(6): p. 1243-53.

225. Richardson, S.I., et al., *IgG3 enhances neutralization potency and Fc effector function of an HIV V2-specific broadly neutralizing antibody.* PLoS Pathog, 2019. **15**(12): p. e1008064.

226. Nyanhete, T.E., et al., *HLA class II-Restricted CD8+ T cells in HIV-1 Virus Controllers.* Sci Rep, 2019. **9**(1): p. 10165.

227. Nabel, G.J., *HIV vaccine strategies.* Vaccine, 2002. **20**(15): p. 1945-7.

228. Tay, M.Z., et al., *Antibody-Mediated Internalization of Infectious HIV-1 Virions Differs among Antibody Isotypes and Subclasses.* PLoS Pathog, 2016. **12**(8): p. e1005817.

229. Heeney, J.L. and S.A. Plotkin, *Immunological correlates of protection from HIV infection and disease.* Nat Immunol, 2006. **7**(12): p. 1281-4.

230. Corey, L., et al., *Immune correlates of vaccine protection against HIV-1 acquisition.* Sci Transl Med, 2015. **7**(310): p. 310rv7.

231. Stephenson, K.E. and D.H. Barouch, *A global approach to HIV-1 vaccine development.* Immunol Rev, 2013. **254**(1): p. 295-304.

232. Hansen, S.G., et al., *Immune clearance of highly pathogenic SIV infection.* Nature, 2013. **502**(7469): p. 100-4.

233. Ranasinghe, S. and B.D. Walker, *Programming CMV for vaccine vector design.* Nat Biotechnol, 2013. **31**(9): p. 811-2.

234. Heemskerk, M.H., et al., *Activation of virus-specific major histocompatibility complex class II-restricted CD8+ cytotoxic T cells in CD4-deficient mice.* Eur J Immunol, 1995. **25**(4): p. 1109-12.

235. Hancock, G., et al., *Identification of effective subdominant anti-HIV-1 CD8+ T cells within entire post-infection and post-vaccination immune responses.* PLoS Pathog, 2015. **11**(2): p. e1004658.

236. Saez-Cirion, A., et al., *HIV controllers exhibit potent CD8 T cell capacity to suppress HIV infection ex vivo and peculiar cytotoxic T lymphocyte activation phenotype.* Proc Natl Acad Sci U S A, 2007. **104**(16): p. 6776-81.

237. Freel, S.A., et al., *Phenotypic and functional profile of HIV-inhibitory CD8 T cells elicited by natural infection and heterologous prime/boost vaccination.* J Virol, 2010. **84**(10): p. 4998-5006.

238. Payne, T.L., et al., *Transcriptional and posttranscriptional regulation of cytokine gene expression in HIV-1 antigen-specific CD8+ T cells that mediate virus inhibition.* J Virol, 2014. **88**(17): p. 9514-28.

239. Frahm, M.A., et al., *CD4+CD8+ T cells represent a significant portion of the anti-HIV T cell response to acute HIV infection.* J Immunol, 2012. **188**(9): p. 4289-96.

240. Dobin, A., et al., *STAR: ultrafast universal RNA-seq aligner.* Bioinformatics, 2013. **29**(1): p. 15-21.

241. Anders, S., P.T. Pyl, and W. Huber, *HTSeq--a Python framework to work with high-throughput sequencing data.* Bioinformatics, 2015. **31**(2): p. 166-9.

242. Love, M.I., W. Huber, and S. Anders, *Moderated estimation of fold change and dispersion for RNA-seq data with DESeq2.* Genome Biol, 2014. **15**(12): p. 550.

243. Montojo, J., et al., *GeneMANIA Cytoscape plugin: fast gene function predictions on the desktop.* Bioinformatics, 2010. **26**(22): p. 2927-8.

244. Bolotin, D.A., et al., *MiXCR: software for comprehensive adaptive immunity profiling.* Nat Methods, 2015. **12**(5): p. 380-1.

245. Nazarov, V.I., et al., *tcR: an R package for T cell receptor repertoire advanced data analysis.* BMC Bioinformatics, 2015. **16**: p. 175.

246. Ochsenbauer, C., et al., *Generation of transmitted/founder HIV-1 infectious molecular clones and characterization of their replication capacity in CD4 T lymphocytes and monocyte-derived macrophages.* J Virol, 2012. **86**(5): p. 2715-28.

247. Keele, B.F., et al., *Identification and characterization of transmitted and early founder virus envelopes in primary HIV-1 infection.* Proc Natl Acad Sci U S A, 2008. **105**(21): p. 7552-7.

248. Klein, M.R., et al., *Kinetics of Gag-specific cytotoxic T lymphocyte responses during the clinical course of HIV-1 infection: a longitudinal*

analysis of rapid progressors and long-term asymptomatics. J Exp Med, 1995. **181**(4): p. 1365-72.

249. Johnson, R.P., et al., *HIV-1 gag-specific cytotoxic T lymphocytes recognize multiple highly conserved epitopes. Fine specificity of the gag-specific response defined by using unstimulated peripheral blood mononuclear cells and cloned effector cells.* J Immunol, 1991. **147**(5): p. 1512-21.

250. Gea-Banacloche, J.C., et al., *Maintenance of large numbers of virus-specific CD8+ T cells in HIV-infected progressors and long-term nonprogressors.* J Immunol, 2000. **165**(2): p. 1082-92.

251. Julg, B., et al., *Enhanced anti-HIV functional activity associated with Gag-specific CD8 T-cell responses.* J Virol, 2010. **84**(11): p. 5540-9.

252. Masemola, A., et al., *Hierarchical targeting of subtype C human immunodeficiency virus type 1 proteins by CD8+ T cells: correlation with viral load.* J Virol, 2004. **78**(7): p. 3233-43.

253. Saez-Cirion, A., et al., *Heterogeneity in HIV suppression by CD8 T cells from HIV controllers: association with Gag-specific CD8 T cell responses.* J Immunol, 2009. **182**(12): p. 7828-37.

254. Vingert, B., et al., *HIV Controller CD4+ T Cells Respond to Minimal Amounts of Gag Antigen Due to High TCR Avidity.* PLoS Pathogens, 2010. **6**(2): p. e1000780.

255. Masopust, D., *Developing an HIV cytotoxic T-lymphocyte vaccine: issues of CD8 T-cell quantity, quality and location.* J Intern Med, 2009. **265**(1): p. 125-37.

256. Sallusto, F., et al., *Two subsets of memory T lymphocytes with distinct homing potentials and effector functions.* Nature, 1999. **401**(6754): p. 708-712.

257. Day, C.L., *Ex vivo analysis of human memory CD4 T cells specific for hepatitis C virus using MHC class II tetramers.* 2003. **112**(6): p. 831-42.

258. Palmer, C., et al., *Cell-type specific gene expression profiles of leukocytes in human peripheral blood.* BMC Genomics, 2006. **7**: p. 115.

259. Awong, G., et al., *Human CD8 T cells generated in vitro from hematopoietic stem cells are functionally mature.* BMC Immunol, 2011. **12**: p. 22.

260. Tokunaga, T., et al., *Regulation of Th-POK and Runx3 in T cell development in human thymoma.* Autoimmunity, 2009. **42**(8): p. 653-60.

261. Vacchio, M.S., et al., *A ThPOK-LRF transcriptional node maintains the integrity and effector potential of post-thymic CD4+ T cells.* Nat Immunol, 2014. **15**(10): p. 947-56.

262. Vacchio, M.S. and R. Bosselut, *What Happens in the Thymus Does Not Stay in the Thymus: How T Cells Recycle the CD4+-CD8+ Lineage Commitment Transcriptional Circuitry To Control Their Function.* J Immunol, 2016. **196**(12): p. 4848-56.

263. Cocchi, F., et al., *Identification of RANTES, MIP-1 alpha, and MIP-1 beta as the major HIV-suppressive factors produced by CD8+ T cells.* Science, 1995. **270**(5243): p. 1811-5.

264. Guzzo, C., et al., *The CD8-derived chemokine XCL1/lymphotactin is a conformation-dependent, broad-spectrum inhibitor of HIV-1.* PLoS Pathog, 2013. **9**(12): p. e1003852.

265. Simonetta, F., et al., *High eomesodermin expression among CD57+ CD8+ T cells identifies a CD8+ T cell subset associated with viral control during chronic human immunodeficiency virus infection.* J Virol, 2014. **88**(20): p. 11861-71.

266. Greenough, T.C., et al., *A Gene Expression Signature That Correlates with CD8+ T Cell Expansion in Acute EBV Infection.* J Immunol, 2015. **195**(9): p. 4185-97.

267. DeVico, A.L. and R.C. Gallo, *Control of HIV-1 infection by soluble factors of the immune response.* Nat Rev Microbiol, 2004. **2**(5): p. 401-13.

268. Tomaras, G.D., et al., *CD8+ T cell-mediated suppressive activity inhibits HIV-1 after virus entry with kinetics indicating effects on virus gene expression.* Proc Natl Acad Sci U S A, 2000. **97**(7): p. 3503-8.

269. Schulte, D., et al., *The HLA-E(R)/HLA-E(R) genotype affects the natural course of hepatitis C virus (HCV) infection and is associated with HLA-E-restricted recognition of an HCV-derived peptide by interferon-gamma-secreting human CD8(+) T cells.* J Infect Dis, 2009. **200**(9): p. 1397-401.

270. Roberts, L., et al., *Plasma cytokine levels during acute HIV-1 infection predict HIV disease progression.* AIDS, 2010. **24**(6): p. 819-31.

271. Burgers, W.A., et al., *Association of HIV-specific and total CD8+ T memory phenotypes in subtype C HIV-1 infection with viral set point.* J Immunol, 2009. **182**(8): p. 4751-61.

272. Hess, C., et al., *HIV-1 specific CD8+ T cells with an effector phenotype and control of viral replication.* Lancet, 2004. **363**(9412): p. 863-6.

273. Addo, M.M., et al., *Fully differentiated HIV-1 specific CD8+ T effector cells are more frequently detectable in controlled than in progressive HIV-1 infection.* PLoS One, 2007. **2**(3): p. e321.

274. Trautmann, L., et al., *Upregulation of PD-1 expression on HIV-specific CD8+ T cells leads to reversible immune dysfunction.* Nat Med, 2006. **12**(10): p. 1198-202.

275. Day, C.L., et al., *PD-1 expression on HIV-specific T cells is associated with T-cell exhaustion and disease progression.* Nature, 2006. **443**(7109): p. 350-4.

276. Hertoghs, K.M., et al., *Molecular profiling of cytomegalovirus-induced human CD8+ T cell differentiation.* J Clin Invest, 2010. **120**(11): p. 4077-90.

277. Ayano, M., et al., *Increased CD226 Expression on CD8+ T Cells Is Associated with Upregulated Cytokine Production and Endothelial Cell Injury in Patients with Systemic Sclerosis.* J Immunol, 2015. **195**(3): p. 892-900.

278. Best, J.A., et al., *Transcriptional insights into the CD8(+) T cell response to infection and memory T cell formation.* Nat Immunol, 2013. **14**(4): p. 404-12.

279. Depper, J.M., et al., *Interleukin 2 (IL-2) augments transcription of the IL-2 receptor gene.* Proc Natl Acad Sci U S A, 1985. **82**(12): p. 4230-4.

280. Pal, R., et al., *Inhibition of HIV-1 infection by the beta-chemokine MDC.* Science, 1997. **278**(5338): p. 695-8.

281. Saez-Cirion, A., et al., *HIV controllers exhibit potent CD8 T cell capacity to suppress HIV infection ex vivo and peculiar cytotoxic T lymphocyte*

activation phenotype. Proceedings of the National Academy of Sciences, 2007. **104**(16): p. 6776-6781.

282. Riou, C., et al., *HIV Skews the Lineage-Defining Transcriptional Profile of Mycobacterium tuberculosis-Specific CD4+ T Cells.* J Immunol, 2016. **196**(7): p. 3006-18.

283. Overgaard, N.H., et al., *CD4+/CD8+ double-positive T cells: more than just a developmental stage?* J Leukoc Biol, 2015. **97**(1): p. 31-8.

284. Soghoian, D.Z. and H. Streeck, *Cytolytic CD4(+) T cells in viral immunity.* Expert review of vaccines, 2010. **9**(12): p. 1453-1463.

285. Weiss, L., et al., *Persistent expansion, in a human immunodeficiency virus-infected person, of V beta-restricted CD4+CD8+ T lymphocytes that express cytotoxicity-associated molecules and are committed to produce interferon-gamma and tumor necrosis factor-alpha.* J Infect Dis, 1998. **178**(4): p. 1158-62.

286. Kitchen, S.G., et al., *CD4 on CD8(+) T cells directly enhances effector function and is a target for HIV infection.* Proc Natl Acad Sci U S A, 2004. **101**(23): p. 8727-32.

287. Qi, Q., et al., *Diversity and clonal selection in the human T-cell repertoire.* Proc Natl Acad Sci U S A, 2014. **111**(36): p. 13139-44.

288. Baum, P.D., et al., *Blood T-cell receptor diversity decreases during the course of HIV infection, but the potential for a diverse repertoire persists.* Blood, 2012. **119**(15): p. 3469-77.

289. Mendoza, D., et al., *HLA B*5701-Positive Long-Term Nonprogressors/Elite Controllers Are Not Distinguished from Progressors by the Clonal Composition of HIV-Specific CD8(+) T Cells.* Journal of Virology, 2012. **86**(7): p. 4014-4018.

290. Ndhlovu, Z., et al., *Magnitude and kinetics of CD8+ T cell activation during hyperacute HIV infection impacts viral set point.* Immunity, 2015. **43**(3): p. 591-604.

291. Pantaleo, G., et al., *Major expansion of CD8+ T cells with a predominant V beta usage during the primary immune response to HIV.* Nature, 1994. **370**(6489): p. 463-7.

292. Butler, A.L., S. Fischinger, and G. Alter, *The Antibodiome-Mapping the Humoral Immune Response to HIV.* Curr HIV/AIDS Rep, 2019. **16**(2): p. 169-179.

293. Moris, A., M. Pereira, and L. Chakrabarti, *A role for antibodies in natural HIV control.* Curr Opin HIV AIDS, 2019. **14**(4): p. 265-272.

294. Sajadi, M.M., et al., *Correlation between circulating HIV-1 RNA and broad HIV-1 neutralizing antibody activity.* J Acquir Immune Defic Syndr, 2011. **57**(1): p. 9-15.

295. Doria-Rose, N.A., et al., *Breadth of human immunodeficiency virus-specific neutralizing activity in sera: clustering analysis and association with clinical variables.* J Virol, 2010. **84**(3): p. 1631-6.

296. Rusert, P., et al., *Determinants of HIV-1 broadly neutralizing antibody induction.* Nat Med, 2016. **22**(11): p. 1260-1267.

297. Walker, B.D. and X.G. Yu, *Unravelling the mechanisms of durable control of HIV-1.* Nat Rev Immunol, 2013. **13**(7): p. 487-98.

298. Euler, Z., et al., *Cross-reactive neutralizing humoral immunity does not protect from HIV type 1 disease progression.* J Infect Dis, 2010. **201**(7): p. 1045-53.

299. Medina-Ramirez, M., et al., *Broadly cross-neutralizing antibodies in HIV-1 patients with undetectable viremia.* J Virol, 2011. **85**(12): p. 5804-13.

300. Carotenuto, P., et al., *Neutralizing antibodies are positively associated with CD4+ T-cell counts and T-cell function in long-term AIDS-free infection.* Aids, 1998. **12**(13): p. 1591-600.

301. Pilgrim, A.K., et al., *Neutralizing antibody responses to human immunodeficiency virus type 1 in primary infection and long-term-nonprogressive infection.* J Infect Dis, 1997. **176**(4): p. 924-32.

302. Lewis, G.K., *Role of Fc-mediated antibody function in protective immunity against HIV-1.* Immunology, 2014. **142**(1): p. 46-57.

303. Horwitz, J.A., et al., *Non-neutralizing Antibodies Alter the Course of HIV-1 Infection In Vivo.* Cell, 2017. **170**(4): p. 637-648.e10.

304. Hu, X., et al., *Profiles of neutralizing antibody response in chronically human immunodeficiency virus type 1 clade B'-infected former plasma donors from China naive to antiretroviral therapy.* J Gen Virol, 2012. **93**(Pt 10): p. 2267-78.

305. deCamp, A., et al., *Global panel of HIV-1 Env reference strains for standardized assessments of vaccine-elicited neutralizing antibodies.* J Virol, 2014. **88**(5): p. 2489-507.

306. Sarzotti-Kelsoe, M., et al., *Optimization and validation of the TZM-bl assay for standardized assessments of neutralizing antibodies against HIV-1.* J Immunol Methods, 2014. **409**: p. 131-46.

307. Platt, E.J., et al., *Effects of CCR5 and CD4 cell surface concentrations on infections by macrophagetropic isolates of human immunodeficiency virus type 1.* J Virol, 1998. **72**(4): p. 2855-64.

308. Hu, X., et al., *Profiling the neutralizing antibody response in chronically HIV-1 CRF07_BC-infected intravenous drug users naive to antiretroviral therapy.* Sci Rep, 2017. **7**: p. 46308.

309. Yates, N.L., et al., *HIV-1 Envelope Glycoproteins from Diverse Clades Differentiate Antibody Responses and Durability among Vaccinees.* J Virol, 2018. **92**(8).

310. Seaton, K.E., et al., *Computational analysis of antibody dynamics identifies recent HIV-1 infection.* JCI Insight, 2017. **2**(24).

311. Campbell, E.M., et al., *Labeling HIV-1 virions with two fluorescent proteins allows identification of virions that have productively entered the target cell.* Virology, 2007. **360**(2): p. 286-93.

312. Shukair, S.A., et al., *Human cervicovaginal mucus contains an activity that hinders HIV-1 movement.* Mucosal Immunol, 2013. **6**(2): p. 427-34.

313. Ackerman, M.E., et al., *A robust, high-throughput assay to determine the phagocytic activity of clinical antibody samples.* J Immunol Methods, 2011. **366**(1-2): p. 8-19.

314. Liu, P., et al., *Capacity for infectious HIV-1 virion capture differs by envelope antibody specificity.* J Virol, 2014. **88**(9): p. 5165-70.

315. Dennison, S.M., et al., *Qualified Biolayer Interferometry Avidity Measurements Distinguish the Heterogeneity of Antibody Interactions with Plasmodium falciparum Circumsporozoite Protein Antigens.* J Immunol, 2018. **201**(4): p. 1315-1326.

316. Lynch, R.M., et al., *The development of CD4 binding site antibodies during HIV-1 infection.* J Virol, 2012. **86**(14): p. 7588-95.

317. Henderson, R., et al., *Disruption of the HIV-1 Envelope allosteric network blocks CD4-induced rearrangements.* Nat Commun, 2020. **11**(1): p. 520.

318. Huang, Y., et al., *Simultaneous Evaluation of the Magnitude and Breadth of a Left and Right Censored Multivariate Response, with Application to HIV Vaccine Development.* Stat Biopharm Res, 2009. **1**(1): p. 81-91.

319. Gilbert, P., et al., *Magnitude and breadth of a nonprotective neutralizing antibody response in an efficacy trial of a candidate HIV-1 gp120 vaccine.* J Infect Dis, 2010. **202**(4): p. 595-605.

320. Cornelissen, M., et al., *The Neutralizing Antibody Response in an Individual with Triple HIV-1 Infection Remains Directed at the First Infecting Subtype.* AIDS Res Hum Retroviruses, 2016. **32**(10-11): p. 1135-1142.

321. Sanchez-Merino, V., et al., *Detection of Broadly Neutralizing Activity within the First Months of HIV-1 Infection.* J Virol, 2016. **90**(11): p. 5231-5245.

322. Liu, P., *Capacity for Infectious HIV-1 Virion Capture Differs by Envelope Antibody Specificity.* 2014. **88**(9): p. 5165-70.

323. Yasmeen, A., et al., *Differential binding of neutralizing and non-neutralizing antibodies to native-like soluble HIV-1 Env trimers, uncleaved Env proteins, and monomeric subunits.* Retrovirology, 2014. **11**: p. 41.

324. Hessell, A.J., et al., *Fc receptor but not complement binding is important in antibody protection against HIV.* Nature, 2007. **449**(7158): p. 101-4.

325. Ko, S.Y., et al., *Enhanced neonatal Fc receptor function improves protection against primate SHIV infection.* Nature, 2014. **514**(7524): p. 642-5.

326. Kouyos, R.D., et al., *Tracing HIV-1 strains that imprint broadly neutralizing antibody responses.* Nature, 2018. **561**(7723): p. 406-410.

327. Caskey, M., et al., *Viraemia suppressed in HIV-1-infected humans by broadly neutralizing antibody 3BNC117.* Nature, 2015. **522**(7557): p. 487-91.

328. Julien, J.P., et al., *Broadly neutralizing antibody PGT121 allosterically modulates CD4 binding via recognition of the HIV-1 gp120 V3 base and multiple surrounding glycans.* PLoS Pathog, 2013. **9**(5): p. e1003342.

329. Pejchal, R., et al., *A potent and broad neutralizing antibody recognizes and penetrates the HIV glycan shield.* Science, 2011. **334**(6059): p. 1097-103.

330. Goonetilleke, N. and A.J. McMichael, *Immunology. Antigen processing takes a new direction.* Science, 2013. **340**(6135): p. 937-8.

331. Huang, J., et al., *Detection, phenotyping, and quantification of antigen-specific T cells using a peptide-MHC dodecamer.* Proc Natl Acad Sci U S A, 2016. **113**(13): p. E1890-7.

332. Zaunders, J.J., et al., *Identification of circulating antigen-specific CD4+ T lymphocytes with a CCR5+, cytotoxic phenotype in an HIV-1 long-term nonprogressor and in CMV infection.* Blood, 2004. **103**(6): p. 2238-47.

333. Lam, S. and C. Bollard, *T-cell therapies for HIV.* Immunotherapy, 2013. **5**(4): p. 407-14.

334. Wagner, T.A., *Quarter Century of Anti-HIV CAR T Cells.* Curr HIV/AIDS Rep, 2018. **15**(2): p. 147-154.

335. Migueles, S.A., et al., *Adoptive lymphocyte transfer to an HIV-infected progressor from an elite controller.* JCI Insight, 2019. **4**(18).

336. Anthony-Gonda, K., et al., *Multispecific anti-HIV duoCAR-T cells display broad in vitro antiviral activity and potent in vivo elimination of HIV-infected cells in a humanized mouse model.* Sci Transl Med, 2019. **11**(504).

337. Moore, P.L., C. Williamson, and L. Morris, *Virological features associated with the development of broadly neutralizing antibodies to HIV-1.* Trends Microbiol, 2015. **23**(4): p. 204-11.

338. Sather, D.N., et al., *Emergence of broadly neutralizing antibodies and viral coevolution in two subjects during the early stages of infection with human immunodeficiency virus type 1.* J Virol, 2014. **88**(22): p. 12968-81.

Biography

Tinashe Edward Nyanhete completed his B.A. in Molecular Biology and Geography at Colgate University in 2014. During his time at Colgate, Tinashe worked in Dr. Kenneth Belanger's laboratory studying the role of nucleoporin proteins in regulating movement of molecules between the cytoplasm and nucleus. Tinashe also worked with Dr. Matthew Scott at Stanford University studying glioblastoma development as part of the Howard Hughes Medical Institute Exceptional Research Opportunities Proram (EXROP). Tinashe completed his undergraduate honors thesis research project at the National Cancer Institute under the mentorship of Dr. Marjorie Robert-Guroff which resulted in a publication titled 'Beyond Oncolytics: E1B55K-Deleted Adenovirus as a Vaccine Delivery Vector.'

After his undergraduate degree at Colgate, Tinashe moved to Duke University in 2014 where he pursued his PhD in Immunology in the laboratory of Dr. Georgia Tomaras. While at Duke Tinashe's publications include the first author publication 'HLA class II-restricted CD8+ T cells in HIV-1 Virus Controllers (Sci Rep. 2019. 9(1):10165)' and co-authorship publications: 'A MUC16 IgG Binding Activity Selects for a Restricted Subset of IgG Enriched for Certain Simian Immunodeficiency Virus Epitope Specificities (J Virol. 2020. 94(5).pii:e01246-19)', 'Antibody-Dependent

Cellular Cytotoxicity (ADCC)-Mediating Antibodies Constrain Neutralizing Antibody Escape Pathway (Front Immunol. 2019. 10.2875)', 'Human Epistatic Interaction Controls IL7R Splicing and Increases Multiple Sclerosis Risk (Cell. 2017. 169(1):72 – 84),' and a commentary article 'CD8+ T cells: Mechanistic Target of Rapamycin and Eukaryotic Initiation Factor 2 in Elite HIV-1 Control (AIDS. 2018. 32(18):2835 – 2838).'

Tinashe also received multiple honors and awards during his time at Duke including the Duke University Chancellor's Scholarship (2014), Duke CFAR Travel Award (2018), HIV4RP International Travel Scholarship (2018), FOCIS Centers of Excellence Travel Award (2017), Howard Hughes Medical Institute International Student Research Fellowship Duke University Finalist (2016), Duke Scholar in Infectious Disease (2017), Duke Graduate School Conference Travel Award (2018), and the BiCoRE Travel Award (2015).